73-4945

KRANE, Robert Joseph, 1938-
THE SOLUTION OF LAMINAR NATURAL CONVECTION FLOWS
IN RECTANGULAR ENCLOSURES BY THE METHOD OF
MATCHED ASYMPTOTIC EXPANSIONS.

The University of Oklahoma, Ph.D., 1972
Engineering, mechanical

University Microfilms, A XEROX Company, Ann Arbor, Michigan

THE UNIVERSITY OF OKLAHOMA

GRADUATE COLLEGE

THE SOLUTION OF LAMINAR NATURAL CONVECTION FLOWS IN RECTANGULAR ENCLOSURES BY THE METHOD OF MATCHED ASYMPTOTIC EXPANSIONS

A DISSERTATION

SUBMITTED TO THE GRADUATE FACULTY

in partial fulfillment of the requirements for the

degree of

DOCTOR OF PHILOSOPHY

BY

ROBERT JOSEPH KRANE

Norman, Oklahoma

1972

THE SOLUTION OF LAMINAR, NATURAL CONVECTION FLOWS

IN RECTANGULAR ENCLOSURES BY THE METHOD OF

MATCHED ASYMPTOTIC EXPANSIONS

APPROVED BY

Martin C. Jischke

William N. Huffb

M. Rasmussen

[illegible]

F. J. Appl

DISSERTATION COMMITTEE

ACKNOWLEDGMENTS

The author wishes to thank his entire doctoral advisory committee for their efforts. Special thanks are due to Dr. Martin Jischke who acted as chairman of this group. His unflagging interest and infectious enthusiasm assured the timely completion of this work.

My doctoral studies would have been impossible without the patience and understanding given so freely by my wife, Toni, and my children, Mike, Mary, Matt, and Greg. They, indeed, made very real contributions to this research.

This work is dedicated to the memory of my late father

Harry Robert Krane

ABSTRACT

Laminar, natural convection flows of a Newtonian fluid in a two-dimensional rectangular enclosure are considered. The two vertical walls of the enclosure are assumed to be isothermal surfaces maintained at two different temperatures and the horizontal walls are assumed to be adiabatic surfaces.

The physical nature of the flows in all regions of the flow-field, including the corners, is explained for the first time. The crucial point of this part of the analysis is the determination of the correct force balance in the core. The resulting pressure force-buoyancy force balance gives the experimentally observed linear temperature profile in the core region.

The vertical wall boundary layers are found to be governed by a second-order set of nonlinear parabolic partial differential equations that are nonsimilar. The exact solution of these equations (even in a numerical sense) presents a formidable problem. It was therefore decided to perform an approximate zeroth-order solution using von Karman integral techniques. This solution is shown to agree reasonably well with previously published experimental data and numerical solutions.

The "pseudo-elliptic" zeroth-order behavior of completely enclosed natural convection flows is revealed here for the first time. A "longtime upstream influence" is shown to exist for the vertical wall boundary layers even though they are governed by parabolic equations.

TABLE OF CONTENTS

Page

Page

LIST OF TABLES

LIST OF ILLUSTRATIONS

NOMENCLATURE

c_n - constants ($n = 1,2,\ldots$) in core solution

f_n - functions of horizontal coordinate ($\bar{y}$) in bottom horizontal wall boundary layer ($n = 1,2,\ldots$)

F_n - functions of horizontal coordinate ($\bar{\bar{y}}$) in top horizontal wall boundary layer

F - product of boundary layer thickness and magnitude of vertical velocity in integral solution of vertical wall boundary layers

g - magnitude of acceleration due gravity

h_n - functions of horizontal coordinate ($\hat{y}$) in bottom right-hand corner region ($n = 1,2,\ldots$)

H - height of enclosure

K_n - constants in horizontal wall boundary layer solutions ($n = 1,2$)

K - thermal conductivity

L - characteristic length

p - pressure

Q - any variable of interest

$\dot{Q}$ - total rate of heat transfer across the enclosure

t - time

T - Temperature

u - vertical component of velocity

U - magnitude of vertical velocity profile assumed for the integral solution

v - horizontal component of velocity

W - width of enclosure

x - vertical spatial coordinate

y - horizontal spatial coordinate

Greek Letters

α - thermal diffusivity, constant in integral solution of vertical wall boundary layer equations

β - coefficient of thermal expansion, constant in integral solution of vertical wall boundary layer equations

δ - vertical wall boundary layer thickness, small change in a variable

Δ - horizontal wall boundary layer thickness

ϵ - small parameter in the problem ($\equiv N_{GR}^{-1/8}$)

μ - dynamic viscosity

ν - kinematic viscosity

ρ - density

Φ_g - gravitational potential

ψ - streamfunction

Superscripts

$*$ - physical variable

i - intermediate coordinate

Nondimensional Variables

N_{GR} - Grashof number, defined as the ratio of buoyant forces to viscous forces, $\left(\frac{\rho_0 g\beta\Delta TL^3}{\nu_0^2}\right)$

$\bar{N}_{NU}$ - Nusselt number, $\left(\frac{\bar{h}L}{K}\right)$

N_{PR} - Prandtl number, defined as the ratio of diffusivity of momentum to the diffusivity of thermal energy, $\left(\frac{\nu_0}{\alpha_0}\right)$

N_{Re} - Reynolds number, defined as the ratio of inertia forces to viscous forces, $\left(\frac{\rho_0 \bar{L}_{rx} \bar{v}_r}{\mu_0}\right)$

Subscripts

a - left-hand, or "cold", vertical wall

b - right-hand, or "hot", vertical wall

c - convection

d - diffusion

0 - reference state

r - reference variable

δ - edge of vertical wall boundary layer

n - order of solution (n = 1,2,3,...)

Mathematical Symbols

O( ) - order

$\sim$ - asymptotically equal to

$(\vec{\ })$ - vector

$(\tilde{\ })$ - right-hand vertical wall boundary-layer variable

$(\bar{\ })$ - bottom horizontal wall boundary-layer variable

$(\bar{\bar{\ }})$ - top horizontal wall boundary-layer variable

$(\hat{\ })$ - bottom right-hand corner region variable

$(\hat{\hat{\ }})$ - top right-hand corner region variable

THE SOLUTION OF LAMINAR NATURAL CONVECTION FLOWS IN RECTANGULAR ENCLOSURES BY THE METHOD OF MATCHED ASYMPTOTIC EXPANSIONS

CHAPTER I

INTRODUCTION

Preliminary Remarks

During the past decade there has been a resurgence of interest in natural convection flow phenomena. This renewed interest has resulted in advances in many areas of fluid mechanics research. The analysis of cryogenic tankage for space vehicles [1 - 10], the design of industrial processes such as glass furnaces [11], [12], a need for improved analytical techniques by heating engineers [13], the analysis of cooling systems for nuclear reactors and turbine blades [14 - 16], and the analysis of geophysical flows [17] are typical of the current problems that have provided the impetus for further research in natural convection. The common interests of researchers working on topics such as these have led to the adoption of what has become a "model problem" in natural convection [11], [13]. The solution of this problem is of direct practical interest to heating engineers, process designers, and those analyzing cooling systems for nuclear reactors and turbomachinery; but, more importantly, it serves as a vehicle for the development of analytical techniques that can eventually be extended to a broader class of natural convection flows.

A Model Problem In Natural Convection

The model problem may be stated in the following manner. Consider a two-dimensional rectangular enclosure of width, W, and height, H, completely filled with a Newtonian fluid (Figure 1.1). There is a steady state natural convection flow in the enclosure as a result of the two vertical walls being maintained at different temperatures, T_a^* and T_b^*. The horizontal walls are assumed to be adiabatic surfaces and the gravitational acceleration vector, $\vec{g}$, is aligned with the negative x^*-axis. The two objectives of any analytical study of this system are:

1. Prediction of the detailed structure of the flowfield, and
2. Prediction of the total rate of heat transfer through the fluid from one vertical wall to the other.

Experimental Results of Previous Investigations

Experimental studies by Elder [17], [18], Eckert and Carlson [19], and MacGregor and Emery [20] have delineated the various possible flow regimes and provide a detailed qualitative description of the flow structure in each regime. The following discussion is based upon the results of these four studies.

Elder's experiments show that the basic laminar circulatory flow in the enclosure can produce steady, large scale secondary flows in the interior regions of the fluid, thereby giving rise to a multicellular flow pattern (Figure 1.2). These experiments suggest, that for a given aspect ratio, there is a "critical Grashof number" above

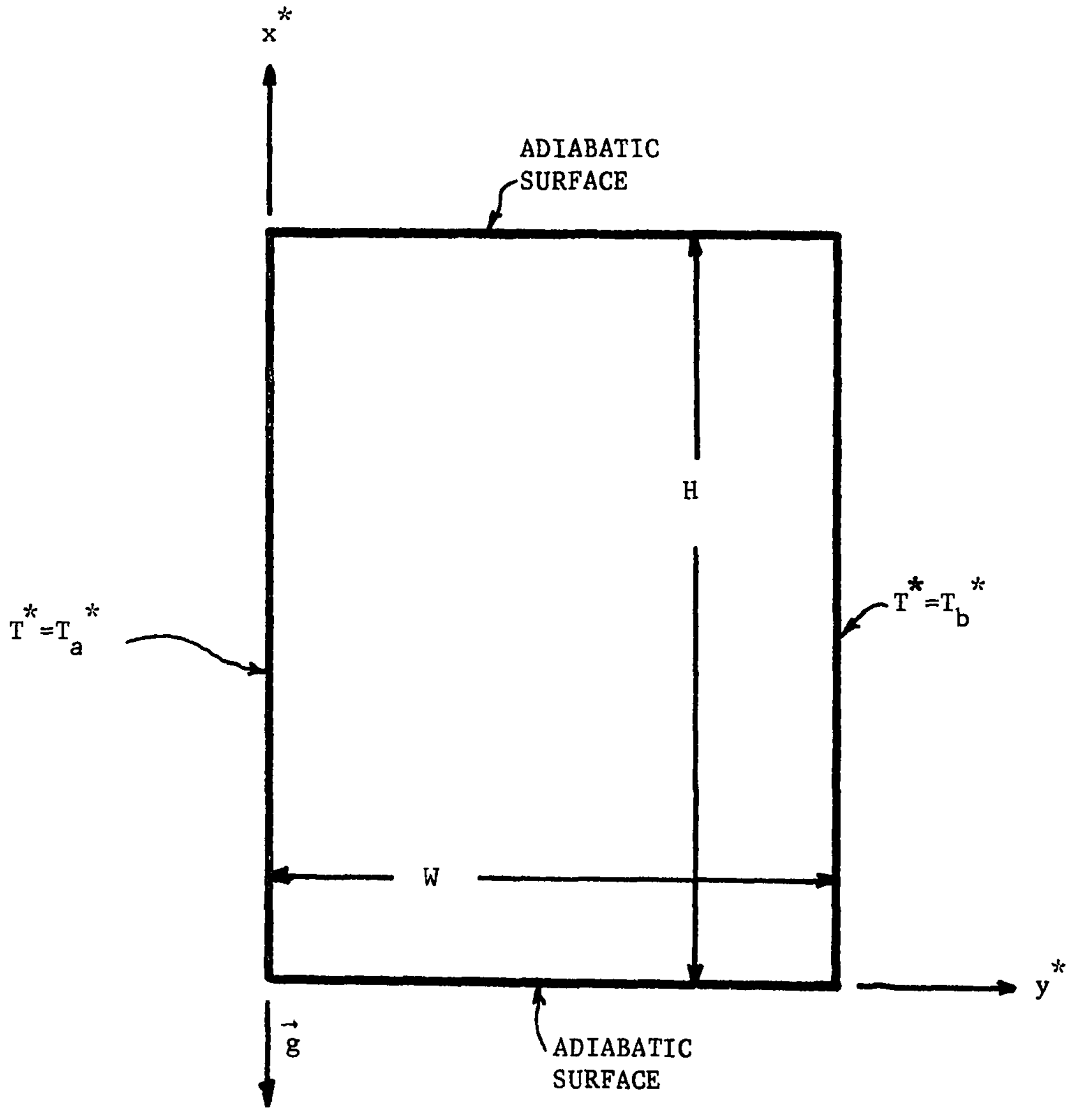

Figure 1.1. System for Model Problem in Natural Convection

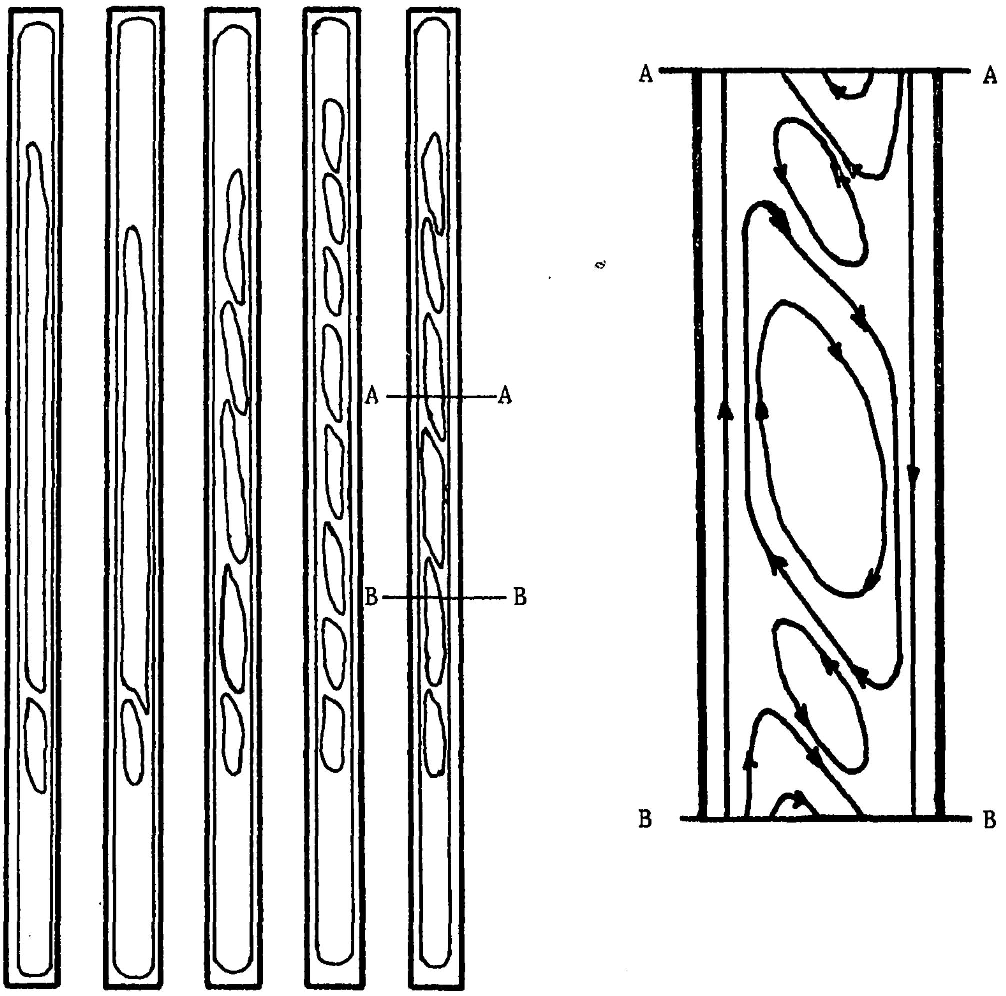

(a) (b) (c) (d) (e)

$\left(\frac{H}{W}\right) = 14$

(a) $N_{GR} = (1.88)(10^5)$

(b) $N_{GR} = (1.0)(10^6)$

(c) $N_{GR} = (1.35)(10^6)$

(d) $N_{GR} = (1.59)(10^6)$

(e) $N_{GR} = (1.87)(10^6)$

Figure 1.2. Streamline Patterns for Some Multicellular Flows Observed by Elder

which the flow is always multicellular. Furthermore, experimental results also suggest that, if the aspect ratio of the enclosure is of $O(1)$, the critical Grashof number is large enough so that the entire laminar boundary layer flow regime is unicellular. Therefore, both this discussion and the work that follows will be limited to the study of unicellular flows; that is, to enclosures with aspect ratio of order unity.

Five distinct unicellular flow regimes have been identified. They have been categorized by various investigators according to Grashof number, N_{GR}, as follows:

1. Conduction regime ($N_{GR} \leq 10^3$)
2. Asymptotic regime ($10^3 \leq N_{GR} \leq 10^4$)
3. Laminar boundary-layer regime ($10^4 \leq N_{GR} \leq 10^9$)
4. Transition regime ($N_{GR} \approx 10^9$)
5. Turbulent boundary-layer regime ($N_{GR} > 10^9$)

The upper limit of the laminar boundary layer regime is not well established with different investigators (see for example [17], [19]) reporting different maximum values of N_{GR}. Typical isotherm and streamline patterns and velocity and temperature profiles for the conduction, asymptotic, and laminar boundary layer regimes are shown in Figure 1.3.

The temperature profiles in the conduction regime are essentially linear across the enclosure except in regions near the top and bottom walls. In these regions the temperature profiles are nonlinear, indicating a convective contribution to the total rate of heat transfer across the enclosure owing to a very weak circulatory flow.

The asymptotic flow regime is characterized by a circulatory flow which is stronger than the one found in the conduction regime, but

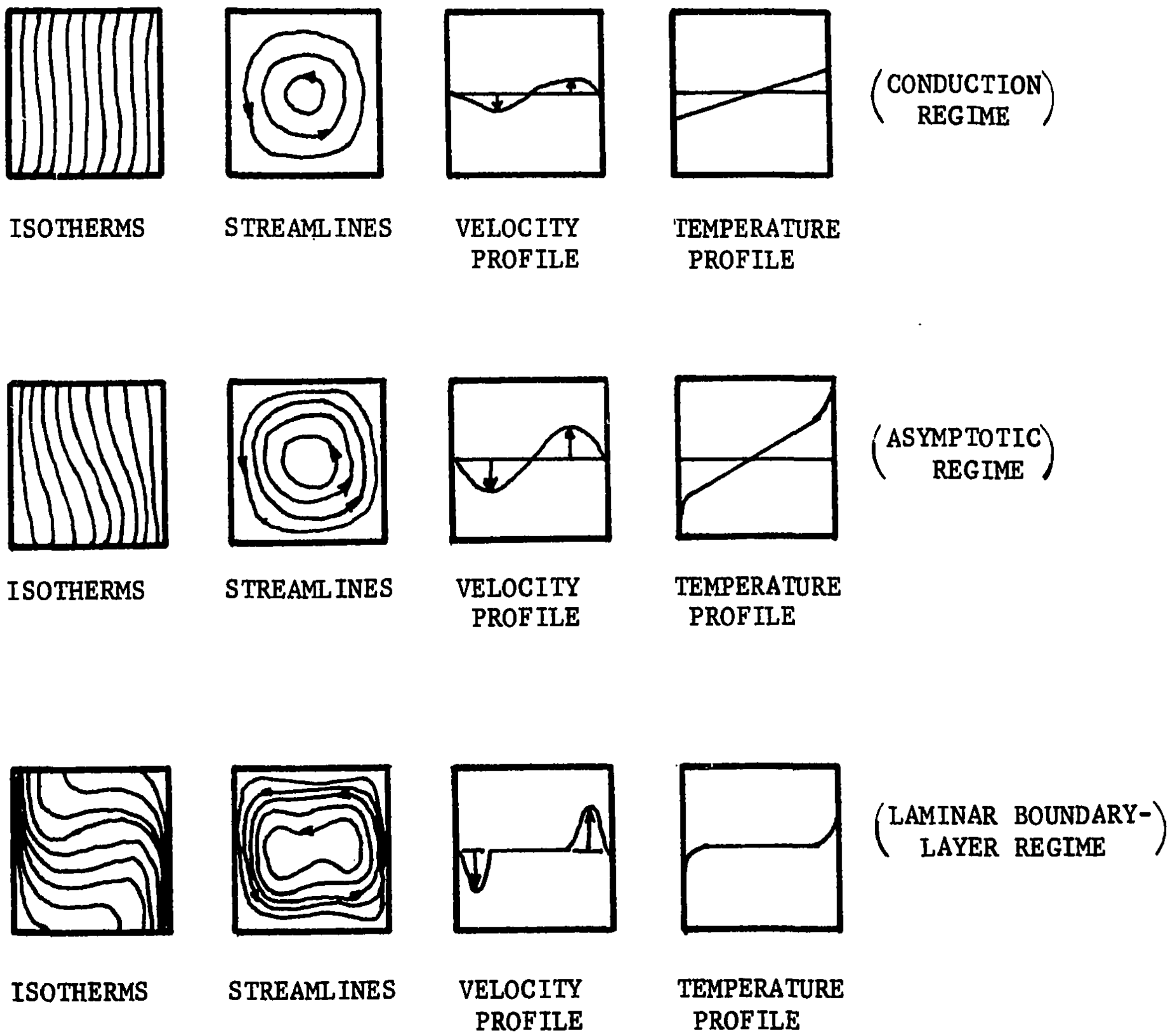

Figure 1.3. Unicellular Flow Regimes for the Enclosure Problem

which is still relatively weak. The velocity and temperature profiles are symmetrical with respect to the centerline of the enclosure. The heat transfer through the central portion of the enclosure is higher in this regime than in the conduction regime because of a larger convective contribution by the stronger circulatory flow.

In the laminar boundary layer regime the isotherms are horizontal except in the vertical wall boundary layers and in the immediate vicinity of the horizontal walls. A uniform vertical temperature gradient is established; that is, the flow in the central, or "core", region of the enclosure is thermally stratified. The heat transfer in this regime is primarily due to the convective flow in the boundary layers with an almost negligible contribution made by conduction through the core region of the fluid. Relatively large velocities occur only in the vertical wall boundary layers. The velocities in the core region are relatively small and have almost no vertical component. Unlike external flow natural convection boundary layers which only entrain fluid, the vertical wall boundary layers in the enclosure both entrain and expel fluid. Thus, the core flow provides the mechanism for feeding and draining these boundary layers.

The transition flow regime that separates the laminar and turbulent boundary layer regimes is characterized by unsteady, wavelike instabilities near the vertical walls similar to those found on a vertical plate immersed in an infinite fluid. In the core regions the isotherms are horizontal and the velocities relatively low. Finally, the turbulent boundary layer regime is qualitatively similar to the laminar boundary layer regime, although the boundary layer thicknesses are larger.

In addition to the detailed field measurements mentioned above, overall heat-transfer measurements have been made [21 -23] and are available for comparison with the results of analytical studies.

Since this work will be concerned only with an analysis of the laminar boundary layer flow regime, all further discussion will be limited to this flow regime.

A Survey of Previous Analytical Investigations

Previous analytical studies may be categorized as those employing:

1. integral methods
2. asymptotic methods
3. finite difference methods

The model of Emery and Chu [21] uses integral methods to calculate the overall rate of heat transfer across the enclosure. It predicts the experimental data with reasonable accuracy but, characteristically, yields no information on the detailed structure of the flowfield. Furthermore, the model is based upon the erroneous assumption that the structure of the flow in the vertical wall boundary layers is identical to that of the flow on a vertical flat plate in an infinite fluid. This is physically impossible since the flat plate boundary layer only entrains fluid while the boundary layer in the enclosure must both entrain and expel fluid in order to conserve mass for the entire enclosure. It must therefore be concluded that the close agreement of this model with experimental data is rather fortuitous.

Gill [13] used asymptotic methods to obtain an exact solution in the neighborhood of the enclosure centerline ($x \approx H/2$). He also found an approximate solution for the limiting case of infinite Prandtl number which is in agreement with Elder's experimental data [17]. Neither of these solutions, however, describes the entire flowfield for an arbitrary Prandtl number which is ultimately the problem of interest.

The main thrust of the research effort on the enclosure problem has been concentrated on the development of numerical solutions of the governing equations [11], [20], [24 - 28]. These studies employ various finite difference techniques to perform numerical solutions of the governing equations. They have all enjoyed some degree of success in predicting both the overall heat-transfer rate and the detailed features of the flowfield. However, limitations on computer storage space and time have prevented finite difference models from being applied to flows in the practically important high Grashof portion of the laminar boundary layer regime ($10^6 < N_{GR} < 10^9$). This is caused by the well-known fact that the boundary layer thickness decreases with increasing Grashof number which, in turn, requires an increase in the number of gridpoints needed to adequately resolve the features of the flow in the boundary layers. Noble [11] estimates that for uniform grid spacing a Grashof number of 10^6 represents a practical upper limit based on computer storage requirements and that an increase in Grashof number from 10^6 to 10^7 would double storage requirements. He does note, however, that this difficulty may be overcome to some extent by refining the grid size only near the enclosure walls and in a later paper [12] he and his colleagues have successfully applied this technique. However, as pointed out by Emmons [29], a number of serious questions exist concerning the adequacy of the convergence criteria in current use by those employing finite difference techniques. In the absence of mathematically rigorous proofs of accuracy and convergence, most numerical solutions are assumed to have "converged" because they "look good" when compared with preconceived trends in the data. Also, numerical solutions by their very nature do not readily indicate parametric trends or lend themselves to an understanding of the basic physical processes occurring in the problem. Finally, even if all the above-mentioned faults of numerical methods could somehow be resolved satisfactorily, an alternative technique would be desirable on the basis of economics alone, since the numerical methods are extremely costly in terms of programming effort and computer time.

It therefore seems apparent that the integral and finite difference methods presently being used to solve the enclosure problem have been extended to their respective limits of application and that a fresh approach is needed if further advances in both understanding and computational efficiency are to be made.

CHAPTER II

THEORETICAL DEVELOPMENT

Preliminary Remarks

The fundamental objective of this research is to systematically obtain an approximate solution for the unicellular laminar boundary layer flow regime. This will be accomplished by formulating the problem within the framework of singular perturbation theory. The decision to employ asymptotic methods is based upon the desired nature of the solution; that is, the solution should not only predict the overall rate of heat transfer across the enclosure, but should also reveal the detailed structure of the flowfield.

The Governing Equations

The flow in the enclosure is assumed to be governed by the Navier-Stokes equations as modified by the Boussinesq approximation. They are given by

$$\nabla \cdot \vec{V}^* = 0 \qquad \text{(continuity)} \tag{2.1a}$$

$$\rho_0 \frac{D\vec{V}^*}{Dt} = -(\delta\rho)\vec{g} - \nabla p^* + \mu_0 \nabla^2 \vec{V}^* \qquad \text{(momentum)} \tag{2.1b}$$

$$\frac{DT^*}{Dt} = \alpha_0 \nabla^2 T^* \qquad \text{(energy)} \tag{2.1c}$$

$$\delta\rho = -(\beta\rho_0)(T^* - T_0^*) \qquad \text{(state)} \tag{2.1d}$$

Here $\vec{V}^*$ is the velocity with components u^* and v^* in the x^* and y^* directions, respectively, ρ_0 is the reference density corresponding to some isothermal reference state at temperature T_0^*, $\vec{g}$ the acceleration of gravity, $\delta\rho$ the disturbance density, p^* the pressure, μ_0 the dynamic viscosity, T^* the temperature, α_0 the thermal diffusivity, and β the coefficient of thermal expansion.

Equations (2.1) are derived subject to the following assumptions:

1. The fluid is Newtonian and all fluid properties, except the density as it appears in the body force term, are constant.
2. Viscous dissipation is negligible.
3. The effect of pressure on density is negligible compared to that of temperature; that is, the isothermal compressibility is much smaller than the coefficient of thermal expansion.
4. The fluid is a radiatively non-participating medium.
5. The pressure, p^*, is defined as the actual pressure in the fluid, p'^*, less the static head, or

   $$p^* = p'^* - \rho_0 \Phi_g$$

   where: Φ_g is the gravitational potential, defined such that $\vec{g} = \text{grad } \Phi_g$
6. Variations in density caused by variations in temperature are small compared with the reference density, or

   $$\left|\frac{\delta\rho}{\rho_0}\right| = \left|\beta(T^* - T_0^*)\right| << 1$$

A rigorous discussion of the adequacy and limitations of these assumptions is given by Noble [11].

For the two-dimensional, steady state flow of interest, equations (2.1) may be expressed in Cartesian coordinates as follows:

$$\frac{\partial u^*}{\partial x^*} + \frac{\partial v^*}{\partial y^*} = 0 \qquad \text{(continuity)} \tag{2.2a}$$

$$u^* \frac{\partial u^*}{\partial x^*} + v^* \frac{\partial u^*}{\partial y^*} = -\frac{1}{\rho_0}\frac{\partial p^*}{\partial x^*} + (\beta g)(T^* - T_0^*) + \nu_o\left(\frac{\partial^2 u^*}{\partial x^{*2}} + \frac{\partial^2 u^*}{\partial y^{*2}}\right)$$

$$(x^*\text{-momentum}) \tag{2.2b}$$

$$u^* \frac{\partial v^*}{\partial x^*} + v^* \frac{\partial v^*}{\partial y^*} = -\frac{1}{\rho_0}\frac{\partial p^*}{\partial y^*} + \nu_0\left(\frac{\partial^2 v^*}{\partial x^{*2}} + \frac{\partial^2 v^*}{\partial y^{*2}}\right)$$

$$(y^*\text{-momentum}) \tag{2.2c}$$

$$u^* \frac{\partial T^*}{\partial x^*} + v^* \frac{\partial T^*}{\partial y^*} = \alpha_0\left(\frac{\partial^2 T^*}{\partial x^{*2}} + \frac{\partial^2 T^*}{\partial y^{*2}}\right) \qquad \text{(energy)} \tag{2.2d}$$

where the equation of state (2.1d) has been substituted in the x^*-momentum equation.

These equations are subject to the following boundary conditions:

$$u^*(x^*,0) = 0 \tag{2.3a}$$

$$v^*(x^*,0) = 0 \tag{2.3b}$$

$$T^*(x^*,0) = T_a^* \tag{2.3c}$$

$$u^*(x^*,W) = 0 \tag{2.3d}$$

$$v^*(x^*,W) = 0 \tag{2.3e}$$

$$T^*(x^*,W) = T_b^* \tag{2.3f}$$

$$u^*(H,y^*) = 0 \tag{2.3g}$$

$$v^*(H,y^*) = 0 \tag{2.3h}$$

$$\frac{\partial T^*(H,y^*)}{\partial x^*} = 0 \tag{2.3i}$$

$$u^*(0,y^*) = 0 \tag{2.3j}$$

$$v^*(0,y^*) = 0 \tag{2.3k}$$

$$\frac{\partial T^*(0,y^*)}{\partial x^*} = 0 \tag{2.3ℓ}$$

Equations (2.2) form a set of four scalar equations in the four unknowns u^*, v^*, p^*, and T^* and, therefore, along with the set of boundary conditions given by equations (2.3), constitute a mathematically "well posed" problem. Gill [13] noticed that the governing equations and their boundary conditions possess the property of remaining unaltered by a simultaneous sign change of the variables u^*, v^*, $(x^* - \frac{H}{2})$, and $(y^* - \frac{W}{2})$ when the signs of the variables p^* and $(T^* - T_0^*)$ remain unchanged. Since this is a symmetry property involving reflection of the velocity components about the geometric center of the enclosure ($x^* = H/2$, $y^* = W/2$); it is called the centro-symmetry property of the equations and boundary conditions. As will be seen later, this property plays a crucial role in obtaining the solution of the problem.

The boundary conditions on u^* and v^* merely reflect the well-known fact that the velocity of a viscous fluid, relative to a solid surface, must be identically zero at the surface. The boundary conditions on T^* and its first derivative with respect to x^* correspond to the problem definition of isothermal vertical walls and adiabatic horizontal walls, respectively. The analysis that follows will be based on the assumption that the right-hand vertical wall of the enclosure is the "hot" wall and the left-hand vertical wall is the "cold" wall; that is $T_b^* > T_a^*$.

The governing equations (2.2) and the boundary conditions will now be put in nondimensional form by introducing the following nondimensional variables

$$u \equiv \frac{u^*}{u_r} \qquad \frac{\partial p}{\partial x} \equiv \frac{\left(\frac{\partial p^*}{\partial x^*}\right)}{\left(\frac{\partial p}{\partial x}\Big|_r\right)} \qquad x \equiv \frac{x^*}{L_{rx}}$$

$$v \equiv \frac{v^*}{v_r}$$

$$T \equiv \frac{T^* - T_0^*}{T_b^* - T_a^*} = \frac{T^* - T_a^*}{\Delta T} \qquad \frac{\partial p}{\partial y} \equiv \frac{\left(\frac{\partial p^*}{\partial y^*}\right)}{\left(\frac{\partial p}{\partial y}\Big|_r\right)} \qquad y \equiv \frac{y^*}{L_{ry}}$$

where u_r, v_r, $\frac{\partial p}{\partial x}\Big|_r$, $\frac{\partial p}{\partial y}\Big|_r$, L_{rx} and L_{ry} are reference quantities that must be selected so as to correctly scale the governing equations in each region of the flowfield. Since the reference temperature, T_0^*, was set equal to the cold wall temperature, T_a^*; the nondimensional temperature, T, will vary between the limits of zero and unity everywhere in the flowfield. Therefore, the temperature scaling will remain unchanged over the entire enclosure. A reference pressure gradient is employed instead of a reference pressure since the pressure gradient represents a pressure force, which is the physically meaningful quantity in the problem. Rewriting the governing equations (2.2) and the boundary conditions (2.3) in terms of the nondimensional variables gives:

$$\left(\frac{u_r}{L_{rx}}\right)\frac{\partial u}{\partial x} + \left(\frac{v_r}{L_{ry}}\right)\frac{\partial v}{\partial y} = 0 \qquad \text{(continuity)} \qquad (2.4a)$$

$$\left(\frac{u_r^2}{L_{rx}}\right) u\frac{\partial u}{\partial x} + \left(\frac{u_r v_r}{L_{ry}}\right) v\frac{\partial u}{\partial y} = -\left(\frac{1}{\rho_0}\right)\left(\frac{\partial p}{\partial x}\bigg|_r\right)\frac{\partial p}{\partial x} + (\beta g \Delta T)T + \left(\frac{\nu_0 u_r}{L_{rx}^2}\right)\frac{\partial^2 u}{\partial x^2} +$$

$$+ \left(\frac{\nu_0 u_r}{L_{ry}^2}\right)\frac{\partial^2 u}{\partial y^2} \qquad \text{(x-momentum)} \qquad (2.4b)$$

$$\left(\frac{u_r v_r}{L_{rx}}\right) u\frac{\partial v}{\partial x} + \left(\frac{v_r^2}{L_{ry}}\right) v\frac{\partial v}{\partial y} = -\left(\frac{1}{\rho_0}\right)\left(\frac{\partial p}{\partial y}\bigg|_r\right)\frac{\partial p}{\partial y} + \left(\frac{\nu_0 v_r}{L_{rx}^2}\right)\frac{\partial^2 v}{\partial x^2} + \left(\frac{\nu_0 v_r}{L_{ry}^2}\right)\frac{\partial^2 v}{\partial y^2}$$

$$\text{(y-momentum)} \qquad (2.4c)$$

$$\left(\frac{u_r}{L_{rx}}\right) u\frac{\partial T}{\partial x} + \left(\frac{v_r}{L_{ry}}\right) v\frac{\partial T}{\partial y} = \left(\frac{\alpha_0}{L_{rx}^2}\right)\frac{\partial^2 T}{\partial x^2} + \left(\frac{\alpha_0}{L_{ry}^2}\right)\frac{\partial^2 T}{\partial y^2} \qquad \text{(energy)} \qquad (2.4d)$$

$$u(x,0) = 0 \qquad (2.5a)$$

$$v(x,0) = 0 \qquad (2.5b)$$

$$T(x,0) = 0 \qquad (2.5c)$$

$$u\left(x,\frac{W}{L_{ry}}\right) = 0 \qquad (2.5d)$$

$$v\left(x,\frac{W}{L_{ry}}\right) = 0 \qquad (2.5e)$$

$$T\left(x,\frac{W}{L_{ry}}\right) = 1 \qquad (2.5f)$$

$$u\left(\frac{H}{L_{rx}},y\right) = 0 \qquad (2.5g)$$

$$v\left(\frac{H}{L_{rx}},y\right) = 0 \qquad (2.5h)$$

$$\frac{\partial T\,(\frac{H}{L_{rx}},y)}{\partial x} = 0 \qquad (2.5i)$$

$$u(0,y) = 0 \qquad (2.5j)$$

$$v(0,y) = 0 \qquad (2.5k)$$

$$\frac{\partial T(0,y)}{\partial x} = 0 \qquad (2.5\ell)$$

Scaling of the Governing Equations

The analytical and experimental results of previous investigations indicate that for the laminar boundary layer flow regime the flowfield may be divided into nine separate and physically distinct regions as shown in Figure 2.1. These regions may be grouped in the following manner:

(1) the "core" region - (region 5)

(2) the vertical wall boundary layers - (regions 4 and 6)

(3) the horizontal wall boundary layers - (regions 2 and 8)

(4) the corner regions - (regions 1, 3, 7 and 9)

Because of the centro-symmetry property of the governing equations their solutions do not have to be obtained in all nine regions of the flowfield. It will be shown that only the solutions in the core, two corners, one vertical wall boundary layer, and both horizontal wall boundary layers must be evaluated to determine all of the unknown constants and functions in the problem. Regions 2 (the top horizontal wall boundary layer), 3 (the top right-hand corner), 5 (core), 6 (right-hand vertical wall boundary layer), 8 (bottom horizontal wall boundary layer), and 9 (bottom right-hand corner) were

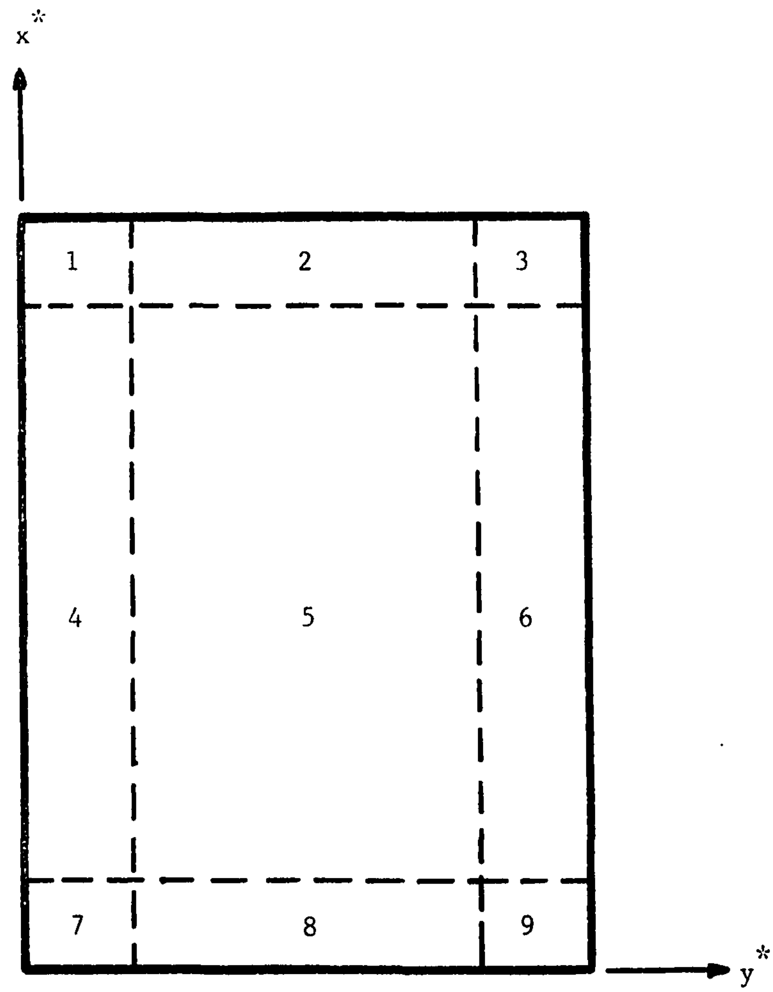

Figure 2.1. Physically Distinct Regions in the Flowfield for the Laminar Boundary-Layer Flow Regime

chosen for this purpose. Any variable of interest, Q, in these regions will be denoted by the symbols shown in Figure 2.2.

The vertical wall boundary layer will be scaled first, followed by the horizontal wall boundary layers. Several assumptions must be made to scale these regions. These assumptions dictate all of the reference quantities in the core region (with the sole exception of the length scales, taken to be the overall dimensions of the enclosure). Thus, the validity of the assumptions made in scaling the vertical and horizontal wall boundary layers may be verified by comparing the resulting core solution with experimental data and numerical solutions. Finally, the scaling will be done for the corner regions.

Scaling of the (Right-Hand) Vertical Wall Boundary Layer Equations

Experimental evidence indicates that distinct natural convection boundary layers are formed on the vertical walls of the enclosure when the Grashof number is greater than about 10^4. This empirical fact is used as a starting point for the analysis. Assume that

$$\tilde{L}_{rx} = H \tag{2.6}$$

$$\tilde{L}_{ry} = \tilde{\delta} \tag{2.7}$$

where: $\tilde{\delta} \equiv$ characteristic vertical wall boundary layer thickness

so that: $H >> \tilde{\delta}$

Thus, the spatial coordinates are given by:

$$\tilde{x} = \frac{x^*}{\tilde{L}_{rx}} = \frac{x^*}{H} \tag{2.8}$$

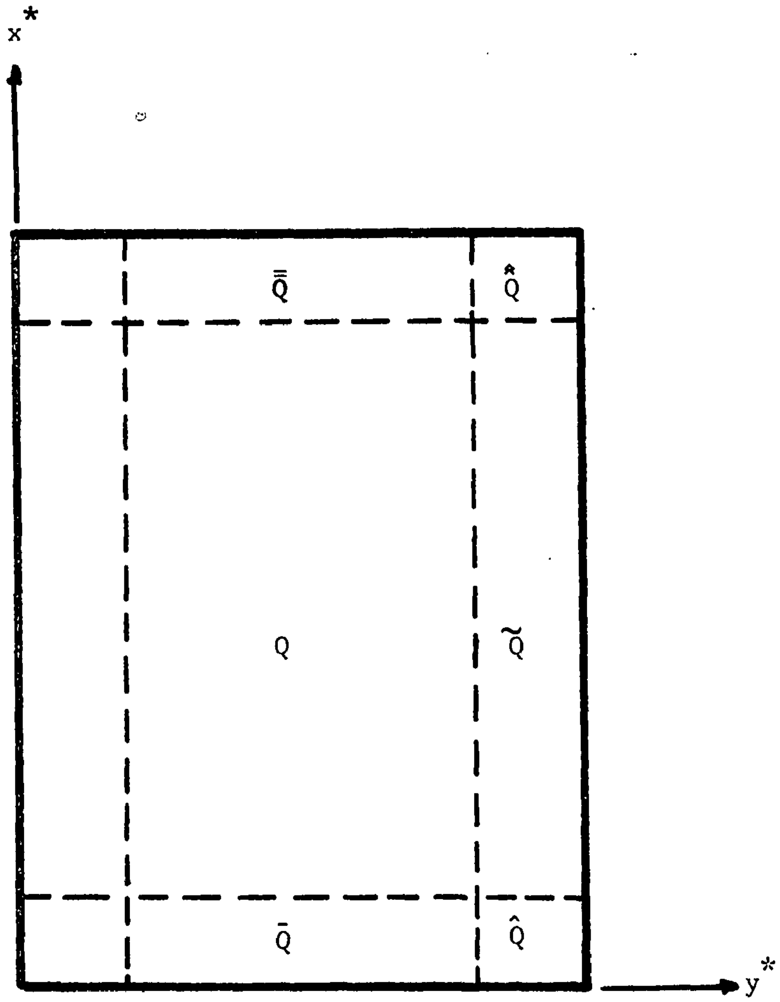

Figure 2.2. Symbols Denoting the Region of Applicability Of Any Variable of Interest, Q

$$\tilde{y} = \frac{W^{o} - y^{*}}{\tilde{L}_{ry}} = \frac{W - y^{*}}{\tilde{\delta}} \tag{2.9}$$

The continuity equation (2.4a) may now be written as:

$$\frac{\partial \tilde{u}}{\partial \tilde{x}} + \left(\frac{\tilde{v}_r H}{\tilde{u}_r \tilde{\delta}}\right) \frac{\partial \tilde{v}}{\partial \tilde{y}} = 0 \tag{2.10}$$

However, in the vertical wall boundary layer both terms in the continuity equation must be of the same order. This may be proven in the following manner. First, suppose that $\left(\frac{\tilde{v}_r H}{\tilde{u}_r \delta}\right) >> 1$. Then, to lowest order, the continuity equation would reduce to

$$\frac{\partial \tilde{v}}{\partial \tilde{y}} = 0$$

so that

$$\tilde{v} = \tilde{v}(\tilde{x}) \text{ only.}$$

But, $\tilde{v} = 0$ at $\tilde{y} = 0$ because there is no flow through a solid surface. Also, $\tilde{v}$ is nonzero as $\tilde{y} \to \infty$ so the boundary layer can entrain or expel fluid. Thus, $\tilde{v}$ must be a function of $\tilde{y}$ as well as $\tilde{x}$ and it is impossible for $\left(\frac{\tilde{v}_r H}{\tilde{u}_r \tilde{\delta}}\right)$ to be $>> 1$. Conversely, if it is assumed that $\left(\frac{\tilde{v}_r H}{\tilde{u}_r \delta}\right) << 1$, the continuity equation, to lowest order, would reduce to

$$\frac{\partial \tilde{u}}{\partial \tilde{x}} = 0$$

so that $\tilde{u} = \tilde{u}(\tilde{y})$ only.

But, since $\tilde{u} = 0$ at $\tilde{x} = 0$ and at $\tilde{x} = 1$ and has some maximum value in between, $\tilde{u}$ must also be a function of $\tilde{x}$ as well as $\tilde{y}$ and it is impossible for $\left(\frac{\tilde{v}_r H}{\tilde{u}_r \tilde{\delta}}\right)$ to be $<< 1$. Therefore,

$$\frac{\tilde{v}_r H}{\tilde{u}_r \tilde{\delta}} = 1 \tag{2.11}$$

Substituting equations (2.6), (2.7), and (2.11) in the $\tilde{x}$-momentum equation (2.4b) yields:

$$\left(\frac{\tilde{u}_r^2}{H}\right)\left(\tilde{u}\frac{\partial\tilde{u}}{\partial\tilde{x}} + \tilde{v}\frac{\partial\tilde{u}}{\partial\tilde{y}}\right) = -\left(\frac{1}{\rho_0}\right)\left(\frac{\partial\tilde{p}}{\partial\tilde{x}}\bigg|_r\right)\frac{\partial\tilde{p}}{\partial\tilde{x}} + (\beta g \Delta T)\tilde{T}$$

$$+\left[\frac{\nu_0\tilde{u}_r}{\tilde{\delta}^2}\right]\left[\left(\frac{\tilde{\delta}}{H}\right)^2\frac{\partial^2\tilde{u}}{\partial\tilde{x}^2} + \frac{\partial^2\tilde{u}}{\partial\tilde{y}^2}\right] \tag{2.12}$$

It is now assumed that an inertia force-viscous force-buoyancy force balance holds in the vertical wall boundary layers. This gives

$$\left(\frac{\tilde{u}_r^2}{H}\right) = (\beta g \Delta T) = \left(\frac{\nu_0\tilde{u}_r}{\tilde{\delta}^2}\right) \tag{2.13}$$

Thus,

$$\tilde{u}_r = \left(\frac{\nu_0}{H}\right) N_{GR}^{\frac{1}{2}} \tag{2.14}$$

and,

$$\frac{\tilde{\delta}}{H} = N_{GR}^{-\frac{1}{4}} \tag{2.15}$$

where N_{GR}, the Grashof number is given by

$$N_{GR} \equiv \left(\frac{\beta g \Delta T H^3}{\nu_0^2}\right) \tag{2.16}$$

and represents a characteristic ratio of buoyant forces to viscous forces in the problem. Therefore, the scaling for the vertical wall boundary layer thickness is identical to the well-known result for external flow laminar natural convection boundary layers. Equation (2.11) now gives:

$$\tilde{v}_r = \left(\frac{\nu_0}{H}\right) N_{GR}^{\frac{1}{4}} \tag{2.17}$$

The pressure gradient (pressure force) in the vertical wall boundary layer is not an applied pressure gradient such as those which occur in forced convection flows. Therefore, the pressure force plays a passive role in the dynamics; that is, the pressure gradient will adjust itself as it "needs to do" in order to satisfy the dynamics of the flow. Thus;

$$\left(\frac{1}{\rho_0}\right)\left(\frac{\partial\tilde{p}}{\partial\tilde{x}}\Big|_r\right) = \frac{\tilde{u}_r^2}{H} \tag{2.18}$$

Substituting equation (2.14) in equation (2.18) gives:

$$\frac{\partial\tilde{p}}{\partial\tilde{x}}\Big|_r = \left(\frac{\rho_0\nu_0^2}{H^3}\right) N_{GR} \tag{2.19}$$

then;

$$\frac{\partial\tilde{p}}{\partial\tilde{y}}\Big|_r = \left(\frac{\tilde{L}_{rx}}{\tilde{L}_{ry}}\right)\left(\frac{\partial\tilde{p}}{\partial\tilde{x}}\Big|_r\right) = \left(\frac{\rho_0\nu_0^2}{H^3}\right) N_{GR}^{5/4} \tag{2.20}$$

All of the reference quantities for the vertical wall boundary layers are now known. Substituting these quantities in the governing equations (2.4) and the boundary conditions (2.5d, e, f) yields

$$\frac{\partial\tilde{u}}{\partial\tilde{x}} + \frac{\partial\tilde{v}}{\partial\tilde{y}} = 0 \tag{2.21a}$$

$$\tilde{u}\frac{\partial\tilde{u}}{\partial\tilde{x}} + \tilde{v}\frac{\partial\tilde{u}}{\partial\tilde{y}} = -\frac{\partial\tilde{p}}{\partial\tilde{x}} + \tilde{T} + \left(N_{GR}^{-\frac{1}{2}}\right)\frac{\partial^2\tilde{u}}{\partial\tilde{x}^2} + \frac{\partial^2\tilde{u}}{\partial\tilde{y}^2} \tag{2.21b}$$

$$\left(N_{GR}^{-\frac{1}{2}}\right)\left(\tilde{u}\frac{\partial \tilde{v}}{\partial \tilde{x}} + \tilde{v}\frac{\partial \tilde{v}}{\partial \tilde{y}}\right) = -\frac{\partial \tilde{p}}{\partial \tilde{y}} + \left(N_{GR}^{-1}\right)\frac{\partial^2 \tilde{v}}{\partial \tilde{x}^2} + \left(N_{GR}^{-\frac{1}{2}}\right)\frac{\partial^2 \tilde{v}}{\partial \tilde{y}^2} \tag{2.21c}$$

$$\tilde{u}\frac{\partial \tilde{T}}{\partial \tilde{x}} + \tilde{v}\frac{\partial \tilde{T}}{\partial \tilde{y}} = \left[\frac{1}{N_{PR}}\right]\left[\left(N_{GR}^{-\frac{1}{2}}\right)\frac{\partial^2 \tilde{T}}{\partial \tilde{x}^2} + \frac{\partial^2 \tilde{T}}{\partial \tilde{y}^2}\right] \tag{2.21d}$$

and,

$$\tilde{u}(\tilde{x},0) = 0 \tag{2.22a}$$

$$\tilde{v}(\tilde{x},0) = 0 \tag{2.22b}$$

$$\tilde{T}(\tilde{x},0) = 1 \tag{2.22c}$$

where the Prandtl number, N_{PR}, is given by

$$N_{PR} \equiv \frac{\nu_0}{\alpha_0} \tag{2.23}$$

and gives the ratio of the diffusivity of momentum to the diffusivity of thermal energy. The Prandtl number is now assumed to be O(1). If the Prandtl number is $>>$ O(1), the vertical wall boundary layers must be rescaled as suggested by Eichhorn [30] since the inertia - viscous - buoyancy force balance would no longer hold across both the momentum and thermal boundary layers. For a Prandtl number much less than order unity, the thermal boundary layer is much thicker than the momentum boundary layer. Then the inertia forces are no longer of the same order as the buoyancy forces in the outer part of the thermal boundary layer. If, however, the Prandtl number is much greater than order unity, the momentum boundary layer is much thicker than the thermal boundary layer. In this case the buoyancy forces are not the same order as the inertia and viscous forces in the outer part of the momentum boundary layer.

The small parameter, ϵ, is now defined as:

$$\epsilon = N_{GR}^{-1/8}$$

This value of the small parameter was chosen because it is the only value that yields expansions in integral powers of ϵ in all regions of the flowfield.

Rewriting equations (2.21) in terms of the small parameter, ϵ, gives:

$$\frac{\partial \tilde{u}}{\partial \tilde{x}} + \frac{\partial \tilde{v}}{\partial \tilde{y}} = 0 \tag{2.24a}$$

$$\tilde{u}\frac{\partial \tilde{u}}{\partial \tilde{x}} + \tilde{v}\frac{\partial \tilde{u}}{\partial \tilde{x}} = -\frac{\partial \tilde{p}}{\partial \tilde{x}} + \tilde{T} + \epsilon^4 \frac{\partial^2 \tilde{u}}{\partial \tilde{x}^2} + \frac{\partial^2 \tilde{u}}{\partial \tilde{y}^2} \tag{2.24b}$$

$$\epsilon^4\left(\tilde{u}\frac{\partial \tilde{v}}{\partial \tilde{x}} + \tilde{v}\frac{\partial \tilde{v}}{\partial \tilde{y}}\right) = -\frac{\partial \tilde{p}}{\partial \tilde{y}} + \epsilon^8 \frac{\partial^2 \tilde{v}}{\partial \tilde{x}^2} + \epsilon^4 \frac{\partial^2 \tilde{v}}{\partial \tilde{y}^2} \tag{2.24c}$$

$$\left(N_{PR}\right)\left(\tilde{u}\frac{\partial \tilde{T}}{\partial \tilde{x}} + \tilde{v}\frac{\partial \tilde{T}}{\partial \tilde{y}}\right) = \epsilon^4 \frac{\partial^2 \tilde{T}}{\partial \tilde{x}^2} + \frac{\partial^2 \tilde{T}}{\partial \tilde{y}^2} \tag{2.24d}$$

The following expansions in integral powers of the small parameter, ϵ, are assumed for the dependent variables:

$$\tilde{u}(\tilde{x},\tilde{y}) \sim \tilde{u}_0(\tilde{x},\tilde{y}) + \epsilon\,\tilde{u}_1(\tilde{x},\tilde{y}) + \epsilon^2\tilde{u}_2(\tilde{x},\tilde{y}) + \ldots \text{ (as } \epsilon \to 0) \tag{2.25a}$$

$$\tilde{v}(\tilde{x},\tilde{y}) \sim \tilde{v}_0(\tilde{x},\tilde{y}) + \epsilon\,\tilde{v}_1(\tilde{x},\tilde{y}) + \epsilon^2\tilde{v}_2(\tilde{x},\tilde{y}) + \ldots \text{ (as } \epsilon \to 0) \tag{2.25b}$$

$$\tilde{p}(\tilde{x},\tilde{y}) \sim \tilde{p}_0(\tilde{x},\tilde{y}) + \epsilon\,\tilde{p}_1(\tilde{x},\tilde{y}) + \epsilon^2\tilde{p}_2(\tilde{x},\tilde{y}) + \ldots \text{ (as } \epsilon \to 0) \tag{2.25c}$$

$$\tilde{T}(\tilde{x},\tilde{y}) \sim \tilde{T}_0(\tilde{x},\tilde{y}) + \epsilon\,\tilde{T}_1(\tilde{x},\tilde{y}) + \epsilon^2\tilde{T}_2(\tilde{x},\tilde{y}) + \ldots \text{ (as } \epsilon \to 0) \tag{2.25d}$$

Substituting these expansions into equations (2.24) and the boundary conditions (2.22), gathering terms of like powers of ϵ, and noting that in order for this result to hold for arbitrary values of ϵ all of the coefficients must identically vanish, gives an infinite number of sets of governing equations and boundary conditions for the various order problems. Only the zeroth-order set of equations and boundary conditions is given here:

$$\frac{\partial \tilde{u}_0}{\partial \tilde{x}} + \frac{\partial \tilde{v}_0}{\partial \tilde{y}} = 0 \tag{2.26a}$$

$$\tilde{u}_0 \frac{\partial \tilde{u}_0}{\partial \tilde{x}} + \tilde{v}_0 \frac{\partial \tilde{u}_0}{\partial \tilde{y}} = - \frac{\partial \tilde{p}_0}{\partial \tilde{x}} + \tilde{T}_0 + \frac{\partial^2 \tilde{u}_0}{\partial \tilde{y}^2} \tag{2.26b}$$

$$\frac{\partial \tilde{p}_0}{\partial \tilde{y}} = 0 \tag{2.26c}$$

$$\left(N_{PR}\right)\left(\tilde{u}_0 \frac{\partial \tilde{T}_0}{\partial \tilde{x}} + \tilde{v}_0 \frac{\partial \tilde{T}_0}{\partial \tilde{y}}\right) = \frac{\partial^2 \tilde{T}_0}{\partial \tilde{y}^2} \tag{2.26d}$$

with,

$$\tilde{u}_0(\tilde{x},0) = 0 \tag{2.27a}$$

$$\tilde{v}_0(\tilde{x},0) = 0 \tag{2.27b}$$

$$\tilde{T}_0(\tilde{x},0) = 1 \tag{2.27c}$$

(plus matching conditions with core and corner regions)

The zeroth-order equations (2.26) for the vertical wall boundary layers form a second-order system of nonlinear, parabolic, partial differential equations. It will be shown that the solutions of these equations must be matched to a flow with a linear temperature profile in the core region. Cheesewright [31], however, has shown that similarity transforms cannot be obtained for this case. Thus, the vertical wall boundary layer equations are <u>nonsimilar</u> which substantially increases the difficulty of their solution.

The governing equations and boundary conditions for the first- and second-order problems are given in Appendix A.

Scaling of the (Bottom) Horizontal Wall Boundary-Layer Equations

A careful study of the flow in the enclosure reveals that the flow in the core region is the only available mechanism for feeding and draining the boundary layers on the vertical walls. Thus, the horizontal reference velocities in these two regions must be identical, or

$$v_r = \tilde{v}_r = \left(\frac{\nu_0}{H}\right) N_{GR}^{\frac{1}{4}} = \left(\frac{\nu_0}{\epsilon^2 H}\right) \tag{2.28}$$

Further examination of experimental and numerical results shows that the flows in the vicinity of the horizontal walls exert only a small effect on the entire flowfield and serve mainly to provide transition regions from the core flow to the zero relative velocity and adiabatic wall boundary conditions at the horizontal walls. Therefore, the horizontal reference velocities in the core and the horizontal wall boundary layers are equal, or

$$\bar{v}_r = v_r = \left(\frac{\nu_0}{\epsilon^2 H}\right) \tag{2.29}$$

The reference length parallel to the horizontal walls is the width of the enclosure, or

$$\bar{L}_{ry} = W \tag{2.30}$$

and the reference length perpendicular to these walls is the horizontal wall boundary layer thickness. Thus;

$$\bar{L}_{rx} = \bar{\Delta} \tag{2.31}$$

where:

$\bar{\Delta} \equiv$ characteristic horizontal wall boundary layer thickness

so that: $W >> \bar{\Delta}$

Therefore, the spatial coordinates for the (bottom) horizontal wall boundary layer are

$$\bar{x} = \frac{x^*}{\bar{L}_{rx}} = \frac{x^*}{\bar{\Delta}} \tag{2.32}$$

$$\bar{y} = \frac{y^*}{\bar{L}_{ry}} = \frac{y^*}{W} \tag{2.33}$$

The reference pressure gradient parallel to the horizontal walls is assumed to be the same as the reference pressure gradient in the core region parallel to the horizontal walls, or

$$\left.\frac{\partial \bar{p}}{\partial \bar{y}}\right|_r = \left.\frac{\partial p}{\partial y}\right|_r \tag{2.34}$$

But, since the vertical pressure gradient in the core region is "impressed" on the vertical wall boundary layers, as shown by equation (2.26c); it follows that

$$\left.\frac{\partial p}{\partial x}\right|_r = \left.\frac{\partial \tilde{p}}{\partial \tilde{x}}\right|_r \tag{2.35}$$

or,

$$\left.\frac{\partial p}{\partial x}\right|_r = \left(\frac{\rho_0 \nu_0^2}{H^3}\right) N_{GR} = \left(\frac{\rho_0 \nu_0^2}{\epsilon^8 H^3}\right) \tag{2.36}$$

The length scales in the core region are the enclosure dimensions, or:

$$L_{rx} = H \tag{2.37}$$

$$L_{ry} = W \tag{2.38}$$

then,

$$\left.\frac{\partial p}{\partial y}\right|_r = \left(\frac{L_{rx}}{L_{ry}}\right)\left(\left.\frac{\partial p}{\partial x}\right|_r\right) = \left(\frac{\rho_0 \nu_0^2}{H^2 W}\right) N_{GR} = \left(\frac{\rho_0 \nu_0^2}{\epsilon^8 H^2 W}\right) \tag{2.39}$$

Equation (2.34) now gives:

$$\left.\frac{\partial \bar{p}}{\partial \bar{y}}\right|_r = \left(\frac{\rho_0 \nu_0^2}{H^2 W}\right) N_{GR} = \left(\frac{\rho_0 \nu_0^2}{\epsilon^8 H^2 W}\right) \tag{2.40}$$

then,

$$\left.\frac{\partial \bar{p}}{\partial \bar{x}}\right|_r = \left(\frac{\bar{L}_{ry}}{\bar{L}_{rx}}\right)\left(\left.\frac{\partial \bar{p}}{\partial \bar{y}}\right|_r\right) = \left(\frac{\rho_0 \nu_0^2}{H^2 \bar{\Delta}}\right) N_{GR} = \left(\frac{\rho_0 \nu_0^2}{\epsilon^8 H^2 \bar{\Delta}}\right) \tag{2.41}$$

The continuity equation (2.4a) may be written as:

$$\frac{\partial \bar{u}}{\partial \bar{x}} + \left(\frac{\bar{L}_{rx} \bar{v}_r}{\bar{L}_{ry} \bar{u}_r}\right) \frac{\partial \bar{v}}{\partial \bar{y}} = 0 \tag{2.42}$$

Arguments similar to those used for the vertical wall boundary layers show that both terms in this equation must be of the same order. Therefore,

$$\frac{\bar{L}_{rx} \bar{v}_r}{\bar{L}_{ry} \bar{u}_r} = 1 \tag{2.43}$$

so that:

$$\bar{u}_r = \left(\frac{\bar{L}_{rx}}{\bar{L}_{ry}}\right) \bar{v}_r \tag{2.44}$$

Substituting equations (2.29), (2.30), and (2.31) in equation (2.44) gives:

$$\bar{u}_r = \left(\frac{\bar{\Delta}\, \nu_0}{HW}\right) N_{GR}^{\frac{1}{2}} = \left(\frac{\bar{\Delta}\, \nu_0}{\epsilon^2 HW}\right) \tag{2.45}$$

All of the reference quantities with the exception of $\bar{\Delta}$, the length scale perpendicular to the horizontal walls, are now known. The characteristic boundary layer thickness, $\bar{\Delta}$, will be determined by considering all of the possible force balances in the $\bar{y}$-momentum equation (2.4c). Writing this equation in terms of the reference quantities gives:

$$\left(N_{GR}^{\frac{1}{2}}\right)\left(\bar{u}\,\frac{\partial \bar{v}}{\partial \bar{x}} + \bar{v}\,\frac{\partial \bar{v}}{\partial \bar{y}}\right) = -\left(N_{GR}\right)\frac{\partial \bar{p}}{\partial \bar{y}} + \left(N_{GR}^{\frac{1}{2}}\right)\left(\frac{HW}{\bar{\Delta}^2}\right)\left(\frac{\partial^2 \bar{v}}{\partial \bar{x}^2} + \left(\frac{\bar{\Delta}}{W}\right)^2 \frac{\partial^2 \bar{v}}{\partial \bar{y}^2}\right) \tag{2.46}$$

There are, in general, four possible force balances in this equation:

1. inertia - pressure - viscous force balance
2. inertia - pressure force balance
3. inertia - viscous force balance
4. pressure - viscous force balance

Cases 1 and 2 may be rejected immediately because the inertia force and pressure force terms are obviously not of the same order. The balance in case 3 cannot be obtained since the pressure force term has the largest coefficient. Thus, the pressure force - viscous force balance of case 4 is the only possible balance. Equating the coefficients of the pressure force and viscous force terms in equation (2.46) gives

$$N_{GR} = \left(\frac{HW}{\bar{\Delta}^2}\right) N_{GR}^{\frac{1}{2}} = \left(\frac{HW}{\epsilon^2 \bar{\Delta}^2}\right) \tag{2.47}$$

or,

$$\frac{\bar{\Delta}}{W} = \left(\frac{H}{W}\right)^{\frac{1}{2}} N_{GR}^{-3/8} = \epsilon^3\left(\frac{H}{W}\right)^{\frac{1}{2}} \tag{2.48}$$

where $\left(\frac{H}{W}\right)$, <u>the aspect ratio of the enclosure</u>, <u>is assumed to be of order unity</u>. Equations (2.15) and (2.48) give

$$\frac{\bar{\Delta}}{\tilde{\delta}} = \epsilon \left(\frac{W}{H}\right)^{\frac{1}{2}}$$

that is, the horizontal wall boundary layers are much thinner than the vertical wall boundary layers. This agrees with the previously mentioned observation that the flows in the vicinity of the horizontal walls exert only a small effect on the entire flowfield and serve mainly to provide transition regions from the core flow to the zero relative velocity and adiabatic wall boundary conditions at the horizontal walls. Equation (2.45) now gives:

$$\bar{u}_r = \left(\frac{\nu_0}{H}\right)\left(\frac{H}{W}\right)^{\frac{1}{2}} N_{GR}^{-1/8} = \epsilon \left(\frac{\nu_0}{H}\right)\left(\frac{H}{W}\right)^{\frac{1}{2}} \qquad (2.49)$$

all of the reference quantities for the horizontal wall boundary layers are now known. Substituting these quantities in the governing equation (2.4) and the boundary conditions (2.5j, k, ℓ) yields:

$$\frac{\partial \bar{u}}{\partial \bar{x}} + \frac{\partial \bar{v}}{\partial \bar{y}} = 0 \qquad (2.50a)$$

$$\epsilon^{10}\left(\frac{H}{W}\right)^2\left(\bar{u}\frac{\partial \bar{u}}{\partial \bar{x}} + \bar{v}\frac{\partial \bar{u}}{\partial \bar{y}}\right) = -\left(\frac{H}{W}\right)\frac{\partial \bar{p}}{\partial \bar{x}} + \epsilon^3 \bar{T} + \epsilon^6\left(\frac{H}{W}\right)^2\frac{\partial^2 \bar{u}}{\partial \bar{x}^2} + \epsilon^{12}\left(\frac{H}{W}\right)^3\frac{\partial^2 \bar{u}}{\partial \bar{y}^2} \qquad (2.50b)$$

$$\epsilon^4\left(\bar{u}\frac{\partial \bar{v}}{\partial \bar{x}} + \bar{v}\frac{\partial \bar{v}}{\partial \bar{y}}\right) = -\frac{\partial \bar{p}}{\partial \bar{y}} + \frac{\partial^2 \bar{v}}{\partial \bar{x}^2} + \epsilon^6\left(\frac{H}{W}\right)\frac{\partial^2 \bar{v}}{\partial \bar{y}^2} \qquad (2.50c)$$

$$\epsilon^4\left(N_{PR}\right)\left(\bar{u}\frac{\partial \bar{T}}{\partial \bar{x}} + \bar{v}\frac{\partial \bar{T}}{\partial \bar{y}}\right) = \frac{\partial^2 \bar{T}}{\partial \bar{x}^2} + \epsilon^6\left(\frac{H}{W}\right)\frac{\partial^2 \bar{T}}{\partial \bar{y}^2} \qquad (2.50d)$$

and,

$$\bar{u}(0,\bar{y}) = 0 \qquad (2.51a)$$

$$\bar{v}(0,\bar{y}) = 0 \qquad (2.51b)$$

$$\frac{\partial \bar{T}(0,\bar{y})}{\partial \bar{x}} = 0 \qquad (2.51c)$$

where the pressure force - viscous force balance is obtained in the $\bar{y}$-momentum equation (2.50c).

The following expansions are assumed for the dependent variables:

$$\bar{u}(\bar{x},\bar{y}) \sim \bar{u}_0(\bar{x},\bar{y}) + \epsilon\,\bar{u}_1(\bar{x},\bar{y}) + \epsilon^2\bar{u}_2(\bar{x},\bar{y}) + \ldots \quad (\text{as } \epsilon \to 0) \quad (2.52a)$$

$$\bar{v}(\bar{x},\bar{y}) \sim \bar{v}_0(\bar{x},\bar{y}) + \epsilon\,\bar{v}_1(\bar{x},\bar{y}) + \epsilon^2\bar{v}_2(\bar{x},\bar{y}) + \ldots \quad (\text{as } \epsilon \to 0) \quad (2.52b)$$

$$\bar{p}(\bar{x},\bar{y}) \sim \bar{p}_0(\bar{x},\bar{y}) + \epsilon\,\bar{p}_1(\bar{x},\bar{y}) + \epsilon^2\bar{p}_2(\bar{x},\bar{y}) + \ldots \quad (\text{as } \epsilon \to 0) \quad (2.52c)$$

$$\bar{T}(\bar{x},\bar{y}) \sim \bar{T}_0(\bar{x},\bar{y}) + \epsilon\,\bar{T}_1(\bar{x},\bar{y}) + \epsilon^2\bar{T}_2(\bar{x},\bar{y}) + \ldots \quad (\text{as } \epsilon \to 0) \quad (2.52d)$$

Substituting these expansions into equations (2.50) and the boundary conditions (2.51), gathering terms of like powers of ϵ, and noting that in order for this result to hold for arbitrary values of ϵ all of the coefficients must identically vanish, gives an infinite number of sets of governing equations and boundary conditions for the various order problems. Only the zeroth-order set of equations and boundary conditions are given here:

$$\frac{\partial \bar{u}_0}{\partial \bar{x}} + \frac{\partial \bar{v}_0}{\partial \bar{y}} = 0 \qquad (2.53a)$$

$$\frac{\partial \bar{p}_0}{\partial \bar{x}} = 0 \qquad (2.53b)$$

$$\frac{\partial \bar{p}_0}{\partial \bar{y}} = \frac{\partial^2 \bar{v}_0}{\partial \bar{x}^2} \qquad (2.53c)$$

$$\frac{\partial^2 \bar{T}_0}{\partial \bar{x}^2} = 0 \qquad (2.53d)$$

and,

$$\bar{u}_0(0,\bar{y}) = 0 \qquad (2.54a)$$

$$\bar{v}_0(0,\bar{y}) = 0 \qquad (2.54b)$$

$$\frac{\partial \bar{T}_0(0,\bar{y})}{\partial \bar{x}} = 0 \qquad (2.54c)$$

(plus matching conditions with core and corner regions)

The zeroth-order equations (2.53) and boundary conditions (2.54) for the horizontal wall boundary layer are linear. Their exact solutions will be obtained later in the analysis. The governing equations and their boundary conditions for the first- and second-order problems are given in Appendix A.

In a similar manner, the zeroth-order set of governing equations and boundary conditions for the top horizontal wall boundary layer are found to be:

$$\frac{\partial \bar{\bar{u}}_0}{\partial \bar{\bar{x}}} + \frac{\partial \bar{\bar{v}}_0}{\partial \bar{\bar{y}}} \qquad (2.55a)$$

$$\frac{\partial \bar{\bar{p}}_0}{\partial \bar{\bar{x}}} = 0 \qquad (2.55b)$$

$$\frac{\partial \bar{\bar{p}}_0}{\partial \bar{\bar{y}}} = \frac{\partial^2 \bar{\bar{v}}_0}{\partial \bar{\bar{x}}^2} \qquad (2.55c)$$

$$\frac{\partial^2 \bar{\bar{T}}_0}{\partial \bar{\bar{x}}^2} = 0 \qquad (2.55d)$$

and, $\bar{\bar{u}}_0(0,\bar{\bar{y}}) = 0 \qquad (2.56a)$

$$\bar{\bar{v}}_0(0,\bar{\bar{y}}) = 0 \qquad (2.56b)$$

$$\frac{\partial \bar{\bar{T}}_0(0,\bar{\bar{y}})}{\partial \bar{\bar{x}}} = 0 \qquad (2.56c)$$

(plus matching conditions with core and corner regions) where the spatial coordinates for the top horizontal wall boundary layer are given by:

$$\bar{\bar{x}} = \frac{H - x^*}{\bar{L}_{rx}} = \frac{H - x^*}{\epsilon^3 (HW)^{\frac{1}{2}}} \tag{2.57}$$

$$\bar{\bar{y}} = \frac{y^*}{\bar{\bar{L}}_{ry}} = \frac{y^*}{W} \tag{2.58}$$

Scaling of the Governing Equations for the Core Region

Several early investigators of the enclosure problem, such as Batchelor [32] and Pillow [33], assumed that the core is an isothermal region. It can easily be demonstrated that this assumption corresponds to an inertia force - viscous force balance in the x-momentum equation. Subsequently, numerical solutions and experimental evidence (i.e., [11] and [19], respectively) have shown that the core is not isothermal but is, instead, thermally stratified. The thermal stratification in the core is characterized by nearly horizontal isotherms such that the temperature is a function of the vertical coordinate only; that is, $T = T(x)$ only. Indeed, experiment shows $T(x)$ to be linear in x. It will be shown that this result corresponds to a pressure force - buoyancy force balance in the x-momentum equation.

Observing that the core flow feeds and drains the horizontal wall boundary layers gives:

$$u_r = \bar{u}_r = \left(\frac{\nu_0}{H}\right)\left(\frac{H}{W}\right)^{\frac{1}{2}} N_{GR}^{-1/8} = \epsilon \left(\frac{\nu_0}{H}\right)\left(\frac{H}{W}\right)^{\frac{1}{2}} \tag{2.59}$$

All of the reference quantities in the core region are now known. The reference lengths, L_{rx} and L_{ry}, are just the overall dimensions of the enclosure, or:

$$L_{rx} = H \tag{2.37}$$

$$L_{ry} = W \tag{2.38}$$

The vertical reference velocity, u_r, was found to be

$$u_r = \left(\frac{\nu_0}{H}\right)\left(\frac{H}{W}\right)^{\frac{1}{2}} N_{GR}^{-1/8} = \epsilon \left(\frac{\nu_0}{H}\right)\left(\frac{H}{W}\right)^{\frac{1}{2}} \tag{2.59}$$

by observing that the core feeds and drains the horizontal wall boundary layers. Similarly, the horizontal reference velocity, v_r, was found to be

$$v_r = \left(\frac{\nu_0}{H}\right) N_{GR}^{\frac{1}{4}} = \left(\frac{\nu_0}{\epsilon^2 H}\right) \tag{2.29}$$

by observing that the core also feeds and drains the vertical wall boundary layers. The vertical reference pressure gradient, $\left.\frac{\partial p}{\partial x}\right|_r$, was obtained by noting that the vertical pressure gradient in the core is "impressed" on the vertical wall boundary layers as shown by equation (2.26c). Thus,

$$\left.\frac{\partial p}{\partial x}\right|_r = \left.\frac{\partial \tilde{p}}{\partial \tilde{x}}\right|_r = \left(\frac{\rho_0 \nu_0^2}{H^3}\right) N_{GR} = \left(\frac{\rho_0 \nu_0^2}{\epsilon^8 H^3}\right) \tag{2.36}$$

The horizontal pressure gradient in the core then follows as:

$$\left.\frac{\partial p}{\partial y}\right|_r = \left(\frac{L_{rx}}{L_{ry}}\right) \left.\frac{\partial p}{\partial x}\right|_r = \left(\frac{\rho_0 \nu_0^2}{H^2 W}\right) N_{GR} = \left(\frac{\rho_0 \nu_0^2}{\epsilon^8 H^2 W}\right) \tag{2.39}$$

The spatial coordinates for the core region are

$$x = \frac{x^*}{L_{rx}} = \frac{x^*}{H} \tag{2.60}$$

$$y = \frac{y^*}{L_{ry}} = \frac{y^*}{W} \tag{2.61}$$

There was no freedom whatsoever in choosing the above reference quantities. Except for the length scales, L_{rx} and L_{ry}, they were all dictated by the assumptions made in scaling the vertical and horizontal wall boundary layers. The validity of these assumptions will now be established by demonstrating that they result in a pressure force - buoyancy force balance in the x-momentum equation which, in turn, yields the experimentally observed linear temperature profile in the core. Substituting these reference quantities in the governing equations gives:

$$\varepsilon^3 \frac{\partial u}{\partial x} + \left(\frac{H}{W}\right)^{\frac{1}{2}} \frac{\partial v}{\partial y} = 0 \tag{2.62a}$$

$$\varepsilon^{10}\left(\frac{H}{W}\right) u \frac{\partial u}{\partial x} + \varepsilon^7 \left(\frac{H}{W}\right)^{3/2} v \frac{\partial u}{\partial y} = -\frac{\partial p}{\partial x} + T + \varepsilon^9 \left(\frac{H}{W}\right)^{\frac{1}{2}} \left[\frac{\partial^2 u}{\partial x^2} + \left(\frac{H}{W}\right)^2 \frac{\partial^2 u}{\partial y^2}\right] \tag{2.62b}$$

$$\varepsilon^7 \left(\frac{H}{W}\right)^{\frac{1}{2}} u \frac{\partial v}{\partial x} + \varepsilon^4 \left(\frac{H}{W}\right) v \frac{\partial v}{\partial y} = -\left(\frac{H}{W}\right) \frac{\partial p}{\partial y} + \varepsilon^6 \left[\frac{\partial^2 v}{\partial x^2} + \left(\frac{H}{W}\right)^2 \frac{\partial^2 v}{\partial y^2}\right] \tag{2.62c}$$

$$\varepsilon^3 \left(N_{PR}\right)\left(\frac{H}{W}\right)^{\frac{1}{2}} u \frac{\partial T}{\partial x} + \left(N_{PR}\right)\left(\frac{H}{W}\right) v \frac{\partial T}{\partial y} = \varepsilon^2 \left[\frac{\partial^2 T}{\partial x^2} + \left(\frac{H}{W}\right)^2 \frac{\partial^2 T}{\partial y^2}\right] \tag{2.62d}$$

these equations do not possess any boundary conditions. Their solutions, however, are required to match with the solutions of the vertical and horizontal wall boundary layers. The equations indicate that:

1. Both terms in the continuity equation do not have to be of the same order in the core. This is because both terms can be identically zero in this region.

2. The reference quantities dictated by the assumptions made in scaling the vertical and horizontal wall boundary layers result in a pressure force - bouyant force balance in the x-momentum equation (2.62b).

The following expansions are assumed for the dependent variables:

$$u(x,y) \sim u_0(x,y) + \epsilon\, u_1(x,y) + \epsilon^2 u_2(x,y) + \ldots \quad (\text{as } \epsilon \to 0) \qquad (2.63a)$$

$$v(x,y) \sim v_0(x,y) + \epsilon\, v_1(x,y) + \epsilon^2 v_2(x,y) + \ldots \quad (\text{as } \epsilon \to 0) \qquad (2.63b)$$

$$p(x,y) \sim p_0(x,y) + \epsilon\, p_1(x,y) + \epsilon^2 p_2(x,y) + \ldots \quad (\text{as } \epsilon \to 0) \qquad (2.63c)$$

$$T(x,y) \sim T_0(x,y) + \epsilon\, T_1(x,y) + \epsilon^2 T_2(x,y) + \ldots \quad (\text{as } \epsilon \to 0) \qquad (2.63d)$$

Substituting these expansions into equations (2.62), gathering terms of like powers of ϵ, and noting that in order for this result to hold for arbitrary values of ϵ that all of the coefficients must identically vanish, gives an infinite number of sets of governing equations for the various order problems. The first four sets of these equations are as follows:

<u>Zeroth Order</u>

$$\frac{\partial v_0}{\partial y} = 0 \qquad (2.64a)$$

$$\frac{\partial p_0}{\partial x} = T_0 \qquad (2.64b)$$

$$\frac{\partial p_0}{\partial y} = 0 \qquad (2.64c)$$

$$v_0 \frac{\partial T_0}{\partial y} = 0 \qquad (2.64d)$$

First-Order

$$\frac{\partial v_1}{\partial y} = 0 \tag{2.65a}$$

$$\frac{\partial p_1}{\partial x} = T_1 \tag{2.65b}$$

$$\frac{\partial p_1}{\partial y} = 0 \tag{2.65c}$$

$$v_0 \frac{\partial T_1}{\partial y} + v_1 \frac{\partial T_0}{\partial y} = 0 \tag{2.65d}$$

Second-Order

$$\frac{\partial v_2}{\partial y} = 0 \tag{2.66a}$$

$$\frac{\partial p_2}{\partial x} = T_2 \tag{2.66b}$$

$$\frac{\partial p_2}{\partial y} = 0 \tag{2.66c}$$

$$\left(N_{PR}\right)\left(\frac{H}{W}\right)\left(v_0 \frac{\partial T_0}{\partial y} + v_1 \frac{\partial T_1}{\partial y} + v_2 \frac{\partial T_0}{\partial y}\right) = \frac{\partial^2 T_0}{\partial x^2} + \left(\frac{H}{W}\right)^2 \frac{\partial^2 T_0}{\partial y^2} \tag{2.66d}$$

Third-Order

$$\frac{\partial u_0}{\partial x} + \left(\frac{H}{W}\right)^{\frac{1}{2}} \frac{\partial v_3}{\partial y} = 0 \tag{2.67a}$$

$$\frac{\partial p_3}{\partial x} = T_3 \tag{2.67b}$$

$$\frac{\partial p_3}{\partial y} = 0 \tag{2.67c}$$

$$\left(N_{PR}\right)\left(\frac{H}{W}\right)^{\frac{1}{2}} u_0 \frac{\partial T_0}{\partial x} + \left(N_{PR}\right)\left(\frac{H}{W}\right)\left(v_0 \frac{\partial T_3}{\partial y} + v_1 \frac{\partial T_2}{\partial y} + v_2 \frac{\partial T_1}{\partial y} + v_3 \frac{\partial T_0}{\partial y}\right)$$
$$= \frac{\partial^2 T_1}{\partial x^2} + \left(\frac{H}{W}\right)^2 \frac{\partial^2 T_1}{\partial y^2} \tag{2.67d}$$

The governing equations for the fourth-order problem are listed in Appendix A.

Zeroth-Order Solution in the Core Region

The zeroth-order continuity equation (2.64a) gives:

$$v_0 = v_0(x) \text{ only} \tag{2.68}$$

The zeroth-order energy equation is given by

$$v_0 \frac{\partial T_0}{\partial y} = 0 \tag{2.64d}$$

But, in general, v_0 is nonzero since the vertical wall boundary layers must entrain and expel fluid. Thus;

$$\frac{\partial T_0}{\partial y} = 0 \tag{2.69}$$

so that:

$$T_0 = T_0(x) \text{ only} \tag{2.70}$$

The zeroth-order y-momentum equation

$$\frac{\partial p_0}{\partial y} = 0 \tag{2.64c}$$

gives:

$$p_0 = p_0(x) \text{ only} \tag{2.71}$$

The zeroth-order x-momentum equation (2.64b) may now be rewritten as:

$$\frac{dp_0}{dx} = T_0 \tag{2.72}$$

Substituting equation (2.69) in the first-order energy equation (2.65d) gives:

$$v_0 \frac{\partial T_1}{\partial y} = 0 \tag{2.73}$$

However, as shown above, v_0 is in general nonzero so that:

$$\frac{\partial T_1}{\partial y} = 0 \qquad (2.74)$$

The second-order y-momentum equation

$$\frac{\partial p_2}{\partial y} = 0 \qquad (2.66c)$$

gives:

$$p_2 = p_2(x) \text{ only} \qquad (2.75)$$

Thus, the second-order x-momentum equation (2.66b) may be rewritten as

$$\frac{d\,p_2}{d\,x} = T_2 \qquad (2.76)$$

Since the left-hand member of equation (2.76) is a function of x only, the right-hand member is either a constant or a function of x only. In either case it follows that:

$$\frac{\partial T_2}{\partial y} = 0 \qquad (2.77)$$

Substituting equations (2.69), (2.74) and (2.77) in the second-order energy equation (2.66d) gives:

$$\frac{d^2 T_0}{d\,x^2} = 0 \qquad (2.78)$$

Integrating yields:

$$T_0 = c_1 x + c_2 \qquad (2.79)$$

<u>This systematically and rationally obtained analytical solution for the zeroth-order temperature distribution in the core region reproduces the experimentally observed linear stratification profile</u>. This establishes

the validity of the assumptions made in scaling the vertical and horizontal wall boundary layers. Equation (2.72) may now be integrated to obtain the zeroth-order pressure distribution in the core. This gives:

$$p_0 = \tfrac{1}{2} c_1 x^2 + c_2 x + c_3 \tag{2.80}$$

The third-order y-momentum equation

$$\frac{\partial p_3}{\partial y} = 0 \tag{2.67c}$$

yields

$$p_3 = p_3 \ (x) \text{ only} \tag{2.81}$$

so that the third-order x-momentum equation (2.67b) may be rewritten as:

$$\frac{d p_3}{d x} = T_3 \tag{2.82}$$

The left-hand member of equation (2.82) is a function of x only. Therefore, the right-hand member is either a constant or a function of x only. In either case it follows that:

$$\frac{\partial T_3}{\partial y} = 0 \tag{2.83}$$

Substituting equations (2.69), (2.74), (2.77), and (2.83) in the third-order energy equation (2.67d), gives:

$$\left(N_{PR}\right)\left(\frac{H}{W}\right)^{\frac{1}{2}} u_0 \frac{d T_0}{d x} = \frac{d^2 T_1}{d x^2} \tag{2.84}$$

or,

$$u_0 = \frac{\left(\frac{d^2 T_1}{d x^2}\right)}{\left(N_{PR}\right)\left(\frac{H}{W}\right)^{\frac{1}{2}}\left(\frac{d T_0}{d x}\right)} \tag{2.85}$$

Since the right-hand member of this equation is a function of x only;

u_0 is either a function of x only, a nonzero constant, or identically zero. However, neither of the first two of these possibilities would allow global conservation of mass for the entire enclosure to be satisfied. Thus,

$$u_0 = 0 \tag{2.86}$$

Summarizing the zeroth-order core solution:

$$u_0 = 0 \tag{2.86}$$

$$v_0 = v_0(x) \tag{2.68}$$

$$p_0 = \tfrac{1}{2} c_1 x^2 + c_2 x + c_3 \tag{2.80}$$

$$T_0 = c_1 x + c_2 \tag{2.79}$$

Since $u_0 = 0$; the flow in the core is, to lowest order, entirely horizontal. This horizontal component of velocity, $v_0(x)$, will be determined by the solution of the vertical wall boundary layers. It will just be the function required to feed and drain these boundary layers. The constants c_1 and c_2 will be given by matching conditions. The pressure, p, is defined as the pressure due to motion. Thus, it would be identically equal to zero if there was no motion in the enclosure. This would occur when the wall temperatures were equal, or $T_a^* = T_b^*$. In that case, the pressure would be given by:

$$p_0 = c_3 = 0 \tag{2.87}$$

Scaling of the (Bottom Right-Hand) Corner Region Equations

The scaling in this region is based on the fact that

the mass flow rate out of the bottom horizontal wall boundary layer	=	the mass flowrate into the bottom right-hand corner region

which requires that:

$$\left(L_{rx} v_r\right) = \left(\hat{L}_{rx}\hat{v}_r\right) = \epsilon\, \nu_0\left(\frac{W}{H}\right)^{\frac{1}{2}} \tag{2.88}$$

Both terms in the continuity equation must be the same order to satisfy global conservation of mass for the corner region. Thus;

$$\frac{\hat{v}_r \hat{L}_{rx}}{\hat{u}_r \hat{L}_{ry}} = 1 \tag{2.89}$$

or,

$$\hat{u}_r\hat{L}_{ry} = \hat{v}_r\hat{L}_{rx} = \epsilon\, \nu_0\left(\frac{W}{H}\right)^{\frac{1}{2}} \tag{2.90}$$

so that:

$$\hat{u}_r = \left(\frac{\epsilon\, \nu_0}{\hat{L}_{ry}}\right)\left(\frac{W}{H}\right)^{\frac{1}{2}} \tag{2.91}$$

$$\hat{v}_r = \left(\frac{\epsilon\, \nu_0}{\hat{L}_{rx}}\right)\left(\frac{W}{H}\right)^{\frac{1}{2}} \tag{2.92}$$

Substituting equations (2.89), (2.91) and (2.92) in the energy equation (2.4d) and rearranging gives:

$$\hat{u}\,\frac{\partial\hat{T}}{\partial\hat{x}} + \hat{v}\,\frac{\partial\hat{T}}{\partial\hat{y}} = \left(\frac{1}{N_{PR}}\right)\left(\frac{\hat{L}_{ry}}{\epsilon\,\hat{L}_{rx}}\right)\left(\frac{H}{W}\right)^{\frac{1}{2}}\frac{\partial^2\hat{T}}{\partial\hat{x}^2} + \left(\frac{1}{N_{PR}}\right)\left(\frac{\hat{L}_{rx}}{\epsilon\,\hat{L}_{ry}}\right)\left(\frac{H}{W}\right)^{\frac{1}{2}}\frac{\partial^2\hat{T}}{\partial\hat{y}^2} \tag{2.93}$$

This equation admits three possibilities for the coefficients of the terms in the right-hand member:

Case 1. $$\left(\frac{1}{N_{PR}}\right)\left(\frac{\hat{L}_{ry}}{\epsilon\,\hat{L}_{rx}}\right)\left(\frac{H}{W}\right)^{\frac{1}{2}} = 1 \tag{2.94a}$$

Case 2. $$\left(\frac{1}{N_{PR}}\right)\left(\frac{\hat{L}_{rx}}{\epsilon\,\hat{L}_{ry}}\right)\left(\frac{H}{W}\right)^{\frac{1}{2}} = 1 \tag{2.94b}$$

Case 3. $$\left(\frac{1}{N_{PR}}\right)\left(\frac{\hat{L}_{ry}}{\epsilon\,\hat{L}_{rx}}\right)\left(\frac{H}{W}\right)^{\frac{1}{2}} = \left(\frac{1}{N_{PR}}\right)\left(\frac{\hat{L}_{rx}}{\epsilon\,\hat{L}_{ry}}\right)\left(\frac{H}{W}\right)^{\frac{1}{2}}$$

or,

$$\hat{L}_{rx} = \hat{L}_{ry} \tag{2.94c}$$

A systematic investigation of these three cases is presented in Appendix B. Through a process of elimination, this analyis proves that the only possible set of governing equations is given by Case 3 for a pressure force - viscous force balance in the $\hat{y}$-momentum equation. The analysis shows that any other set of governing equations is impossible since they either require a force balance that cannot be obtained or produce a solution that cannot be matched. The resulting reference quantities and spatial coordinates are as follows:

$$\hat{L}_{rx} = \hat{L}_{ry} = \epsilon^3 \, H^{5/6} \, W^{1/6} \tag{2.95}$$

$$\hat{x} = \frac{x^*}{\hat{L}_{rx}} = \frac{x^*}{\epsilon^3 \, H^{5/6} \, W^{1/6}} \tag{2.96}$$

$$\hat{y} = \frac{W - y^*}{\hat{L}_{ry}} = \frac{W - y^*}{\epsilon^3 \, H^{5/6} \, W^{1/6}} \tag{2.97}$$

$$\hat{u}_r = \hat{v}_r = \left(\frac{\nu_0}{\epsilon^2 \, H}\right)\left(\frac{W}{H}\right)^{1/3} \tag{2.98}$$

$$\left.\frac{\partial \hat{p}}{\partial \hat{x}}\right|_r = \left.\frac{\partial \hat{p}}{\partial \hat{y}}\right|_r = \left(\frac{\rho_0 \nu_0^2}{\epsilon^8 \, H^3}\right) \tag{2.99}$$

Substituting these reference quantities in the governing equations (2.4) and the boundary conditions (2.5 d,e,f,j,k,ℓ) gives:

$$\frac{\partial \hat{u}}{\partial \hat{x}} + \frac{\partial \hat{v}}{\partial \hat{y}} = 0 \tag{2.100a}$$

$$\epsilon \left(\frac{W}{H}\right)^{\frac{1}{2}} \left(\hat{u} \frac{\partial \hat{u}}{\partial \hat{x}} + \hat{v} \frac{\partial \hat{u}}{\partial \hat{y}}\right) = - \frac{\partial \hat{p}}{\partial \hat{x}} + \hat{T} + \frac{\partial^2 \hat{u}}{\partial \hat{x}^2} + \frac{\partial^2 \hat{u}}{\partial \hat{y}^2} \qquad (2.100b)$$

$$\epsilon \left(\frac{W}{H}\right)^{\frac{1}{2}} \left(\hat{u} \frac{\partial \hat{v}}{\partial \hat{x}} + \hat{v} \frac{\partial \hat{v}}{\partial \hat{y}}\right) = - \frac{\partial \hat{p}}{\partial \hat{y}} + \frac{\partial^2 \hat{v}}{\partial \hat{x}^2} + \frac{\partial^2 \hat{v}}{\partial \hat{y}^2} \qquad (2.100c)$$

$$\epsilon \left(N_{PR}\right)\left(\frac{W}{H}\right)^{\frac{1}{2}}\left(\hat{u} \frac{\partial \hat{T}}{\partial \hat{x}} + \hat{v} \frac{\partial \hat{T}}{\partial \hat{y}}\right) = \frac{\partial^2 \hat{T}}{\partial \hat{x}^2} + \frac{\partial^2 \hat{T}}{\partial \hat{y}^2} \qquad (2.100d)$$

and, $\hat{u}(\hat{x},0) = 0$ (2.101a)

$$\hat{v}(\hat{x},0) = 0 \qquad (2.101b)$$

$$\hat{T}(\hat{x},0) = 1 \qquad (2.101c)$$

$$\hat{u}(0,\hat{y}) = 0 \qquad (2.101d)$$

$$\hat{v}(0,\hat{y}) = 0 \qquad (2.101e)$$

$$\frac{\partial \hat{T}(0,\hat{y})}{\partial \hat{x}} = 0 \qquad (2.101f)$$

Thus, a pressure force - buoyancy force - viscous force balance is obtained in the $\hat{x}$-momentum equation and a pressure force - viscous force balance in the $\hat{y}$-momentum equation.

The following expansions are assumed for the dependent variables:

$$\hat{u}(\hat{x},\hat{y}) \sim \hat{u}_0(\hat{x},\hat{y}) + \epsilon\, \hat{u}_1(\hat{x},\hat{y}) + \epsilon^2 \hat{u}_2(\hat{x},\hat{y}) + \ldots \text{ (as } \epsilon \to 0) \qquad (2.102a)$$

$$\hat{v}(\hat{x},\hat{y}) \sim \hat{v}_0(\hat{x},\hat{y}) + \epsilon\, \hat{v}_1(\hat{x},\hat{y}) + \epsilon^2 \hat{v}_2(\hat{x},\hat{y}) + \ldots \text{ (as } \epsilon \to 0) \qquad (2.102b)$$

$$\hat{p}(\hat{x},\hat{y}) \sim \hat{p}_0(\hat{x},\hat{y}) + \epsilon\, \hat{p}_1(\hat{x},\hat{y}) + \epsilon^2 \hat{p}_2(\hat{x},\hat{y}) + \ldots \text{ (as } \epsilon \to 0) \qquad (2.102c)$$

$$\hat{T}(\hat{x},\hat{y}) \sim \hat{T}_0(\hat{x},\hat{y}) + \epsilon\, \hat{T}_1(\hat{x},\hat{y}) + \epsilon^2 \hat{T}_2(\hat{x},\hat{y}) + \ldots \text{ (as } \epsilon \to 0) \qquad (2.102d)$$

Substituting these expansions into equations (2.100) and the boundary conditions (2.101), gathering terms of like powers of ϵ, and noting that in order for this result to hold for arbitrary values of ϵ that all of the coefficients must identically vanish, gives an infinite number of sets of governing equations and boundary conditions for the various order problems. Only the zeroth-order set of equations and boundary conditions are given here:

$$\frac{\partial \hat{u}_0}{\partial \hat{x}} + \frac{\partial \hat{v}_0}{\partial \hat{y}} = 0 \tag{2.103a}$$

$$\frac{\partial \hat{p}_0}{\partial \hat{x}} = \hat{T}_0 + \frac{\partial^2 \hat{u}_0}{\partial \hat{x}^2} + \frac{\partial^2 \hat{u}_0}{\partial \hat{y}^2} \tag{2.103b}$$

$$\frac{\partial \hat{p}_0}{\partial \hat{y}} = \frac{\partial^2 \hat{v}_0}{\partial \hat{x}^2} + \frac{\partial^2 \hat{v}_0}{\partial \hat{y}^2} \tag{2.103c}$$

$$\frac{\partial^2 \hat{T}_0}{\partial \hat{x}^2} + \frac{\partial^2 \hat{T}_0}{\partial \hat{y}^2} = 0 \tag{2.103d}$$

and,

$$\hat{u}_0(\hat{x},0) = 0 \tag{2.104a}$$

$$\hat{v}_0(\hat{x},0) = 0 \tag{2.104b}$$

$$\hat{T}_0(\hat{x},0) = 1 \tag{2.104c}$$

$$\hat{u}_0(0,\hat{y}) = 0 \tag{2.104d}$$

$$\hat{v}_0(0,\hat{y}) = 0 \tag{2.104e}$$

$$\frac{\partial \hat{T}_0(0,\hat{y})}{\partial \hat{x}} = 0 \tag{2.104f}$$

(plus matching conditions with the vertical and horizontal wall boundary layers)

The governing equations and their boundary conditions for the first- and second-order problems are given in Appendix A.

In a similar manner, the zeroth-order set of governing equations and boundary conditions for the top right-hand corner region are found to be:

$$\frac{\partial \hat{\hat{u}}_0}{\partial \hat{\hat{x}}} + \frac{\partial \hat{\hat{v}}_0}{\partial \hat{\hat{y}}} = 0 \tag{2.105a}$$

$$\frac{\partial \hat{\hat{p}}_0}{\partial \hat{\hat{x}}} = - \hat{\hat{T}}_0 + \frac{\partial^2 \hat{\hat{u}}_0}{\partial \hat{\hat{x}}^2} + \frac{\partial^2 \hat{\hat{u}}_0}{\partial \hat{\hat{y}}^2} \tag{2.105b}$$

$$\frac{\partial \hat{\hat{p}}_0}{\partial \hat{\hat{y}}} = \frac{\partial^2 \hat{\hat{v}}_0}{\partial \hat{\hat{x}}^2} + \frac{\partial^2 \hat{\hat{v}}_0}{\partial \hat{\hat{y}}^2} \tag{2.105c}$$

$$\frac{\partial^2 \hat{\hat{T}}_0}{\partial \hat{\hat{x}}^2} + \frac{\partial^2 \hat{\hat{T}}_0}{\partial \hat{\hat{y}}^2} = 0 \tag{2.105d}$$

and,

$$\hat{\hat{u}}_0(\hat{\hat{x}},0) = 0 \tag{2.106a}$$

$$\hat{\hat{v}}_0(\hat{\hat{x}},0) = 0 \tag{2.106b}$$

$$\hat{\hat{T}}_0(\hat{\hat{x}},0) = 1 \tag{2.106c}$$

$$\hat{\hat{u}}_0(0,\hat{\hat{y}}) = 0 \tag{2.106d}$$

$$\hat{\hat{v}}_0(0,\hat{\hat{y}}) = 0 \tag{2.106e}$$

$$\frac{\partial \hat{\hat{T}}_0(0,\hat{\hat{y}})}{\partial \hat{\hat{x}}} = 0 \tag{2.106f}$$

(plus matching conditions with the vertical and horizontal wall boundary layer equations)

where the spatial coordinates for the top right-hand corner region are given by:

$$\hat{x} = \frac{H - x^*}{\hat{\hat{L}}_{rx}} = \frac{H - x^*}{\epsilon^3 H^{5/6} W^{1/6}} \tag{2.107}$$

$$\hat{y} = \frac{W - y^*}{\hat{\hat{L}}_{ry}} = \frac{W - y^*}{\epsilon^3 H^{5/6} W^{1/6}} \tag{2.108}$$

The zeroth-order equations (2.103) for the (bottom right-hand) corner region are a second-order set of linear, elliptic, partial differential equations. The pressure-buoyancy-viscous force balance in the $\hat{x}$-momentum equation (2.103b) and the pressure-viscous force balance in the $\hat{y}$-momentum equation (2.103c) characterize the flow as a "slow flow" with buoyancy. The energy equation (2.103d) shows that the energy transport in the corner is by conduction only and that the temperature distribution is given by a solution of the energy equation alone, independent of the dynamics of the flow.

The solution of equations (2.103) will be outlined here but not carried to completion since the equations are elliptic and thus require boundary conditions on all four sides of the corner region. The boundary conditions on the side of the corner region that matches with the vertical wall boundary layer are, however, unknown at this point in the analysis. Cross-differentiating the momentum equations (2.103b) and (2.103c) and eliminating the pressure terms gives:

$$\frac{\partial^3 \hat{u}_0}{\partial \hat{x}^2 \partial \hat{y}} + \frac{\partial^3 \hat{u}_0}{\partial \hat{y}^3} - \frac{\partial^3 \hat{v}_0}{\partial \hat{x}^3} - \frac{\partial^3 \hat{v}_0}{\partial \hat{y}^2 \partial \hat{x}} + \hat{T}_0 = 0 \tag{2.109}$$

A streamfunction, $\hat{\psi}_0$, is now defined so that

$$\frac{\partial \hat{\psi}_0}{\partial \hat{y}} = \hat{u}_0 \qquad (2.110a)$$

$$\frac{\partial \hat{\psi}_0}{\partial \hat{x}} = - \hat{v}_0 \qquad (2.110b)$$

The function satisfies identically the continuity equation (2.103a). Substituting equation (2.110) in equation (2.109) gives

$$\frac{\partial^4 \hat{\psi}_0}{\partial \hat{x}^4} + 2 \frac{\partial^4 \hat{\psi}_0}{\partial \hat{x}^2 \partial \hat{y}^2} + \frac{\partial^4 \hat{\psi}_0}{\partial \hat{y}^4} + \frac{\partial \hat{T}_0}{\partial \hat{y}} = 0 \qquad (2.111)$$

which is the nonhomogeneous biharmonic equation.

When all the boundary conditions for the corner region have been determined, the energy equation (2.103d) may be solved for the temperature distribution, $\hat{T}_0 = \hat{T}_0(\hat{x},\hat{y})$. This result is then substituted in equation (2.111) which is solved for the streamfunction.

Solution of the Zeroth-Order Problem for the Entire Enclosure

In general, this solution would require solving the zeroth-order governing equations in all nine of the physically distinct regions of the flowfield. However, it has already been shown that, because of the centro-symmetry property of the governing equations, only six of the nine regions must be considered. The core, the right-hand vertical wall boundary layers, the top and bottom right-hand corner regions, and the top and bottom horizontal wall boundary layers were chosen for this purpose. The solutions in these regions will be in terms of a number of unknown constants and functions which are determined by matching conditions.

The solutions in the core have already been determined. The solutions of the top and bottom horizontal wall boundary layers will be determined next. This will be followed by a discussion of the nature of the exact solutions for the corners and vertical wall boundary layers. Finally, an approximate solution of the vertical wall boundary layer equations will be obtained by means of integral techniques.

Solution of the (Bottom) Horizontal Wall Boundary Layer Equations

As before, the bottom horizontal wall boundary layer is governed by the following zeroth-order set of equations

$$\frac{\partial \bar{u}_0}{\partial \bar{x}} + \frac{\partial \bar{v}_0}{\partial \bar{y}} = 0 \tag{2.53a}$$

$$\frac{\partial \bar{p}_0}{\partial \bar{x}} = 0 \tag{2.53b}$$

$$\frac{\partial \bar{p}_0}{\partial \bar{y}} = \frac{\partial^2 \bar{v}_0}{\partial \bar{x}^2} \tag{2.53c}$$

$$\frac{\partial^2 \bar{T}_0}{\partial \bar{x}^2} = 0 \tag{2.53d}$$

with, $$\bar{u}_0(0,\bar{y}) = 0 \tag{2.54a}$$

$$\bar{v}_0(0,\bar{y}) = 0 \tag{2.54b}$$

$$\frac{\partial \bar{T}_0(0,\bar{y})}{\partial \bar{x}} = 0 \tag{2.54c}$$

(plus matching conditions with core and corner regions)

These equations (2.53) and their boundary conditions (2.54) are linear and may be solved exactly (at least in terms of unknown functions of $\bar{y}$).

Integrating the $\bar{x}$-momentum equation (2.53b) gives

$$\bar{p}_0 = f_1(\bar{y}) \tag{2.112}$$

where: $f_1 \equiv$ function of $\bar{y}$ only

Substituting this result in the $\bar{y}$-momentum equation (2.53c) and integrating gives:

$$\bar{v}_0 = \tfrac{1}{2}\, \bar{x}^2\, f_1' + \bar{x}\, f_2(\bar{y}) + f_3(\bar{y}) \tag{2.113}$$

Substituting this expression for $\bar{v}_0$ into the continuity equation (2.53a) and integrating yields:

$$\bar{u}_0 = -\, 1/6\, \bar{x}^3\, f_1''(\bar{y}) - 1/2\, \bar{x}^2\, f_2'(\bar{y}) - \bar{x}f_3'(\bar{y}) + f_4(\bar{y}) \tag{2.114}$$

Integration of the energy equation (2.53d) gives:

$$\bar{T}_0 = \bar{x}\, f_5(\bar{y}) + f_6(\bar{y}) \tag{2.115}$$

The no-slip condition at $\bar{x} = 0$ (2.54b) and the expression for $\bar{v}_0$ (2.113) now give:

$$f_3(\bar{y}) = f_3'(\bar{y}) = 0 \tag{2.116}$$

Similarly, the condition for no normal flow at the wall (2.54b) and the expression for $\bar{u}_0$ (2.114) yield

$$f_4(\bar{y}) = 0 \tag{2.117}$$

while the adiabatic wall condition (2.54c) and the temperature distribution (2.115) give:

$$f_5(\bar{y}) = 0 \tag{2.118}$$

Substituting equations (2.116), (2.117), and (2.118) in equations (2.112), (2.113), (2.114), and (2.115) gives the following solutions of the bottom horizontal wall boundary layer equations:

$$\bar{u}_0 = -1/6\ \bar{x}^3\ f_1''(\bar{y}) - 1/2\ \bar{x}^2\ f_2'(\bar{y}) \qquad (2.119a)$$

$$\bar{v}_0 = 1/2\ \bar{x}^2\ f_1'(\bar{y}) + \bar{x}\ f_2(\bar{y}) \qquad (2.119b)$$

$$\bar{p}_0 = f_1(\bar{y}) \qquad (2.119c)$$

$$\bar{T}_0 = f_6(\bar{y}) \qquad (2.119d)$$

Similarly, the solutions of the zeroth-order set of governing equations for the top horizontal wall boundary layer are given by:

$$\bar{\bar{u}}_0 = -1/6\ \bar{\bar{x}}^3\ F_1''(\bar{\bar{y}}) - 1/2\ \bar{\bar{x}}^2\ F_2'(\bar{\bar{y}}) \qquad (2.120a)$$

$$\bar{\bar{v}}_0 = 1/2\ \bar{\bar{x}}^2\ F_1'(\bar{\bar{y}}) + \bar{\bar{x}}\ F_2(\bar{\bar{y}}) \qquad (2.120b)$$

$$\bar{\bar{p}}_0 = F_1(\bar{\bar{y}}) \qquad (2.120c)$$

$$\bar{\bar{T}}_0 = F_6(\bar{\bar{y}}) \qquad (2.120d)$$

where the F_n's are unknown functions of $\bar{\bar{y}}$ only.

The unknown functions f_1, f_2, f_6, F_1, F_2, F_6 will be determined by matching with the core solutions.

Matching of the (Bottom) Horizontal Wall Boundary Layer and Core Solutions

Pressure Matching

The core region, or "outer", solution for the pressure distribution is given by equations (2.80) and (2.87) as:

$$p_0 = 1/2\ c_1 x^2 + c_2 x \qquad (2.121)$$

Rewriting this solution in horizontal wall boundary layer, or "inner", variables gives:

$$p_0^{oi} = \epsilon^6 (1/2)(c_1)(W/H)\ \bar{x}^2 + \epsilon^3 (c_2)(W/H)^{\frac{1}{2}}\ \bar{x} \qquad (2.122)$$

Taking the "inner limit" of this outer solution as $\epsilon \to 0$ yields:

$$\lim_{\epsilon \to 0} \left(p_0^{oi}\right) = 0 \qquad (2.123)$$

This limit may be rewritten in outer variables as:

$$\lim_{\epsilon \to 0} \left(p_0^{oi}\right) = 0 \qquad (2.124)$$

The horizontal wall boundary layer, or "inner", solution for the pressure distribution is given by equation (2.119c) as:

$$\bar{p}_0 = f_1(\bar{y}) \qquad (2.119c)$$

Rewriting this solution in core, or "outer", variables gives:

$$\bar{p}_0^{io} = f_1(y) \qquad (2.125)$$

Taking the "outer limit" of this inner solution as $\epsilon \to 0$ yields:

$$\lim_{\epsilon \to 0} \left(\bar{p}_0^{io}\right) = f_1(y) \qquad (2.126)$$

The limit matching principle [34]

$$\begin{bmatrix} \text{inner limit} \\ \text{of the outer solution} \end{bmatrix} = \begin{bmatrix} \text{outer limit} \\ \text{of the inner solution} \end{bmatrix}$$

gives:

$$\lim_{\epsilon \to 0} \left(p_0^{oi}\right) = \lim_{\epsilon \to 0} \left(\bar{p}_0^{io}\right) \qquad (2.127)$$

or,

$$f_1(y) = f_1(\bar{y}) = 0 \qquad (2.128)$$

Thus,

$$f_1'(\bar{y}) = f_1''(\bar{y}) = 0 \qquad (2.129)$$

Temperature Matching

The core region, or outer, solution for the temperature distribution is given by equation (2.79) as:

$$T_0 = c_1 x + c_2 \tag{2.79}$$

Rewriting this solution in horizontal wall boundary layer, or inner, variables gives:

$$T_0^{oi} = \varepsilon^3 (c_1)(W/H)^{\frac{1}{2}} \bar{x} + c_2 \tag{2.130}$$

Taking the inner limit of this outer solution as $\varepsilon \to 0$ yields:

$$\lim_{\varepsilon \to 0} \left(T_0^{oi}\right) = c_2 \tag{2.131}$$

This limit may be rewritten in outer variables as:

$$\lim_{\varepsilon \to 0} \left(T_o^{oi}\right) = c_2 \tag{2.132}$$

The horizontal wall boundary layer, or inner, solution for the temperature distribution is given by equation (2.119d) as:

$$\bar{T}_0 = f_6(\bar{y}) \tag{2.119d}$$

Rewriting this solution in core, or outer, variables gives:

$$\bar{T}_0^{io} = f_6(y) \tag{2.133}$$

Taking the outer limit of this inner solution as $\varepsilon \to 0$ yields

$$\lim_{\varepsilon \to 0} \left(\bar{T}_0^{io}\right) = f_6(y) \tag{2.134}$$

The limit matching principle now gives:

$$\lim_{\epsilon\to 0} \left(T_0^{oi}\right) = \lim_{\epsilon\to 0} \left(T_0^{io}\right) \tag{2.135}$$

or,

$$f_6(y) = f_6(\bar{y}) = c_2 \tag{2.136}$$

Substituting equation (2.129) in equation (2.119b) yields:

$$\bar{v}_0 = \bar{x}\ f_2(\bar{y}) \tag{2.137}$$

Matching this solution for $\bar{v}_0$ with the core solution

$$v_0 = v_0(x) \text{ only} \tag{2.68}$$

gives:

$$f_2(\bar{y}) = (\text{constant}) \equiv K_1 \tag{2.138}$$

Therefore;

$$f_2'(\bar{y}) = 0 \tag{2.139}$$

Substituting these results in the zeroth-order solutions for the (bottom) horizontal wall boundary layer gives:

$$\bar{u}_0 = 0 \tag{2.140a}$$

$$\bar{v}_0 = K_1\ \bar{x} \tag{2.140b}$$

$$\bar{p}_0 = 0 \tag{2.140c}$$

$$\bar{T}_0 = c_2 \tag{2.140d}$$

In a similar manner, matching the solutions (2.120) of the zeroth-order governing equations for the top horizontal wall boundary layer to the core solutions gives:

$$\bar{\bar{u}}_0 = 0 \tag{2.141a}$$

$$\bar{\bar{v}}_0 = K_2 \, \bar{\bar{x}} \tag{2.141b}$$

$$\bar{\bar{p}}_0 = \tfrac{1}{2} c_1 + c_2 \tag{2.141c}$$

$$\bar{\bar{T}}_0 = c_1 + c_2 \tag{2.141d}$$

Equations (2.140) and (2.141) show that the horizontal wall boundary layers are regions of constant pressure and temperature.

Summary of Zeroth-Order Solutions

The following zeroth-order solutions were obtained for the core region:

$$u_0 = 0 \tag{2.86}$$

$$v_0 = v_0(x) \tag{2.68}$$

$$p_0 = \tfrac{1}{2} c_1 x^2 + c_2 x \tag{2.80}$$

$$T_0 = c_1 x + c_2 \tag{2.79}$$

As before, the zeroth-order solutions for the bottom and top horizontal wall boundary layers were found to be given by:

$$\bar{u}_0 = 0 \tag{2.140a}$$

$$\bar{v}_0 = K_1 \bar{x} \tag{2.140b}$$

$$\bar{p}_0 = 0 \tag{2.140c}$$

$$\bar{T}_0 = c_2 \tag{2.140d}$$

and,

$$\bar{\bar{u}}_0 = 0 \tag{2.141a}$$

$$\bar{\bar{v}}_0 = K_2 \bar{\bar{x}} \tag{2.141b}$$

$$\bar{\bar{p}}_0 = \tfrac{1}{2}\, c_1 + c_2 \tag{2.141c}$$

$$\bar{\bar{T}}_0 = c_1 + c_2 \tag{2.141d}$$

respectively.

The zeroth-order solutions for the bottom and top right-hand corner regions may be represented symbolically as follows:

$$\hat{u}_0 = \hat{u}_0(\hat{x},\hat{y}) \tag{2.142a}$$

$$\hat{v}_0 = \hat{v}_0(\hat{x},\hat{y}) \tag{2.142b}$$

$$\hat{p}_0 = \hat{p}_0(\hat{x},\hat{y}) \tag{2.142c}$$

$$\hat{T}_0 = \hat{T}_0(\hat{x},\hat{y}) \tag{2.142d}$$

and,

$$\hat{\hat{u}}_0 = \hat{\hat{u}}_0(\hat{\hat{x}},\hat{\hat{y}}) \tag{2.143a}$$

$$\hat{\hat{v}}_0 = \hat{\hat{v}}_0(\hat{\hat{x}},\hat{\hat{y}}) \tag{2.143b}$$

$$\hat{\hat{p}}_0 = \hat{\hat{p}}_0(\hat{\hat{x}},\hat{\hat{y}}) \tag{2.143c}$$

$$\hat{\hat{T}}_0 = \hat{\hat{T}}_0(\hat{\hat{x}},\hat{\hat{y}}) \tag{2.143d}$$

In a similar manner, the zeroth-order solutions for the (right-hand) vertical wall boundary layer may be given symbolically as:

$$\tilde{u}_0 = \tilde{u}_0(c_1,\ c_2,\ N_{PR},\ \tilde{x},\ \tilde{y}) \tag{2.144a}$$

$$\tilde{v}_0 = \tilde{v}_0(c_1,\ c_2,\ N_{PR},\ \tilde{x},\ \tilde{y}) \tag{2.144b}$$

$$\tilde{p}_0 = \tilde{p}_0(c_1,\ c_2,\ N_{PR},\ \tilde{x},\ \tilde{y}) \tag{2.144c}$$

$$\tilde{T}_0 = \tilde{T}_0(c_1,\ c_2,\ N_{PR},\ \tilde{x},\ \tilde{y}) \tag{2.144d}$$

If the exact solutions in all of the above regions were known, the constants could be determined at this point by matching.

The only parameter appearing in the normalized zeroth-order solutions is the Prandtl number. The Grashof number was not expected to appear since the lowest order solution is for a fixed value of this parameter; that is, for an infinite Grashof number. The absence of the aspect ratio, (H/W), is; however, quite an interesting result as this implies that variations in this parameter affect the present steady state solution only in the higher order corrections. This will be discussed in more detail when the results of this analysis are compared with the results of other investigations.

The vertical component of velocity in the core flow is identically zero, while the horizontal component is given by the unknown function $v_0(x)$. This function is, in turn, given by the entrainment-extrainment velocity profiles of the vertical wall boundary layers. Thus, the flow in the core merely serves to feed and drain these boundary layers. This flow must be such that continuity is maintained for the entire enclosure, centro-symmetry is preserved, and matching with the solutions of the horizontal wall boundary layers is achieved.

The exact nature of the flows in the horizontal wall boundary layers and the core region may now be understood. It is well known that in a boundary layer the velocity component normal to the wall is much smaller than the velocity component parallel to the wall. In fact, for the vertical wall boundary layers the characteristic velocities were found to be

$$\tilde{u}_r = \frac{\nu_0}{\epsilon^4 H} \tag{2.14}$$

and,

$$\tilde{v}_r = \frac{\nu_0}{\epsilon^2 H} \qquad (2.17)$$

so that the ratio of the physical velocities, $\tilde{u}^*$ and $\tilde{v}^*$ is given by:

$$\frac{\tilde{v}^*}{\tilde{u}^*} = \left(\frac{v}{\tilde{u}}\right)\left(\frac{\tilde{v}_r}{\tilde{u}_r}\right) \sim O(\epsilon^2) \qquad (2.145)$$

However, since the core flow feeds and drains the vertical wall boundary layers, the horizontal velocity scale in the core region must also be $\tilde{v}_r$. Therefore; since the vertical velocity in the core, u_0, was shown to zero; the velocities in the core are also extremely small ($O(\epsilon^2)$) relative to the vertical velocities in the vertical wall boundary layers.

The scaling of the core region gave a pressure-buoyancy force balance. Thus, the flow in the core is an inviscid, bouyancy dominated flow in which both inertia and viscous forces are, to the lowest order, completely negligible. Inasmuch as the horizontal wall boundary layers must match with the core flow, they must also have a characteristic horizontal velocity given by $\tilde{v}_r$, that is, they must also be flows in which inertia is unimportant. This is reflected in the pressure-viscous force balance obtained in scaling these regions. This balance is characteristic of "slow", or "low Reynolds number" flows.

Thus, if a Reynold's number, N_{Re}, for the horizontal wall boundary layers is defined as

$$N_{Re} = \frac{\rho_0 \bar{L}_{rx} \bar{v}_r}{\mu_0} \qquad (2.146)$$

then,

$$N_{Re} = \left(\frac{W}{H}\right)^{\frac{1}{2}} N_{GR}^{-1/8} \tag{2.147}$$

so that:

$$N_{Re} \to 0 \qquad \text{as} \qquad N_{GR} \to \infty \tag{2.148}$$

Therefore, there are no momentum boundary layers on the horizontal walls. Since they are regions of constant temperature, however, they are actually thermal boundary layers because they provide a rapid transition from the linear temperature distribution in the core to the adiabatic boundary conditions at the horizontal walls.

The governing equations (2.103) in the (bottom right-hand) corner region are a second-order system of linear, elliptic, partial differential equations. It appears that, at least in principle, their exact solutions could be obtained in the manner previously outlined. It will be shown, however, that the vertical wall boundary layer equations may be solved without first solving the corner equations. Furthermore, since the corner regions are extremely small ($\hat{L}_{rx} = \hat{L}_{ry} \sim O(\varepsilon^3)$), they do not numerically affect the overall rate of heat transfer across the enclosure to any great extent. Hence, the corner solutions were not obtained and are given above only in symbolic form (2.142). Nevertheless, these solutions may be discussed from a physical point of view. The flow in (say) the bottom right-hand corner region serves to turn the flow in the bottom horizontal wall boundary layer into the right-hand vertical wall boundary layer and to insure that the no-slip boundary conditions are satisfied on both walls. The solution also has to meet the adiabatic boundary condition on the horizontal wall, the constant temperature boundary condition on the vertical wall, and must match with the solutions of the horizontal and vertical wall boundary layers.

The (right-hand) vertical wall boundary layer equations (2.26) are a second-order system of nonlinear, parabolic, partial differential equations whose solutions must match with the solutions of the top and bottom (right-hand) corners and the core region. The vertical wall boundary layers are, however, nonsimilar [30], [31] and as such their solution presents a formidable problem (even in a numerical sense), as will be shown below. Therefore, the solutions of the (right-hand) vertical wall boundary layer equations are also given only in symbolic form (2.144).

Integration of the nonsimilar vertical wall boundary layer equations requires initial conditions at $\tilde{x} = 0$ and the values of the unknown constants, c_1 and c_2. The initial conditions, in turn, provide one set of boundary conditions for the corner problem which is governed by elliptic equations and hence requires boundary conditions on all four boundaries for its solution. Thus the values of the unknown constants, c_1 and c_2, the initial conditions for the vertical wall boundary layer, and one set of boundary conditions for the corner problem are apriori unknown. If the values the constants, c_1 and c_2, and of each point on the initial profiles are regarded as parameters, there are $(2\infty + 2)$ parameters in the problem. The criteria for selecting the constants, c_1 and c_2, and the initial profiles follow from the centro-symmetry property of the governing equations and from the matching conditions. In principle, one guesses the initial profiles, $\tilde{T}_0(0,\tilde{y})$, $\tilde{u}_0(0,\tilde{y})$, $\tilde{p}_0(0,\tilde{y})$, and the values of the constants, c_1 and c_2, and then proceeds to integrate the governing equations. The resulting solution is then examined to determine if it is centro-symmetric and if it matches with the core and corner solutions. For a unique solution, only one set of constants and profiles will yield these results.

Matching of the Right-Hand Vertical Wall Boundary Layer and the Bottom Right-Hand Corner Region

Because of the nonsimilar nature of the vertical wall boundary layers, it was decided to perform an approximate solution using von Karman integral techniques. This solution will aid in understanding the gross nature of these flows and what is required to obtain their exact solutions. Before this can be accomplished, it remains to be shown that the corner regions do not have to be solved in order to solve the vertical wall boundary layers. This will be done by examining the matching of the right-hand vertical wall boundary layer and the bottom right-hand corner region. These regions definitely overlap in the direction perpendicular to the vertical wall (y^*-direction). However, ensuring overlap in the direction perpendicular to the horizontal wall (x^*-direction) leads to nontrivial matching conditions for the solutions in these two regions. To obtain these conditions, an intermediate coordinate, $\tilde{x}^i$, is introduced. This coordinate is defined for convenience as:

$$\tilde{x}^i \equiv \frac{x^*}{\tilde{L}^i_{rx}} = \frac{x^*}{\epsilon H} \qquad (2.149)$$

(the intermediate coordinate, $\tilde{x}^i$, is not unique.)

The one-term vertical wall boundary layer, or outer, solution for the streamfunction is given by:

$$\tilde{\psi} = \tilde{\psi}_0[\tilde{x},\tilde{y}] \tag{2.150}$$

Rewriting this solution in intermediate variables gives

$$\tilde{\psi} = \tilde{\psi}_0[\epsilon\ \tilde{x}^i,\tilde{y}] \tag{2.151}$$

Then, in physical variables the streamfunction is:

$$\tilde{\psi}^* = \frac{\nu_0}{\epsilon^2}\tilde{\psi}_0[\epsilon\ \tilde{x}^i,\tilde{y}] \tag{2.152}$$

The one-term bottom right-hand corner region, or inner, solution for the streamfunction may be written as:

$$\hat{\psi} = \hat{\psi}_0[\hat{x},\hat{y}] \tag{2.153}$$

Rewriting this solution in intermediate and outer variables gives

$$\hat{\psi} = \hat{\psi}_0\left[\left(\frac{\tilde{x}^i}{\epsilon^2}\right)\left(\frac{H}{W}\right)^{1/6},\ \left(\frac{\tilde{y}}{\epsilon}\right)\left(\frac{H}{W}\right)^{1/6}\right] \tag{2.154}$$

so that in physical variables the solution becomes:

$$\hat{\psi}^* = (\epsilon\nu_0)\left(\frac{W}{H}\right)^{\frac{1}{2}}\hat{\psi}_0\left[\left(\frac{\tilde{x}^i}{\epsilon^2}\right)\left(\frac{H}{W}\right)^{1/6},\ \left(\frac{\tilde{y}}{\epsilon}\right)\left(\frac{H}{W}\right)^{1/6}\right] \tag{2.155}$$

Comparison of equations (2.152) and (2.155) shows that the mass flowrate out of the corner into the vertical wall boundary layer is, to lowest order, zero even though the velocity is nonzero. (The mass flowrate is of higher order because of the small length scale perpendicular to the vertical wall.)

The one-term vertical wall boundary layer, or outer, solution for the vertical velocity is given by:

$$\tilde{u} = \tilde{u}_0[\tilde{x},\tilde{y}] \tag{2.156}$$

Rewriting this solution in intermediate variables yields:

$$\tilde{u} = \tilde{u}_0[\epsilon\ \tilde{x}^i, \tilde{y}] \tag{2.157}$$

Thus, in physical variables the velocity may be written as:

$$\tilde{u}^* = \left(\frac{\nu_0}{\epsilon^4 H}\right) \tilde{u}_0\left[\epsilon\ \tilde{x}^i, \tilde{y}\right] \tag{2.158}$$

The one-term bottom right-hand corner region, or inner, solution for the vertical velocity may be written as:

$$\hat{u} = \hat{u}_0[\hat{x}, \hat{y}] \tag{2.159}$$

Rewriting this solution in intermediate and outer variables

$$\hat{u} = \hat{u}_0\left[\left(\frac{\tilde{x}^i}{\epsilon^2}\right)\left(\frac{H}{W}\right)^{1/6}, \left(\frac{\tilde{y}}{\epsilon}\right)\left(\frac{H}{W}\right)^{1/6}\right] \tag{2.160}$$

so that in physical variables the vertical velocity is given by:

$$\hat{u}^* = \left(\frac{\nu_0}{\epsilon^2 H}\right)\left(\frac{W}{H}\right)^{1/3} \hat{u}_0\left[\left(\frac{\tilde{x}^i}{\epsilon^2}\right)\left(\frac{H}{W}\right)^{1/6}, \left(\frac{\tilde{y}}{\epsilon}\right)\left(\frac{H}{W}\right)^{1/6}\right] \tag{2.161}$$

Since the physical variables must match in the intermediate region, equations (2.158) and (2.161) give

$$\tilde{u}^* = \hat{u}^* \tag{2.162}$$

or,

$$\left(\frac{\nu_0}{\epsilon^4 H}\right) \tilde{u}_0[\epsilon\ \tilde{x}^i, \tilde{y}] = \left(\frac{\nu_0}{\epsilon^2 H}\right)\left(\frac{W}{H}\right)^{1/3} \hat{u}_0\left[\left(\frac{\tilde{x}^i}{\epsilon^2}\right)\left(\frac{H}{W}\right)^{1/6}, \left(\frac{\tilde{y}}{\epsilon}\right)\left(\frac{H}{W}\right)^{1/6}\right] \tag{2.163}$$

Thus;

$$\frac{\partial \tilde{\Psi}_0}{\partial \tilde{y}} = \tilde{u}_0[\epsilon\ \tilde{x}^i, \tilde{y}] = \epsilon^2\left(\frac{W}{H}\right)^{1/3} \hat{u}_0\left[\left(\frac{\tilde{x}^i}{\epsilon^2}\right)\left(\frac{H}{W}\right)^{1/6}, \left(\frac{\tilde{y}}{\epsilon}\right)\left(\frac{H}{W}\right)^{1/6}\right] \tag{2.164}$$

Integrating with respect to $\tilde{y}$ gives:

$$\tilde{\Psi}_0[\epsilon\,\tilde{x}^i,\tilde{y}] \sim \epsilon^3 \int \hat{u}_o \, d\left(\frac{\tilde{y}}{\epsilon}\right) \sim \epsilon^3 \, \hat{\Psi}_0\left[\left(\frac{\tilde{x}^i}{\epsilon^2}\right)\left(\frac{H}{W}\right)^{1/6}, \left(\frac{\tilde{y}}{\epsilon}\right)\left(\frac{H}{W}\right)^{1/6}\right] \qquad (2.165)$$

This implies that $\tilde{\Psi}_0 \to 0$ as $\tilde{x} \to 0$ unless $\tilde{\Psi} \to \infty$, or $\hat{\Psi}_0\left[\left(\frac{\tilde{x}^i}{\epsilon^2}\right)\left(\frac{H}{W}\right)^{1/6}, \left(\frac{\tilde{y}}{\epsilon}\right)\left(\frac{H}{W}\right)^{1/6}\right] \sim \frac{1}{\epsilon^3}$ as $\epsilon \to 0$.

On a physical basis the former of these two possibilities, that is,

$$\tilde{\Psi}_0 \to 0 \qquad \text{as } \tilde{x} \to 0 \qquad (2.166)$$

is taken as the correct result. Equation (2.166) shows that an approximate solution of the vertical wall boundary layer equations can be performed without first solving the corner equations.

Overall Rate of Heat Transfer Across the Enclosure

If an average heat transfer coefficient for the enclosure, $\bar{h}$, is defined as

$$\bar{h} \equiv \frac{\dot{Q}}{(T_b^* - T_a^*)(H)} \qquad (2.167)$$

where $\dot{Q}$ is the total rate of heat transfer across the enclosure, then:

$$\dot{Q} = \bar{h}\,(T_b^* - T_a^*)(H) = -\int_0^H K \left.\frac{\partial T^*}{\partial y^*}\right|_{y^*=H} dx^* \qquad (2.168)$$

Rewriting this equation in nondimensional form gives:

$$\bar{N}_{NU} = \left(\int_0^1 \left.\frac{\partial \tilde{T}}{\partial \tilde{y}}\right|_{\tilde{y}=0} d\tilde{x}\right) N_{GR}^{1/4} \qquad (2.169)$$

where: $\bar{N}_{NU} = \left(\frac{\bar{h}H}{K}\right) \equiv$ average Nusselt Number

In principle, the Nusselt number would be determined by finding the exact solutions of the right-hand corner regions, forming a composite expansion for $\left.\frac{\partial \tilde{T}}{\partial \tilde{y}}\right|_{\tilde{y}=0}$, and integrating this expression over the right-hand vertical wall as shown above.

CHAPTER III

APPROXIMATE SOLUTION OF THE ZEROTH-ORDER PROBLEM

Preliminary Remarks

The exact solution of the nonlinear set of partial differential equations (2.26) that govern the flow in the vertical wall boundary layers presents a formidable problem as these boundary layers are *non-similar*. Thus, in order to facilitate an understanding of the overall structure of the zeroth-order solution, it was necessary to resort to an approximate method of solving these equations. It was, therefore, decided to perform a Von Karman integral solution of the vertical wall boundary layer equations.

Formulation of the Integral Equations for the (Right-Hand) Vertical Wall Boundary Layer

As before, the governing equations and their boundary conditions for the (right-hand) vertical wall boundary layer are given by:

$$\frac{\partial \tilde{u}_0}{\partial \tilde{x}} + \frac{\partial \tilde{v}_0}{\partial \tilde{y}} = 0 \qquad \text{(continuity)} \tag{2.26a}$$

$$\tilde{u}_0 \frac{\partial \tilde{u}_0}{\partial \tilde{x}} + \tilde{v}_0 \frac{\partial \tilde{u}_0}{\partial \tilde{y}} = - \frac{\partial \tilde{p}_0}{\partial \tilde{x}} + \tilde{T}_0 + \frac{\partial^2 \tilde{u}_0}{\partial \tilde{y}^2} \qquad (\tilde{x}\text{-momentum}) \tag{2.26b}$$

$$\frac{\partial \tilde{p}_0}{\partial \tilde{y}} = 0 \qquad (\tilde{y}\text{-momentum}) \tag{2.26c}$$

$$\left(N_{PR}\right)\left(\tilde{u}_0 \frac{\partial \tilde{T}_0}{\partial \tilde{x}} + \tilde{v}_0 \frac{\partial \tilde{T}_0}{\partial \tilde{y}}\right) = \frac{\partial^2 \tilde{T}_0}{\partial \tilde{y}^2} \qquad \text{(energy)} \tag{2.26d}$$

with, $\tilde{u}_0(\tilde{x},0) = 0$ (2.27a)

$\tilde{v}_0(\tilde{x},0) = 0$ (2.27b)

$\tilde{T}_0(\tilde{x},0) = 1$ (2.27c)

(plus matching conditions with core and corner regions)

The spatial coordinate perpendicular to the vertical wall, $\tilde{y}$, has been nondimensionalized by a "characteristic" boundary layer thickness, $\tilde{\delta}$, as follows:

$$\tilde{y} = \frac{W - y^*}{\tilde{\delta}} = \frac{W - y^*}{\epsilon^2 H} \tag{2.9}$$

The variable, δ, used in the following analysis is defined as the actual boundary layer thickness, δ^*, normalized by the characteristic boundary layer thickness, $\tilde{\delta}$, or:

$$\delta \equiv \frac{\delta^*}{\tilde{\delta}} = \frac{\delta^*}{\epsilon^2 H} \tag{3.1}$$

Integrating the $\tilde{x}$-momentum equation (2.26b) from $\tilde{y} = 0$ to $\tilde{y} = \delta$, we have

$$\int_0^\delta \tilde{u}_0 \frac{\partial \tilde{u}_0}{\partial \tilde{x}}\, d\tilde{y} - \int_0^\delta \tilde{u}_0 \frac{\partial \tilde{v}_0}{\partial \tilde{y}}\, d\tilde{y} = - \int_0^\delta \frac{\partial \tilde{p}_0}{\partial \tilde{x}} + \int_0^\delta \tilde{T}_0\, d\tilde{y} - \left.\frac{\partial \tilde{u}_0}{\partial \tilde{y}}\right|_{\tilde{y}=0} \tag{3.2}$$

The continuity equation (2.26a) and the $\tilde{y}$-momentum equation (2.26c) may be written as

$$\frac{\partial \tilde{v}_0}{\partial \tilde{y}} = - \frac{\partial \tilde{u}_0}{\partial \tilde{x}} \tag{3.3}$$

and,

$$\tilde{p}_0 = \tilde{p}_0(\tilde{x}) \text{ only} \tag{3.4}$$

respectively.

Substituting these results in equation (3.2) and rearranging gives

$$\frac{d}{d\tilde{x}}\left[\int_0^{\delta} \tilde{u}_0^2 \, d\tilde{y}\right] = - \left(\frac{\partial \tilde{p}_0}{\partial \tilde{x}}\right)(\delta) + \int_0^{\delta} \tilde{T}_0 d\tilde{y} - \left.\frac{\partial \tilde{u}_0}{\partial \tilde{y}}\right|_{\tilde{y}=0} \tag{3.5}$$

which is the momentum integral equation for the (right-hand) vertical wall boundary layer.

Noting that the temperature at the edge of the boundary layer, $\tilde{T}_{0_\delta}$, is just the core temperature T_0,(which is a function of x only); the energy equation (2.26d) may be rewritten as

$$\left(N_{PR}\right)\left[\tilde{u}_0 \frac{\partial(\tilde{T}_0 - \tilde{T}_{0_\delta})}{\partial \tilde{x}} + \tilde{v}_0 \frac{\partial(\tilde{T}_0 - \tilde{T}_{0_\delta})}{\partial \tilde{y}}\right] = \frac{\partial^2(\tilde{T}_0 - \tilde{T}_{0_\delta})}{\partial \tilde{y}^2} - \left(N_{PR}\right)\left[\tilde{u}_0 \frac{\partial \tilde{T}_{0_\delta}}{\partial \tilde{x}}\right] \tag{3.6}$$

Integrating this equation from $\tilde{y} = 0$ to $\tilde{y} = \delta$ gives:

$$\int_0^{\delta} \tilde{u}_0 \frac{\partial(\tilde{T}_0 - \tilde{T}_{0_\delta})}{\partial \tilde{x}} d\tilde{y} - \int_0^{\delta} (\tilde{T}_0 - \tilde{T}_{0_\delta}) \frac{\partial \bar{v}_0}{\partial \tilde{y}} d\tilde{y}$$

$$= - \left(\frac{1}{N_{PR}}\right)\left[\left.\frac{\partial(\tilde{T}_0 - \tilde{T}_{0_\delta})}{\partial \tilde{y}}\right|_{\tilde{y}=0}\right] - \int_0^{\delta} \tilde{u}_0 \frac{\partial \tilde{T}_{0_\delta}}{\partial \tilde{x}} d\tilde{y} \tag{3.7}$$

Substituting the continuity equation (3.3) in equation (3.7) and rearranging we have

$$\frac{d}{d\tilde{x}}\left[\int_0^{\delta}(\tilde{u}_0)(\tilde{T}_0 - \tilde{T}_{0_\delta})d\tilde{y}\right] = -\left(\frac{1}{N_{PR}}\right)\left[\frac{\partial(\tilde{T}_0-\tilde{T}_{0_\delta})}{\partial\tilde{y}}\Bigg|_{\tilde{y}=0}\right] - \int_0^{\delta}\tilde{u}_0\,\frac{\partial\tilde{T}_{0_\delta}}{\partial\tilde{x}}\,d\tilde{y} \tag{3.8}$$

which is the energy integral equation for the (right-hand) vertical wall boundary layer.

The following set of approximate velocity and temperature profiles will be assumed in order to integrate equations (3.5) and (3.8):

$$\tilde{u}_0 = [\tilde{U}_0(\tilde{x})](\tilde{y}/\delta)(1 - \tilde{y}/\delta)^2 \tag{3.9a}$$

$$\tilde{T}_0 = \tilde{T}_{0_\delta} + (1 - \tilde{T}_{0_\delta})(1 - \tilde{y}/\delta)^2 \tag{3.9b}$$

where: $\tilde{U}_0(\tilde{x})$ is a function of $\tilde{x}$ only.

These profiles do not depict some of the details of the flow such as the velocity and temperature "overshooting" at the outer edge of the boundary layer (see for example, [11], [31]). However, as with all integral methods, even though the assumed profiles may not accurately portray the detailed structure of the flow; integrals of the profiles are fairly accurately represented because of the "smoothing" qualities of the integration process.

The temperature at the edge of the boundary layer, $\tilde{T}_{0_\delta}$, is given by the temperature in the core region, or:

$$\tilde{T}_{0_\delta} = T_0 \tag{3.10}$$

Equations (2.8) and (2.60) show that the vertical coordinate, in the vertical wall boundary layer, $\tilde{x}$, and the vertical coordinate in the core, x, are both scaled by the same reference length, H, or:

$$\tilde{x} = x = (x^*/H) \tag{3.11}$$

Therefore, equation (2.79) for the temperature distribution in the core and equation (3.11) may be substituted in equation (3.10) to yield:

$$\tilde{T}_{0_\delta} = c_1 \tilde{x} + c_2 \tag{3.12}$$

The $\tilde{y}$-momentum equation (2.25c) gives

$$\tilde{p}_0 = \tilde{p}_0(\tilde{x}) \tag{3.13}$$

that is, the pressure distribution in the core region is impressed on the vertical wall boundary layers. Therefore, equations (2.80), (2.87), (3.11) and (3.13) give:

$$\tilde{p}_0 = \tfrac{1}{2} c_1 \tilde{x}^2 + c_2 \tilde{x} \tag{3.14}$$

Substituting the assumed velocity and temperature profiles (3.9) and the expressions for the temperature at the edge of the boundary layer (3.12) and the pressure distribution (3.14) in the momentum integral (3.5) and energy integral (3.8) equations gives:

$$\frac{1}{105} \frac{d}{d\tilde{x}} \left[\delta \tilde{U}_0^2\right] = \left(\frac{\delta}{3}\right)\left(1 - c_1 \tilde{x} - c_2\right) - \left(\frac{\tilde{U}_0}{\delta}\right) \tag{3.15a}$$

$$\frac{1}{30} \frac{d}{d\tilde{x}} \left[\left(\delta \tilde{U}_0\right)\left(1 - c_1 \tilde{x} - c_2\right)\right] = \left(\frac{1}{N_{PR}}\right)\left(\frac{2}{\delta}\right)\left(1 - c_1 \tilde{x} - c_2\right) - \left(\frac{c_1}{12}\right)\left(\delta \tilde{U}_0\right) \tag{3.15b}$$

respectively.

These equations form a simultaneous set of two nonlinear, first-order, ordinary differential equations with variable coefficients and as such cannot be solved analytically in terms of known functions. Therefore, equations (3.15) will be solved numerically by means of a digital computer.

Numerical Solution of the Momentum Integral and Energy Integral Equations for the (Right-Hand) Vertical Wall Boundary Layer

Evaluation of the Unknown Constants, c_1 and c_2

Since equations (3.15) must be solved numerically, it is necessary at this point to specify the values of the unknown constants, c_1 and c_2. It was previously noted that if the exact solutions were known in all regions, these constants could be evaluated by matching. However, since the exact solutions are not known and yet the values of c_1 and c_2 are still required, plausibility arguments supplemented by the results of previous investigations will be used to evaluate these constants.

A typical streamline plot for the unicellular, laminar boundary layer flow regime is shown in Figure 3.1. Consider a fluid particle that traverses the enclosure on one of the "outside" streamlines; that is, a particle that travels almost the entire length of each of the vertical wall boundary layers. In the limit of $N_{GR} \to \infty$, one might intuitively expect that the particle would be heated up to the hot wall temperature by the time it reached the top of the hot wall boundary layer and began moving across the enclosure in the vicinity of the top horizontal wall. The plausibility of this intuitive result may be seen by examining the ratio of the characteristic time a fluid particle spends in the vertical wall boundary layer ("convection time") over the characteristic time for the diffusion of thermal energy from the wall out to the fluid particle ("diffusion time"). The convection time, t_c, for a

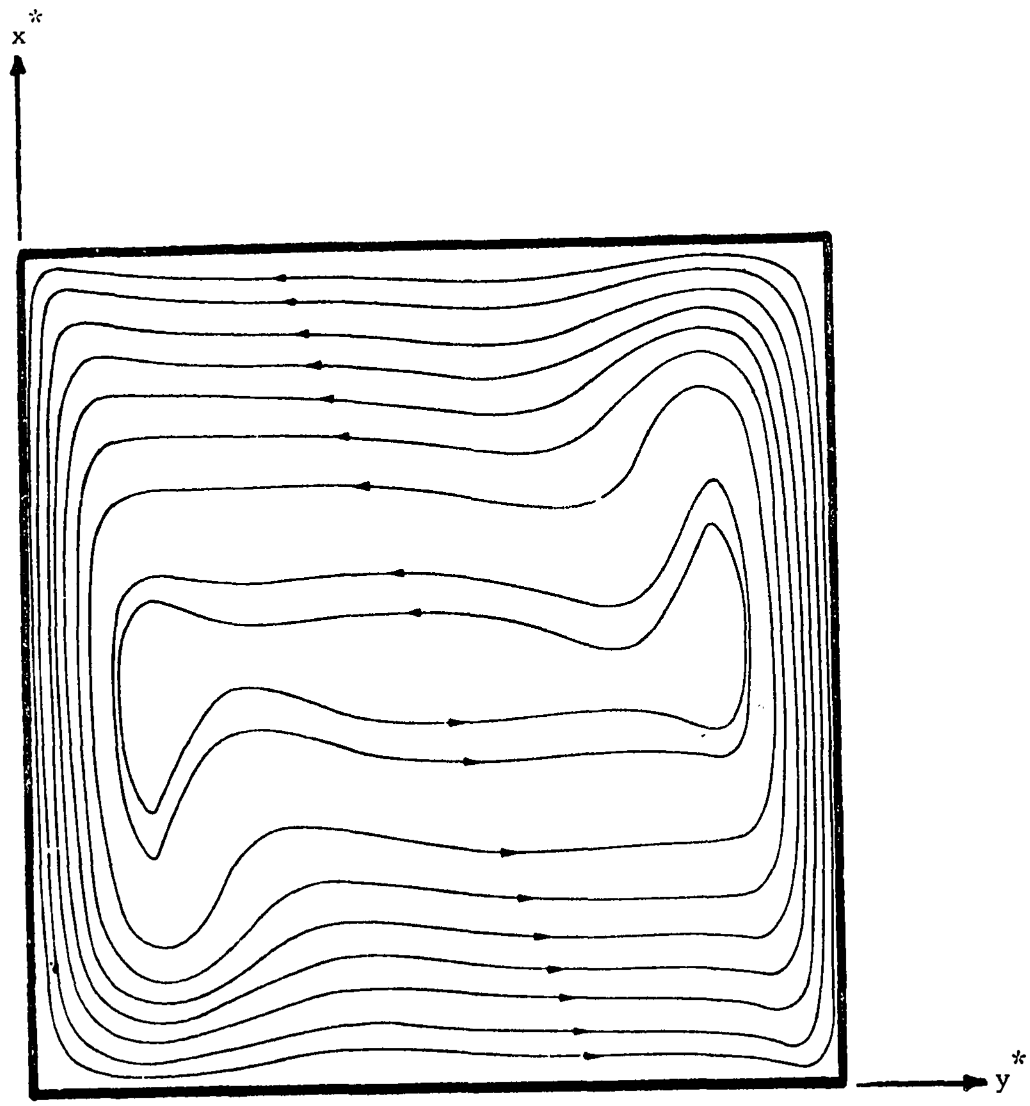

$N_{GR} = 10^6$

$N_{PR} = 1$

$H/W = 1$

Figure 3.1. Typical Streamline Configuration for the Unicellular Laminar Boundary-Layer Flow Regime

fluid particle moving at a distance y^* from the vertical wall is given by:

$$t_c \sim \frac{H}{(\tilde{u}_r)\left(\frac{y^*}{\tilde{\delta}}\right)} \tag{3.16}$$

Substituting the expressions for $\tilde{u}_r$ (2.14) and $\tilde{\delta}$ (2.15) in equation (3.16) gives:

$$t_c \sim \frac{H\,\tilde{y}}{N_{GR}^{1/4}} \tag{3.17}$$

The diffusion time, t_D, for the same particle may be written as:

$$t_D \sim \frac{y^{*2}}{\alpha_0} \tag{3.18}$$

or,

$$t_D \sim \frac{H^2\tilde{y}^2}{\alpha_0 N_{GR}^{1/2}} \tag{3.19}$$

The desired ratio of the convection time over the diffusion time is now given by equations (3.17) and (3.19) as:

$$\frac{t_c}{t_D} \sim \frac{1}{N_{PR}\tilde{y}^3} \tag{3.20}$$

For a fluid particle that enters the vertical wall boundary layer from the corner region, the distance from the vertical wall, $\tilde{y}$, may be approximated by the following expression:

$$\tilde{y} = \frac{\hat{\delta}}{\tilde{\delta}} \tag{3.21}$$

Substituting equations (2.15), (2.95), and (3.21) in equation (3.20) gives:

$$\frac{t_c}{t_D} \sim \left(\frac{1}{N_{PR}}\right)\left(\frac{H}{W}\right)^{\frac{1}{2}} N_{GR}^{3/8} \tag{3.22}$$

Thus, for Prandtl number, N_{PR}, and aspect ratio, (H/W), of order unity equation (3.22) yields

$$\frac{t_c}{t_D} \rightarrow \infty \quad \text{as} \quad N_{GR} \rightarrow \infty \quad ; \tag{3.23}$$

that is, the fluid particle spends a much greater time in the vertical wall boundary layer than is required for thermal energy to diffuse out from the wall to the particle.

Similarly, the fluid particle would be cooled to the cold wall temperature after traversing the cold wall boundary layer. Thus, the fluid in the top horizontal wall boundary layer would have a temperature of unity and the temperature of the fluid in the bottom horizontal wall boundary layer would be zero. Therefore, for the linear core temperature profile

$$T_0 = c_1 x + c_2 \tag{3.24}$$

to match these results, it is required that:

$$c_1 = 1 \tag{3.25a}$$

and,

$$c_2 = 0 \tag{3.25b}$$

The numerical results of Noble [11], the analytical results of Gill [13], and the experimental results of Ekert and Carlson [19] all suggest the validity of equations (3.25). Therefore, the values of c_1 and c_2 given by equations (3.25) will be used in the numerical solution of equations (3.15).

Substituting equations (3.25) in equations (3.15) gives:

$$\frac{1}{105}\frac{d}{d\tilde{x}}\left[\delta\, \tilde{U}_0^2\right] = \left(\frac{\delta}{3}\right)(1 - \tilde{x}) - \left(\frac{\tilde{U}_0}{\delta}\right) \tag{3.26a}$$

$$\frac{1}{30}\frac{d}{d\tilde{x}}\left[(\delta\, \tilde{U}_0)(1 - \tilde{x})\right] = \frac{(2)(1 - \tilde{x})}{(N_{PR})(\delta)} - \left(\frac{\delta\, \tilde{U}_0}{12}\right) \tag{3.26b}$$

Forms of the Momentum and Energy Integral Equations

Required for Numerical Integration

The momentum and energy integral equations (3.26) are integrated numerically using a fourth-order Runge-Kutta technique [35]. Thus, before proceeding, these equations must be recast in a form suitable for solution by this method. It proves convenient to define a new variable, F, as

$$F \equiv \delta\, \tilde{U}_0 \tag{3.27}$$

where F is analogous to a streamfunction.

Rewriting equations (3.26) in terms of the variables F and $\tilde{U}_0$ gives:

$$\frac{1}{105}\frac{d}{d\tilde{x}}(F\, \tilde{U}_0) = \frac{(F)(1 - \tilde{x})}{(3)(\tilde{U}_0)} - \frac{(\tilde{U}_0^2)}{(F)} \tag{3.28a}$$

$$\frac{1}{30}\frac{d}{d\tilde{x}}\left[(F)(1 - \tilde{x})\right] = \frac{(2)(\tilde{U}_0)(1-\tilde{x})}{(N_{PR})(F)} - \frac{(F)}{(12)} \tag{3.28b}$$

Equations (3.28) may be rearranged to give

$$\frac{dF}{d\tilde{x}} = \frac{(60)(\tilde{U}_0)}{(N_{PR})(F)} - \frac{(3)(F)}{(2)(1-\tilde{x})} \tag{3.29a}$$

$$\frac{d\tilde{U}_0}{d\tilde{x}} = \frac{(35)(1-\tilde{x})}{(\tilde{U}_0)} + \frac{(3)(\tilde{U}_0)}{(2)(1-\tilde{x})} - \left(\frac{60}{N_{PR}} + 105\right)\left(\frac{\tilde{U}_0^2}{F^2}\right) \tag{3.29b}$$

which are the "standard" forms required for the application of the Runge-Kutta technique.

Initial Values of the Variables F and $\tilde{U}_0$

In order to initiate the integration process it is necessary to obtain approximate analytical solutions of equations (3.29) that are valid near $\tilde{x} = 0$. These approximate solutions are found by recasting equations (3.29) as integral equations and then employing an iterative process to solve the integral equations near $\tilde{x} = 0$.

The momentum and energy integral equations (3.29) may be rewritten as:

$$\frac{dF^2}{d\tilde{x}} + \frac{3\ F^2}{(1-\tilde{x})} = \frac{(120)(\tilde{U}_0)}{(N_{PR})} \tag{3.30a}$$

$$\frac{d\tilde{U}_0^2}{d\tilde{x}} - \frac{(3)(\tilde{U}_0^2)}{(1-\tilde{x})} = (70)(1-\tilde{x}) - (21)\left(\frac{60}{N_{PR}} + 105\right)\left(\frac{\tilde{U}_0^3}{F^2}\right) \tag{3.30b}$$

These equations are both of the form

$$\frac{dy}{dx} + P(x)y = Q(x) \tag{3.31}$$

for which the general solution is given by:

$$y = e^{-\int P\,dx}\left[\int Q\, e^{\int P\,dx}\, dx + (\text{constant})\right] \tag{3.32}$$

Thus, equations (3.30) may be rewritten as the following set of integral equations:

$$F^2 = [1-\tilde{x}]^3\left[F^2(0) + \left(\frac{120}{N_{PR}}\right)\int_0^{\tilde{x}} \frac{\tilde{U}_0}{(1-\tilde{x})^3}\, d\tilde{x}\right] \tag{3.33a}$$

$$\tilde{U}_0^2 = \left[\frac{1}{(1-\tilde{x})^3}\right]\left\{\tilde{U}_0^2(0) + [14][1 - (1-\tilde{x})^5] - \left[\frac{120}{N_{PR}} + 210\right]\int_0^{\tilde{x}} \frac{(1-\tilde{x})^3\tilde{U}_0^3}{F^2}\, d\tilde{x}\right\} \tag{3.33b}$$

Near $\tilde{x} = 0$, equations (3.33) reduce to

$$F^2 = \left(\frac{120}{N_{PR}}\right) \int_0^{\tilde{x}} \tilde{U}_0 \, d\tilde{x} \tag{3.34a}$$

$$\tilde{U}_0^2 = (70)\tilde{x} - \left(\frac{120}{N_{PR}} + 210\right) \int_0^{\tilde{x}} \frac{\tilde{U}_0^3}{F^2} \, d\tilde{x} \tag{3.34b}$$

where it has been assumed that $F(0) = \tilde{U}_0(0) = 0$. Assume the following solutions to be valid near $\tilde{x} = 0$

$$\tilde{U}_0 = \alpha \, \tilde{x}^{1/2} \tag{3.35a}$$

$$F^2 = \beta \, \tilde{x}^{3/2} \tag{3.35b}$$

where α and β are constants.

Substituting these assumed solutions (3.35) in equations (3.34) and performing the required integration yields:

$$(\beta)\tilde{x}^{3/2} = \left(\frac{80\ \alpha}{N_{PR}}\right) \tilde{x}^{3/2} \tag{3.36a}$$

$$(\alpha^2)\tilde{x} = \left[(70) - \left(\frac{120}{N_{PR}} + 210\right)\left(\frac{\alpha^3}{\beta}\right)\right] \tilde{x} \tag{3.36b}$$

Thus, if

$$\beta = \frac{80\alpha}{N_{PR}} \tag{3.37}$$

and,

$$\alpha = \left[\frac{70}{\frac{5}{2} + \frac{21\ N_{PR}}{8}}\right]^{\frac{1}{2}} \tag{3.38}$$

the solutions (3.35) are exact near $\tilde{x} = 0$ and no further iteration is required. Substituting equations (3.37) and (3.38) in equations (3.35) gives:

$$\tilde{U}_0 = \left[\frac{70}{\frac{5}{2} + \frac{21\ N_{PR}}{8}}\right]^{\frac{1}{2}} \tilde{x}^{\frac{1}{2}} \tag{3.39}$$

$$F = \left[\frac{80}{N_{PR}}\right]^{\frac{1}{2}} \left[\frac{70}{\frac{5}{2} + \frac{21\ N_{PR}}{8}}\right]^{\frac{1}{2}} \tilde{x}^{3/4} \tag{3.39b}$$

Equations (3.39) are used to start the integration process by computing the values of F and $\tilde{U}_0$ at the end of the first integration interval ($\tilde{x}$ = h). These equations, however, do not contain any free parameters and, hence, the results of the numerical integration are dependent upon the nature of the approximate solutions (3.39) used to initiate the process. Therefore, some criterion must be established for determining the validity of the approximate solutions (3.39) inasmuch they affect the overall results of the numerical integration process.

Criterion For Evaluating the Suitability of the Approximate Solutions Used to Initiate the Integration Process

The criterion for evaluating the suitability of the appoximate solutions used to start the numerical integration is based upon the centro-symmetry property of the flow. This property requires that the velocities be "reflected" about the geometric center of the enclosure ($x^* = H/2$, $y^* = W/2$). Consider the core velocities at the edges of the vertical wall boundary layers as shown in Figure 3.2. Centro-symmetry requires that:

$$(\vec{V})_A = - (\vec{V})_C \tag{3.40}$$

However, to lowest order, it has been shown that the vertical velocity in the core is identically zero, or:

$$u_0 = 0 \tag{2.86}$$

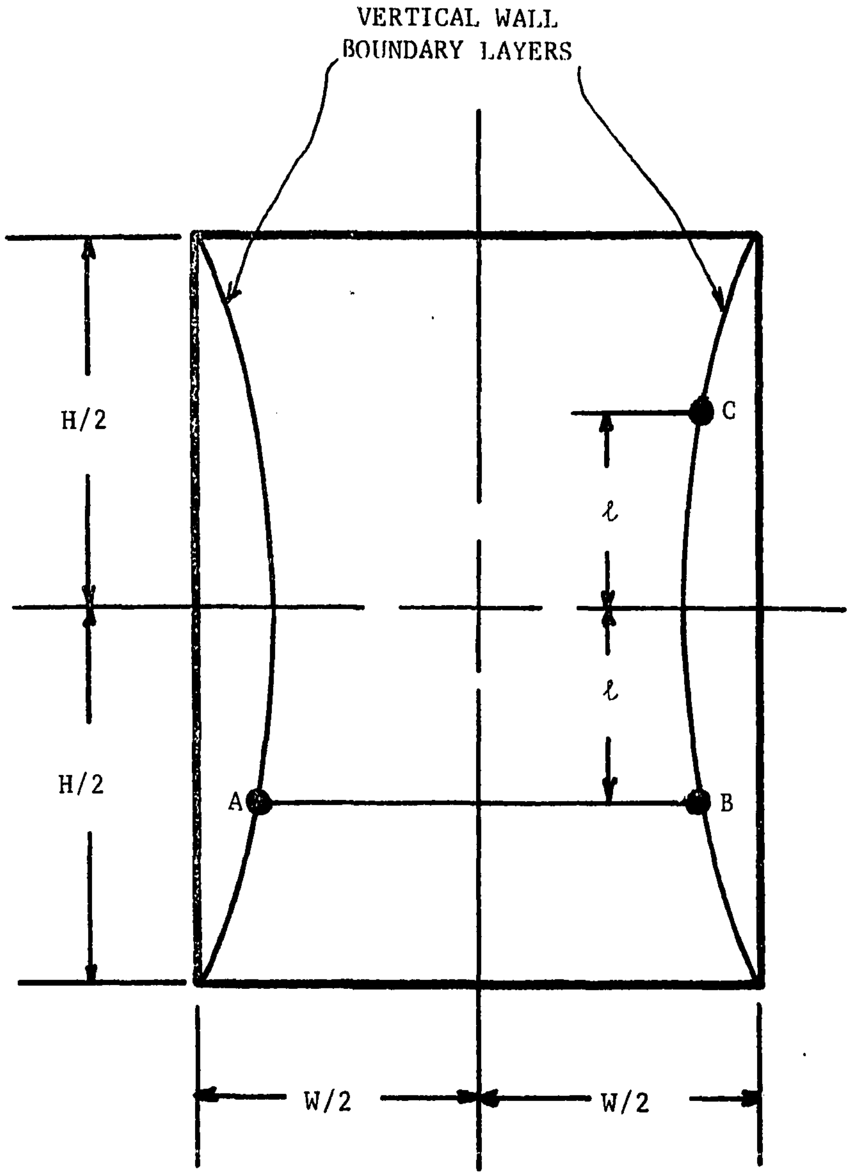

Figure 3.2. Velocity Components in the Core Region

Therefore, equation (3.40) reduces to

$$(v_0)_A = - (v_0)_C \tag{3.41}$$

Furthermore, since $u_0 = 0$, it can be seen that

$$(v_0)_A = (v_0)_B \tag{3.42}$$

Thus, equations (3.41) and (3.42) give

$$(v_0)_B = - (v_0)_C \tag{3.43}$$

that is, the entrainment-extrainment flow for the vertical wall boundary layer must be antisymmetric about $x^* = H/2$. This, in turn, requires that:

$$v_0\Big|_{x^*} = H/2 = 0 \tag{3.44}$$

Therefore, the centro-symmetry property of the flow requires that the resulting solutions be such that the horizontal velocitiy at the edge of the boundary layer is identically zero at $x^* = H/2$.

Expression for the Horizontal Velocity at the Edge of the (Right-Hand) Vertical Wall Boundary Layer

The horizontal velocity at the edge of the vertical wall boundary layer must be calculated since it provides the criterion for evaluating the method used to initiate the numerical solution. Also, since the velocity is just the entrainment-extrainment velocity, it is the velocity distribution in the core region.

The continuity equation for the (right-hand) vertical wall boundary layer equation is given by:

$$\frac{\partial \tilde{u}_0}{\partial \tilde{x}} + \frac{\partial \tilde{v}_0}{\partial \tilde{y}} = 0 \qquad (2.26a)$$

Integrating this equation across the boundary layer gives:

$$(\tilde{v}_0)_\delta = - \frac{d}{d\tilde{x}} \left[\int_0^1 (\delta\ \tilde{u}_0)\ d(\tilde{y}/\delta) \right] \qquad (3.45)$$

Substituting equation (3.9a) for $\tilde{u}_0$ in equation (3.45) yields:

$$(v_0)_\delta = - \frac{1}{12} \frac{d(\delta \tilde{u}_0)}{d\tilde{x}} = - \frac{1}{12} \frac{dF}{d\tilde{x}} \qquad (3.46)$$

Finally, substituting equation (3.29a) in equation (3.46) gives

$$(v_0)_\delta = - \frac{(5)(\tilde{U}_0)}{(N_{PR})(F)} + \frac{(F)}{(8)(1-\tilde{x})} \qquad (3.47)$$

which is the horizontal velocity at the edge of the vertical wall boundary layer.

Nusselt Number For the Approximate Solution

An expression for the Nusselt number was found to be:

$$\bar{N}_{NU} = N_{GR}^{1/4} \int_0^1 \left. \frac{\partial \tilde{T}}{\partial \tilde{y}} \right|_{\tilde{y}=0} d\tilde{x} \qquad (2.169)$$

Thus, for the zeroth-order solution:

$$\bar{N}_{NU} = N_{GR}^{1/4} \int_0^1 \left. \frac{\partial \tilde{T}_0}{\partial \tilde{y}} \right|_{\tilde{y}=0} d\tilde{x} \qquad (3.48)$$

Substituting equation (3.9b) in equation (3.48) gives:

$$\bar{N}_{NU} = - 2\ N_{GR}^{1/4} \int_0^1 \left(\frac{1 - \tilde{x}}{\delta} \right) d\tilde{x} \qquad (3.49)$$

Equation (3.49) is integrated numerically.

CHAPTER IV

PRESENTATION OF RESULTS

Preliminary Remarks

The stated objectives of this analysis are:

(1) prediction of the detailed structure of the flowfield, and

(2) prediction of the total rate of heat transfer through the fluid from one vertical wall to the other.

Thus, the accuracy of the solution will be assessed by comparing both the velocity and temperature profiles and the correlation for the overall rate of heat transfer with the results of previous investigations. After making these comparisons the implications of the present study about the general nature of enclosed natural convection flows will be discussed.

Comparison of the Velocity and Temperature Distributions With the Numerical Results Obtained by Noble

The vertical velocity and the temperature profiles at H/2 and the horizontal velocity profile in the core will be compared with the finite difference solutions of Noble [11] for a flow with a Grashof number, N_{GR}, of 10^6, a Prandtl number, N_{PR}, of unity, and an aspect ratio, (H/W), of unity. These comparisons are shown in Figures 4.1 to

4.3, respectively. The velocity and temperature profiles exhibit the expected nature of a von Karman integral solution; that is, they do not accurately predit the detailed structure of the flowfield. The most serious discrepancy, however, is shown in Figure 4.3 which reveals that the core velocity, v_0, becomes infinite near x = 0 and x = 1. Indeed, equations (3.35b) and (3.46) show that

$$v_0 \sim x^{-\frac{1}{4}} \tag{4.1}$$

near x = 0. Thus, the core velocity in the appoximate zeroth-order solution cannot be matched with the linear velocity profiles in the horizontal wall boundary layers (2.140b), (2.141b). This appears to be due to the nature of the assumed profiles in the approximate solution of the vertical wall boundary layers. The singularity is identical to the leading edge singularity found in the integral solution of the natural convection flow on a vertical, isothermal plate immersed in an isothermal fluid of infinite extent [36].

Comparison of the Correlation for the Overall Rate of Heat Transfer Across the Enclosure with the Results of Previous Investigations

Equation (3.49) for the Nusselt number, $\bar{N}_{NU}$, was integrated numerically on a digital computer. The results are shown in Table 4.1. Correcting these results for Prandtl number gives

$$\bar{N}_{NU} = \left(\frac{\bar{h}H}{K}\right) = (.18)\left(N_{RA}\right)^{1/4} \tag{4.2}$$

where the Rayleigh number, N_{RA}, is defined as the product of the Grashof number, N_{GR}, and the Prandtl number, N_{PR}. This correlation will now be

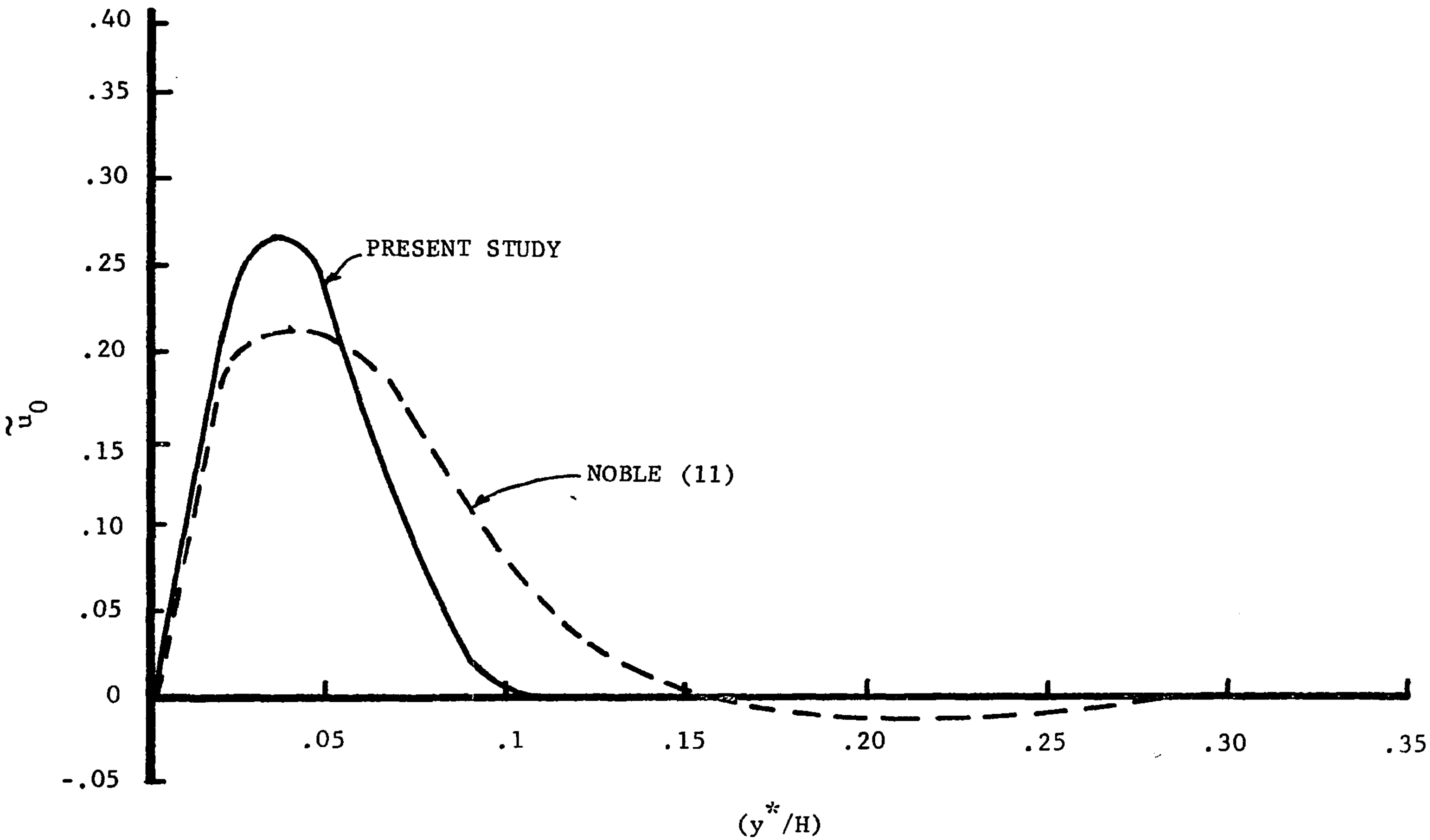

Figure 4.1. Vertical Velocity Traverse at H/2

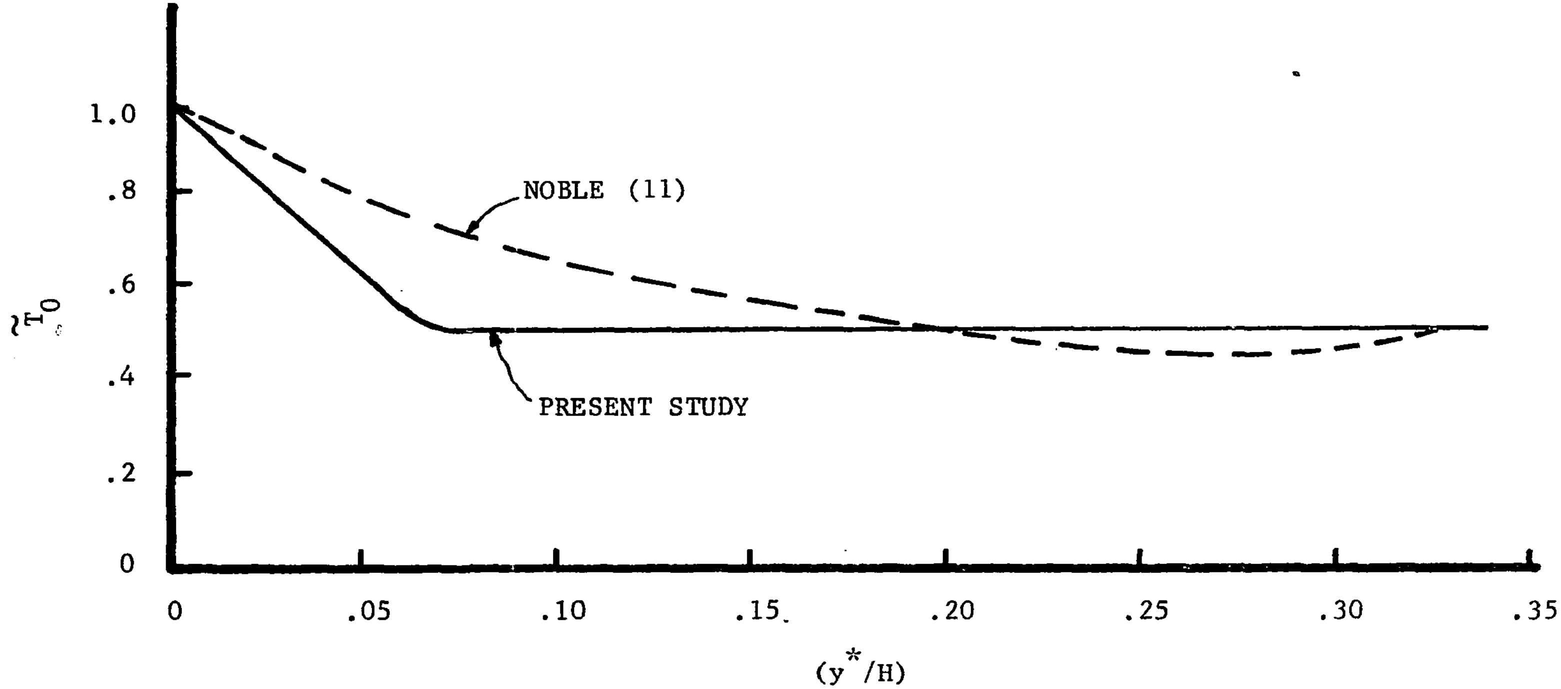

Figure 4.2. Temperature Traverse at H/2

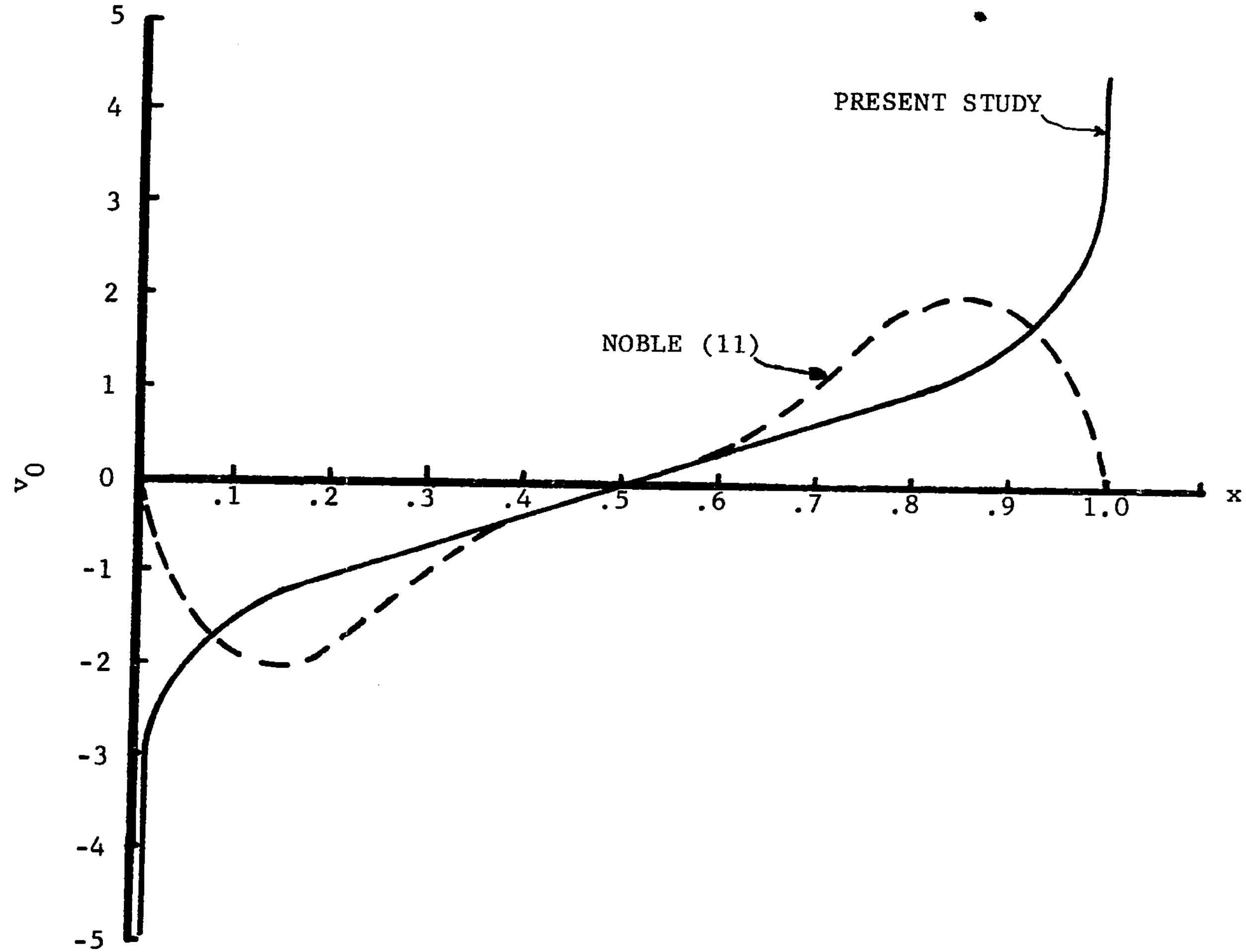

Figure 4.3. Velocity Distribution in the Core

Prandtl Number	$\int_0^1 \left. \frac{\partial \tilde{T}_0}{\partial \tilde{y}} \right\|_{\tilde{y}=0} d\tilde{x}$
.73	.16678
1.00	.18038
1.05	.18590
1.10	.18637
2.00	.21872

Table 4.1. Coefficients for Equation (3.49)
Obtained by Numerical Integration

compared with the numerical and experimental results of several previous investigations.

Jakob [23] analyzed the experimental data of Mull and Reiher [37] and proposed the following correlations:

$$\bar{N}_{NU} = (.18)\left(N_{GR}\right)^{1/4}\left(\frac{H}{W}\right)^{5/36} \qquad (4.3)$$

for $(2)(10^4) < N_{GR}(W/H)^3 < (10^5)$. Correcting for Prandtl number gives:

$$\bar{N}_{NU} = (.19)\left(N_{RA}\right)^{1/4}\left(\frac{H}{W}\right)^{5/36} \qquad (4.4)$$

Based on their experimental results, Eckert and Carlson [19] suggested that

$$\bar{N}_{NU} = (.119)\left(N_{GR}\right)^{.3} \qquad (4.5)$$

for $(10^4) < N_{GR} < (5)(10^6)$, which may be corrected for Prandtl number to give:

$$\bar{N}_{NU} = (.126)\left(N_{RA}\right)^{.3} \qquad (4.6)$$

The exponent (.3) in this correlation suggests that the flows in the vertical wall boundary layers of Eckert and Carlsons' experiments were turbulent. Their visual observations with a Zehnder-Mach interferometer, however, confirmed that these flows were laminar. They assumed that the thermally stratified flow in the core is somehow responsible for the relatively high value of the exponent. At the present time, this point has not been resolved and other investigators, such as de Vahl Davis [26] and Newell and Schmidt [25], have reported even higher values of this exponent (.315 and .397, respectively).

Noble [11] has shown that the data from both his finite difference solution and those of Wilkes [37] correlate with:

$$\bar{N}_{NU} = (.233)\left(N_{RA}\right)^{.28}\left(\frac{H}{W}\right)^{.16} \qquad (4.7)$$

for $(10^4) < (N_{RA})(W/H)^3 < (10^6)$.

The correlation derived in the present study (4.2) and the correlation of Eckert and Carlson (4.6) do not exhibit any dependence of the Nusselt number, $\bar{N}_{NU}$, on the aspect ratio, (H/W), while the correlations of Jakob (4.4) and Noble (4.7) show only a weak dependence of the Nusselt number on this parameter. This implies that the rate of heat transfer across the enclosure is essentially independent of the width of the enclosure, W. This appears to result as in the laminar boundary layer regime the vertical wall boundary layers are separate and distinct with a structure which is independent of the enclosure width.

All of the above correlations are plotted in Figure 4.4 for an aspect ratio, (H/W), of unity. The results of this work are shown to be in good agreement with the results of both the numerical and the experimental studies. Thus, as is typical with integral methods, the overall, or gross, aspects of the flow, such as the total rate of heat transfer, are predicted with some degree of accuracy.

Remarks on the General Problem of Contained Natural Convection Flows

Van Dyke [34] has pointed out that a most curious feature of perturbation methods is that they may supriously change the type of the governing partial differential equations. The most striking example of this feature is the "boundary layer approximation" where the Navier-Stokes equations, which are elliptic, are replaced by parabolic equations inside the boundary layer. Thus, as was shown in Chapter II, the zeroth-order

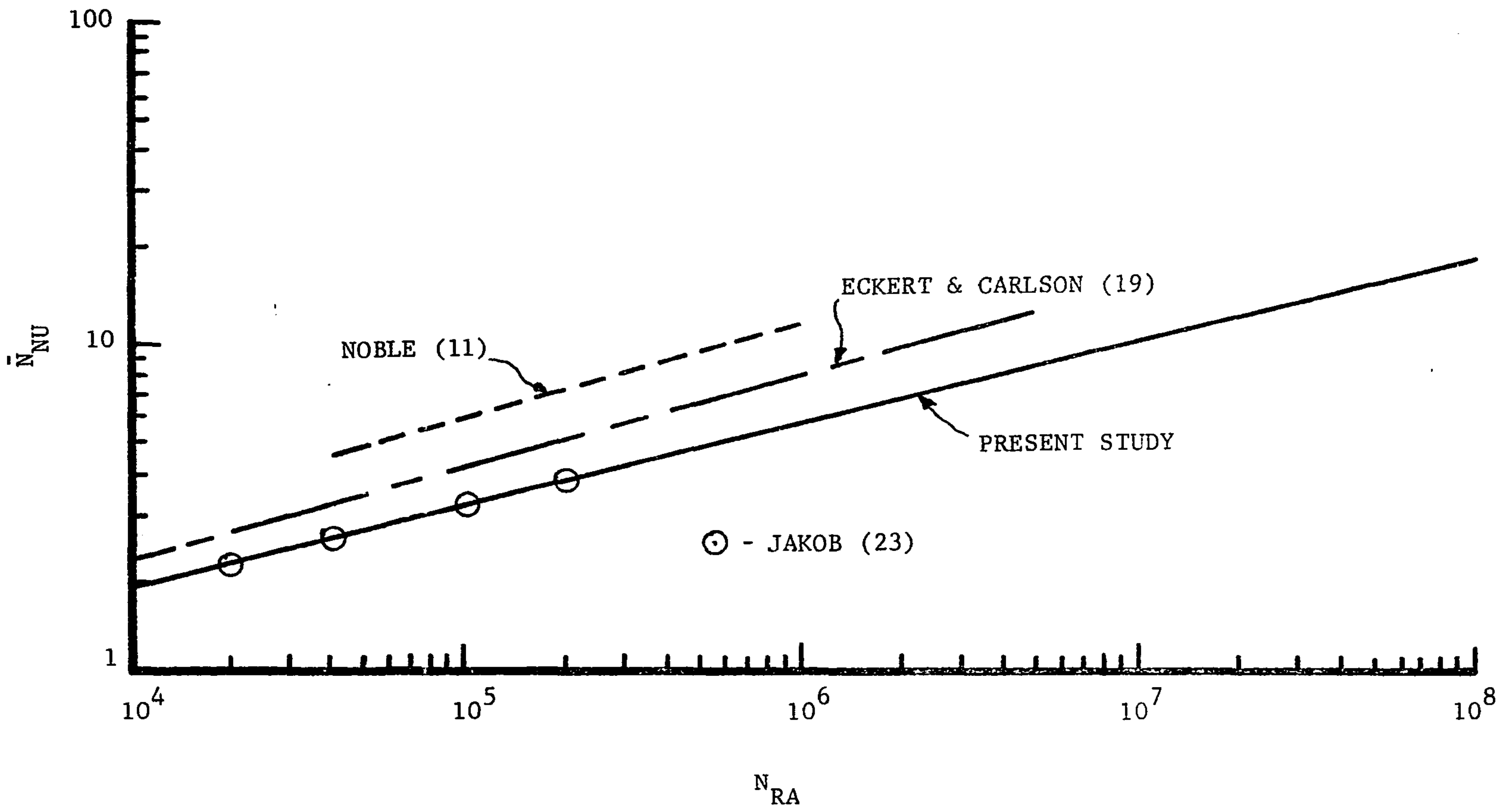

Figure 4.4. Heat Transfer Correlations

is ejected from the bottom of the left-hand vertical wall boundary layer, moves across the core in the manner described above, and enters the bottom of the right-hand vertical wall boundary layer. This completes an entire circuit around the enclosure and the particle is now able to again influence the flow at the point where it began the circuit. The characteristic time for a fluid particle to make a complete circuit around the enclosure is given by:

$$t_{cir} = \left(\frac{2H}{\tilde{u}_r}\right) + \left(\frac{2W}{v_r}\right) \approx \epsilon^2 \left(\frac{2HW}{\nu_0}\right) \tag{4.8}$$

Similarly, the characteristic time spent in the vertical wall boundary layers by a typical fluid particle is:

$$t_{VWBL} = \left(\frac{2H}{\tilde{u}_r}\right) = \epsilon^4 \left(\frac{2H^2}{\nu_0}\right) \tag{4.9}$$

The time scale for the "upstream influence" on the vertical wall boundary layers (t_{cir}) must, however, be considered in relation to the time a fluid particle spends in the vertical wall boundary layers (t_{VWBL}). Thus, forming their ratio gives:

$$\frac{t_{cir}}{t_{VWBL}} = \left(\frac{1}{\epsilon^2}\right)\left(\frac{W}{H}\right) = \left(\frac{W}{H}\right) N_{GR}^{1/4} \tag{4.10}$$

so that

$$\frac{t_{cir}}{t_{VWBL}} \to \infty \qquad \text{as} \qquad N_{GR} \to \infty$$

unless $(H/W) \sim N_{GR}^{1/4}$. This latter possibility is excluded, however, since the present analysis is only for aspect ratios of order unity. Therefore, even though the vertical wall boundary layers are governed vertical wall boundary layer equations (2.26) are a second order set of nonlinear, parabolic partial differential equations. It is well-known that flows governed by parabolic equations may be characterized as having "no upstream influence"; that is, the flow at any point in the flowfield depends only on the flow upstream of that point and is not influenced by the downstream flow. Thus, in external boundary layer flows where a given fluid particle is assumed to pass through the flow-field only once, there is never any "upstream influence", on the lowest order solution. In completely enclosed natural convection flows, however, a fluid particle passes through a given point in the flowfield again and again. Consider a fluid particle that traverses the enclosure on one of the "outside" streamlines as shown in Figure 3.1, that is, a particle that traverses almost the entire length of each of the vertical wall boundary layers. As the particle (say) enters the bottom of the right-hand vertical wall boundary layer, its temperature is increased by an energy transfer from the wall and it is accelerated up the wall in the boundary layer by the resulting bouyant force. In order to conserve mass for the entire enclosure, the particle is ejected from the right-hand vertical wall boundary layer near the top horizontal wall and travels across the enclosure on a horizontal streamline in the core. Since the isotherms are also horizontal in the core, the temperature of the particle remains constant as it crosses this region. The particle then enters the left-hand vertical wall boundary layer, where its temperature is decreased by an energy transfer to the wall, and it is accelerated down the wall in the boundary layer by the bouyant force. Again, in order to conserve mass for the entire enclosure, the particle by parabolic partial differential equations, there is a "longtime upstream influence" on the zeroth-order flow implied by the matching conditions. Thus, the flow will exhibit a "pseudo-elliptic" type of behavior and, in this respect, it is significantly different from external natural convection boundary layer flows.

CHAPTER V

CONCLUSIONS AND RECOMMENDATIONS

Conclusions

The following major conclusions may be drawn from the results of this work:

(1) The physical nature of the flows in all regions of the flowfield, including the corners, have been explained for the first time. The crucial point of this part of the analysis is the determination of the correct force balance in the core. The resulting pressure-buoyancy force balance gives the empirically observed linear temperature profile in the core-region, which, in turn, validates the assumptions made in scaling the vertical and horizontal wall boundary layers.

(2) The most difficult mathematical problem is encountered in the solution of the nonsimilar vertical wall boundary layers which are governed by a second-order set of nonlinear, parabolic differential equations.

(3) As expected, the approximate integral solution of the vertical wall boundary layer equations does not accurately portray the details of the flow but does give a reasonably accurate correlation for the overall rate of heat transfer across the enclosure. The accuracy of the integral solution could probably be improved by a

more judicious choice of velocity and temperature profiles.

(4) The "pseudo-elliptic" behavior of completely enclosed natural convection flows is shown here for the first time.

Recommendations for Future Research

The problems recommended for future research may be divided into two categories:

(1) improvements of the present solution, and

(2) problems similar to the one analyzed in this work that may be analyzed by applying the methodology developed here.

The first of the above categories includes the following problems:

(a) the "exact" (at least in a numerical sense) solution of the vertical wall boundary layer equations

(b) investigation of the above solution to determine if it can be used to predict the onset of multicell flows

(c) higher order solutions

(d) solutions for which the Prandtl number is not of order unity, and

(e) exact solutions of the flows in the corner regions

The exact solution of the vertical wall boundary layer equations presents a formidable mathematical problem as they are <u>nonsimilar</u>. The most fruitful approach would probably be to use the asymptotic methods developed by Meksyn [39], since these methods would yield analytical solutions that would allow the matching to be carried out explicitly. The variational techniques proposed by Schechter [40] also have the potential for giving the solution in an analytical form. Even the purely numerical techniques, such as those developed by Merkin [41] and Clutter and Smith [42], would be difficult to apply, since it has already been shown that their application would require guessing the values of each of the points on the initial profiles in addition to the values of the constants c_1 and c_2 ($2\infty + 2$ parameters) before integrating the equations.

Inspection of finite difference solutions and experimental data suggests that carrying out the higher order solutions may be important since they may add significant corrections to the lowest order solution. These corrections may be relatively large since the expansions proceed in integral powers of the smaller parameter, ϵ; that is, in powers of $N_{GR}^{-1/8}$. Thus, at a Grashof number of (say) 10^4, the first order corrections would have a value of approximately .3.

Solutions for which the Prandtl number is not of order unity would require that the governing equations be rescaled; since there would be a second small parameter (the Prandtl number, N_{PR}, raised to a power) in the problem.

The exact solutions of the flows in the corner regions also pose a difficult mathematical problem as the method of matching these solutions with the solutions of the horizontal and vertical wall boundary layer equations is not completely understood at the present time.

The second category of problems recommended for future research includes:

(a) investigation of the present problem for the case of turbulent flow

(b) flows resulting from applying different boundary conditions to the present problem , and

(c) flows for which the usual Boussinesq approximation breaks down.

In general, the methodology developed in the present problem can be applied to the case of turbulent flow; however, the governing equations would have a different form in order to model the turbulence.

Flows that result from applying different boundary conditions to the present problem include the cases of constant temperature (or heat flux) horizontal walls, the case of a free upper horizontal surface, and the so-called "mixed case" of a constant temperature on one vertical wall and a constant heat flux on the other. The solutions of these problems should not differ significantly from the present solution except in cases where the thermal boundary conditions on the horizontal walls would tend to produce an unstable stratification of the core region. The latter situation could occur, for instance, if the bottom horizontal wall was maintained at a temperature higher than that of the "cold" vertical wall.

One of the most important flows for which the Boussinesq approximation breaks down is the case of variable fluid properties. In a discussion of a paper by MacGregor and Emery [20], Landis has shown that the temperature distribution may be affected to the same order of a variable thermal conductivity as by a variable viscosity. Thus, any study of the variable property case would have to include a variable thermal conductivity as well as a variable viscosity.

REFERENCES

1. Anderson, B.H., and Kolar, M.J.,"Experimental Investigation of the Behavior of a Confined Fluid Subjected to Nonuniform Source and Wall Heating," NASA Technical Note D-2079, 1963.
2. Barakat, H.Z., and Clark, J.A., "Analytical and Experimental Study of the Transient Laminar Natural Convection Flows in Partially Filled Containers," Proceedings of the Third International Heat Transfer Conference, 1966, pp. 113-120.
3. Barrett, D.O., Winstead, T.W., and McReynolds, L.S., "An Investigation of Liquid Hydrogen Stratification in a Large Cylindrical Tank of the Saturn Configuration," Advances in Cryogenic Engineering, Vol. 10, K.D. Timmerhaus, ed., Plenum Press, New York, 1965, pp. 314-324.
4. Bourgarel, M.H., Segel, M.P., and Huffenus, J.P., "Study of Stratification Similitude Laws in Liquid Hydrogen," Advances in Cryogenic Engineering, Vol. 12, K.D. Timmerhaus, ed., Plenum Press, New York, 1967, pp. 103-111.
5. Harper, E.Y., et al., "Analytical and Experimental Study of Stratification in Standard and Reduced Gravity Fields," Proceedings of the Conference on Propellant Tank Pressurization and Stratification, Vol. II, Marshall Space Flight Center, January, 1965.
6. Kolar, M.J., "Experimental Investigation of the Thermal Boundary Layer in a Confined Liquid," NASA Technical Note D-3393, 1966.

7. Ruder, J.M., "Stratification in a Pressurized Container with Side-wall Heating," AIAA Journal, Vol. 2, No. 1, 1964, p. 135.

8. Segel, M.P., "Experimental Study of the Phenomena of Stratification and Pressurization of Liquid Hydrogen," Advances in Cryogenic Engineering, Vol. 10, K.D. Timmerhaus, ed., Plenum Press, New York, 1965, pp. 308-313.

9. Vliet, G.E., et al., "Stratified Layer Flow Model: A Numerical Approach to Liquid Temperature Stratification," Journal of Space-craft and Rockets, Vol. 1, No. 6, 1964.

10. Chin, J.H., et al., "Analytical and Experimental Study of Stratification and Liquid-Ullage Coupling," Lockheed Missiles and Space Company Report 2-05-65-1, Aug. 1, 1965.

11. Noble, J.J., "The Effect of Radiative Transfer on Natural Convection in Enclosures: A Numerical Investigation," Ph.D. dissertation, Massachusetts Institute of Technology, April, 1968.

12. Noble, J.J., et al., "Mathematical and Experimental Modeling of the Circulation Patterns in Glass Melts," Journal of Heat Transfer, Trans. ASME, Series C, Vol. 94, May 1962, p. 149.

13. Gill, A.E., "The Boundary Layer Regime for Convection in a Rectangular Cavity," Journal of Fluid Mechanics, Vol. 26, Part 3, 1966, pp. 515-536.

14. Bayley, F.J., and Lock, G.S.H., "Heat Transfer Characteristics of the Closed Thermosyphon," Journal of Heat Transfer, Trans. ASME, Series C, Vol. 87, No. 1, Feb. 1965, pp. 30-40.

15. Japikse, D., and Winter, E.R.F., "Single Phase Transport Processes in the Open Thermosyphon," International Journal of Heat Transfer, Vol. 14, No. 3, March 1971, pp. 427-442.

16. Japikse, D., Jallouk, P.A., and Winter, E.R.F., "Single Phase Transport Processes in the Closed Thermosyphon," International Journal of Heat and Mass Transfer, Vol. 14, No. 7, July 1971, pp. 869-888.

17. Elder, J.W., "Laminar Free Convection in a Vertical Slot," Journal of Fluid Mechanics, Vol. 23, Part 1, 1965, pp. 77-98.

18. Elder, J.W., "Turbulent Free Convection in a Vertical Slot," Journal of Fluid Mechanics, Vol. 23, Part 1, 1965, pp. 99-111.

19. Eckert, E.R.G., and Carlson, W.O.,"Natural Convection in an Air Layer Enclosed Between Two Vertical Plates with Different Temperatures," International Journal of Heat and Mass Transfer, Vol. 2, 1961, pp. 106-120.

20. MacGregor, R.K., and Emery, A.F., "Free Convection Through Vertical Plane Layers - Moderate and High Prandtl Number Fluids," ASME Paper 68-WA/HT-4, 1968.

21. Emery, A., and Chu, N.C., "Heat Transfer Across Vertical Layers," Journal of Heat Transfer, Trans. ASME, Series C, Vol. 87, No. 1, Feb. 1965, pp. 110-116.

22. Dropkin, D., and Somerscales, E., "Heat Transfer by Natural Convection in Liquids Confined by Two Parallel Plates Which Are Inclined at Various Angles with Respect to the Horizontal," Journal of Heat Transfer, Trans. ASME, Series C, Vol. 87, No. 1, Feb. 1965, pp. 77-84.

23. Jakob, M., Heat Transfer, Vol. 1, Wiley, New York, 1949.

24. Rubel, A., and Landis, F., "Numerical Study of Natural Convection in a Vertical Rectangular Enclosure," The Physics of Fluids, Vol. 12, No. 12, Part II, December, 1969.

25. Newell, M.E., and Schmidt, F.W., "Heat Transfer by Laminar Natural Convection Within Rectangular Enclosures," Journal of Heat Transfer, Trans. ASME, Series C, Vol. 93, No. 1, Feb. 1970, pp. 159-168.

26. De Vahl Davis, G., "Laminar Natural Convection in an Enclosed Rectangular Cavity," International Journal of Heat and Mass Transfer, Vol. 11, 1968, pp. 1675-1693.

27. Szekely, J., and Todd, M.R., "Natural Convection in a Rectangular Cavity - Transient Behavior and Two-Phase Systems in Laminar Flow," International Journal of Heat and Mass Transfer, Vol. 14, No. 3, March 1971, pp. 467-482.

28. Elder, J.W., "Numerical Experiments with Free Convection in a Vertical Slot," Journal of Fluid Mechanics, Vol. 24, Part 4, 1966, pp. 823-843.

29. Emmons, H.W., "Critique of Numerical Modeling of Fluid Mechanics Phenomena," Annual Review of Fluid Mechanics, Vol. 2, 1970, Annual Reviews, Inc., Palo Alto, California.

30. Eichhorn, R., "Natural Convection in a Thermally Stratified Fluid," Progress in Heat and Mass Transfer, Vol. 2, Irvine, T.F., et al., eds., Pergamon Press, New York, 1969, pp. 41-53.

31. Cheesewright, R., "Natural Convection From a Plane, Vertical Surface in Non-Isothermal Surroundings," International Journal of Heat and Mass Transfer, Vol. 10, 1967, pp. 1847-1859.

32. Batchelor, G.K., "Heat Transfer by Free Convection Across a Closed Cavity Between Vertical Boundaries at Different Temperatures," Quarterly of Applied Mathematics, Vol. 12, 1954, pp. 209-233.

33. Pillow, A.F., "The Free Convection Cell in Two Dimensions," Aero. Research Lab Rept. A79, Melbourne, Australia, 1952.

34. Van Dyke, M., Perturbation Methods in Fluid Mechanics, Academic Press, New York, 1964.

35. Abramowitz, M., and Stegun, I.A., Handbook of Mathematical Functions, National Bureau of Standards Applied Mathematics Series, U.S. Government Printing Office, 1964.

36. Goldstein, S., Modern Developments in Fluid Dynamics, Vol. II, Dover Publications, New York, 1965.

37. Wilkes, J.O., "The Finite Difference Computation of Natural Convection in an Enclosed Rectangular Cavity," Ph.D. thesis, University of Michigan, Ann Arbor, 1963.

38. Mull, W., and Reiher, H., "Der Wärmeschutz von Luftschichten," Beihefte zum Gesundh-Ingenieur, Reihe 1, Heft 28, 1930.

39. Meksyn, D., New Methods in Laminar Boundary Layer Theory, Pergamon Press, New York, 1961.

40. Schechter, R.S., The Variational Method in Engineering, McGraw-Hill, New York, 1967.

APPENDIX A

SUMMARY OF THE GOVERNING DIFFERENTIAL EQUATIONS AND BOUNDARY CONDITIONS FOR THE ZEROTH AND HIGHER-ORDER PROBLEMS IN EACH REGION OF THE ENCLOSURE

The zeroth and some of the higher order governing differential equations and their boundary conditions are summarized below for each of the physically distinct regions in the enclosure.

The (Right-Hand) Vertical Wall Boundary Layer

Zeroth-Order

$$\frac{\partial \tilde{u}_0}{\partial \tilde{x}} + \frac{\partial \tilde{v}_0}{\partial \tilde{y}} = 0$$

$$\tilde{u}_0 \frac{\partial \tilde{u}_0}{\partial \tilde{x}} + \tilde{v}_0 \frac{\partial \tilde{u}_0}{\partial \tilde{y}} = -\frac{\partial \tilde{p}_0}{\partial \tilde{x}} + \tilde{T}_0 + \frac{\partial^2 \tilde{u}_0}{\partial \tilde{y}^2}$$

$$\frac{\partial \tilde{p}_0}{\partial \tilde{y}} = 0$$

$$\left(N_{PR}\right)\left(\tilde{u}_0 \frac{\partial \tilde{T}_0}{\partial \tilde{x}} + \tilde{v}_0 \frac{\partial \tilde{T}_0}{\partial \tilde{y}}\right) = \frac{\partial^2 \tilde{T}_0}{\partial \tilde{y}^2}$$

with,

$$\tilde{u}_0(\tilde{x},0) = 0$$

$$\tilde{v}_0(\tilde{x},0) = 0$$

$$\tilde{T}_0(\tilde{x},0) = 1$$

(plus matching conditions with core and corner regions)

First-Order

$$\frac{\partial \tilde{u}_1}{\partial \tilde{x}} + \frac{\partial \tilde{v}_1}{\partial \tilde{y}} = 0$$

$$\tilde{u}_0 \frac{\partial \tilde{u}_1}{\partial \tilde{x}} + \tilde{u}_1 \frac{\partial \tilde{u}_0}{\partial \tilde{x}} + \tilde{v}_0 \frac{\partial \tilde{u}_1}{\partial \tilde{y}} + \tilde{v}_1 \frac{\partial \tilde{u}_0}{\partial \tilde{y}} = -\frac{\partial \tilde{p}_1}{\partial \tilde{x}} + \tilde{T}_1 + \frac{\partial^2 \tilde{u}_1}{\partial \tilde{y}^2}$$

$$\frac{\partial \tilde{p}_1}{\partial \tilde{y}} = 0$$

$$\left(N_{PR}\right)\left(\tilde{u}_0 \frac{\partial \tilde{T}_1}{\partial \tilde{x}} + \tilde{u}_1 \frac{\partial \tilde{T}_0}{\partial \tilde{x}} + \tilde{v}_0 \frac{\partial \tilde{T}_1}{\partial \tilde{y}} + \tilde{v}_1 \frac{\partial \tilde{T}_0}{\partial \tilde{y}}\right) = \frac{\partial^2 \tilde{T}_1}{\partial \tilde{y}^2}$$

with,

$$\tilde{u}_1(\tilde{x},0) = 0$$

$$\tilde{v}_1(\tilde{x},0) = 0$$

$$\tilde{T}_1(\tilde{x},0) = 0$$

(plus matching conditions with the core and corner regions)

Second Order

$$\frac{\partial \tilde{u}_2}{\partial \tilde{x}} + \frac{\partial \tilde{v}_2}{\partial \tilde{y}} = 0$$

$$\tilde{u}_0 \frac{\partial \tilde{u}_2}{\partial \tilde{x}} + \tilde{u}_1 \frac{\partial \tilde{u}_1}{\partial \tilde{x}} + \tilde{u}_2 \frac{\partial \tilde{u}_0}{\partial \tilde{x}} + \tilde{v}_0 \frac{\partial \tilde{u}_2}{\partial \tilde{y}} + \tilde{v}_1 \frac{\partial \tilde{u}_1}{\partial \tilde{y}} + \tilde{v}_2 \frac{\partial \tilde{u}_0}{\partial \tilde{y}}$$

$$= \frac{\partial \tilde{p}_2}{\partial \tilde{x}} + \tilde{T}_2 + \frac{\partial^2 \tilde{u}_2}{\partial \tilde{y}^2}$$

$$\frac{\partial \tilde{p}_2}{\partial \tilde{y}} = 0$$

$$\left(N_{PR}\right)\left(\tilde{u}_0 \frac{\partial \tilde{T}_2}{\partial \tilde{x}} + \tilde{u}_1 \frac{\partial \tilde{T}_1}{\partial \tilde{x}} + \tilde{u}_2 \frac{\partial \tilde{T}_0}{\partial \tilde{x}} + \tilde{v}_0 \frac{\partial \tilde{T}_2}{\partial \tilde{y}} + \tilde{v}_1 \frac{\partial \tilde{T}_1}{\partial \tilde{y}} + \tilde{v}_2 \frac{\partial \tilde{T}_0}{\partial \tilde{y}}\right) = \frac{\partial^2 \tilde{T}_0}{\partial \tilde{y}^2}$$

with,

$$\tilde{u}_2(\tilde{x},0) = 0$$

$$\tilde{v}_2(\tilde{x},0) = 0$$

$$\tilde{T}_2(\tilde{x},0) = 0$$

(plus matching conditions with core and corner regions)

The (Bottom) Horizontal Wall Boundary Layer

Zeroth-Order

$$\frac{\partial \bar{u}_0}{\partial \bar{x}} + \frac{\partial \bar{v}_0}{\partial \bar{y}} = 0$$

$$\frac{\partial \bar{p}_0}{\partial \bar{x}} = 0$$

$$\frac{\partial \bar{p}_0}{\partial \bar{y}} = \frac{\partial^2 \bar{v}_0}{\partial \bar{x}^2}$$

$$\frac{\partial^2 \bar{T}_0}{\partial \bar{x}^2} = 0$$

with,

$$\bar{u}_0(0,\bar{y}) = 0$$

$$\bar{v}_0(0,\bar{y}) = 0$$

$$\frac{\partial \bar{T}_0(0,\bar{y})}{\partial \bar{x}} = 0$$

(plus matching conditions with core and corner regions)

First-Order

$$\frac{\partial \bar{u}_1}{\partial \bar{x}} + \frac{\partial \bar{v}_1}{\partial \bar{y}} = 0$$

$$\frac{\partial \bar{p}_1}{\partial \bar{x}} = 0$$

$$\frac{\partial \bar{p}_1}{\partial \bar{y}} = \frac{\partial^2 \bar{v}_1}{\partial \bar{x}^2}$$

$$\frac{\partial^2 \bar{T}_1}{\partial \bar{x}^2} = 0$$

with,

$$\bar{u}_1(0,\bar{y}) = 0$$

$$\bar{v}_1(0,\bar{y}) = 0$$

$$\frac{\partial \bar{T}_1(0,\bar{y})}{\partial \bar{x}} = 0$$

(plus matching conditions with core and corner regions)

Second-Order

$$\frac{\partial \bar{u}_2}{\partial \bar{x}} + \frac{\partial \bar{v}_2}{\partial \bar{y}} = 0$$

$$\frac{\partial \bar{p}_2}{\partial \bar{x}} = 0 \qquad \text{with,} \quad \bar{u}_2(0,\bar{y}) = 0$$

$$\frac{\partial \bar{p}_2}{\partial \bar{y}} = \frac{\partial^2 \bar{v}_2}{\partial \bar{x}^2} \qquad \bar{v}_2(0,\bar{y}) = 0$$

$$\frac{\partial^2 \bar{T}_2}{\partial \bar{x}^2} = 0 \qquad \frac{\partial \bar{T}_2(0,\bar{y})}{\partial \bar{x}} = 0$$

(plus matching conditions with the core and corner regions)

The Core Region

The equations in this region do not possess any boundary conditions. Their solutions must, however, match with the solutions of the vertical and horizontal wall boundary layer equations.

Zeroth-Order

$$\frac{\partial v_0}{\partial y} = 0$$

$$\frac{\partial p_0}{\partial x} = T_0$$

$$\frac{\partial p_0}{\partial y} = 0$$

$$v_0 \frac{\partial T_0}{\partial y} = 0$$

First Order

$$\frac{\partial v_1}{\partial y} = 0$$

$$\frac{\partial p_1}{\partial x} = T_1$$

$$\frac{\partial p_1}{\partial y} = 0$$

$$v_0 \frac{\partial T_1}{\partial y} + v_1 \frac{\partial T_0}{\partial y} = 0$$

Second-Order

$$\frac{\partial v_2}{\partial y} = 0$$

$$\frac{\partial p_2}{\partial x} = T_2$$

$$\frac{\partial p_2}{\partial y} = 0$$

$$\left(N_{PR}\right)\left(\frac{H}{W}\right)\left(v_0 \frac{\partial T_2}{\partial y} + v_1 \frac{\partial T_1}{\partial y} + v_2 \frac{\partial T_0}{\partial y}\right) = \frac{\partial^2 T_0}{\partial x^2} + \left(\frac{H}{W}\right)^2 \frac{\partial^2 T_0}{\partial y^2}$$

Third-Order

$$\frac{\partial u_0}{\partial x} + \left(\frac{H}{W}\right)^{\frac{1}{2}} \frac{\partial v_3}{\partial y} = 0$$

$$\frac{\partial p_3}{\partial x} = T_3$$

$$\frac{\partial p_3}{\partial y} = 0$$

$$\left(N_{PR}\right)\left(\frac{H}{W}\right)^{\frac{1}{2}} u_0 \frac{\partial T_0}{\partial x} + \left(N_{PR}\right)\left(\frac{H}{W}\right)\left(v_0 \frac{\partial T_3}{\partial y} + v_1 \frac{\partial T_2}{\partial y} + v_2 \frac{\partial T_1}{\partial y} + v_3 \frac{\partial T_0}{\partial y}\right)$$

$$= \frac{\partial^2 T_0}{\partial x^2} + \left(\frac{H}{W}\right)^2 \frac{\partial^2 T_1}{\partial y^2}$$

Fourth-Order

$$\frac{\partial u_1}{\partial x} + \left(\frac{H}{W}\right)^{\frac{1}{2}} \frac{\partial v_4}{\partial y} = 0$$

$$\frac{\partial p_4}{\partial x} = T_4$$

$$\frac{\partial p_4}{\partial y} + v_0 \frac{\partial v_0}{\partial y} = 0$$

$$\left(N_{PR}\right)\left(\frac{H}{W}\right)^{\frac{1}{2}} \left(u_0 \frac{\partial T_1}{\partial x} + u_1 \frac{\partial T_0}{\partial x}\right) + \left(N_{PR}\right)\left(\frac{H}{W}\right)\left(v_0 \frac{\partial T_4}{\partial y} + v_1 \frac{\partial T_3}{\partial y} + v_2 \frac{\partial T_2}{\partial y}\right.$$

$$\left. + v_3 \frac{\partial T_1}{\partial y} + v_4 \frac{\partial T_0}{\partial y}\right) = \frac{\partial^2 T_2}{\partial x^2} + \left(\frac{H}{W}\right)^2 \frac{\partial^2 T_2}{\partial y^2}$$

The (Bottom Right-Hand) Corner Region

Zeroth-Order

$$\frac{\partial \hat{u}_0}{\partial \hat{x}} + \frac{\partial \hat{v}_0}{\partial \hat{y}} = 0$$

$$\frac{\partial \hat{p}_0}{\partial \hat{x}} = \hat{T}_0 + \frac{\partial^2 \hat{u}_0}{\partial \hat{x}^2} + \frac{\partial^2 \hat{u}_0}{\partial \hat{y}^2}$$

$$\frac{\partial \hat{p}_0}{\partial \hat{y}} = \frac{\partial^2 \hat{v}_0}{\partial \hat{x}^2} + \frac{\partial^2 \hat{v}_0}{\partial \hat{y}^2}$$

$$\frac{\partial^2 \hat{T}_0}{\partial \hat{x}^2} + \frac{\partial^2 \hat{T}_0}{\partial \hat{y}^2} = 0$$

with, $\hat{u}_0(\hat{x},0) = 0$ $\qquad \hat{u}_0(0,\hat{y}) = 0$

$\hat{v}_o(\hat{x},0) = 0$ $\qquad \hat{v}_0(0,\hat{y}) = 0$

$\hat{T}_0(\hat{x},0) = 1$ $\qquad \dfrac{\partial \hat{T}_0(0,\hat{y})}{\partial \hat{x}} = 0$

(plus matching conditions with the vertical and horizontal wall boundary layers)

First Order

$$\frac{\partial \hat{u}_1}{\partial \hat{x}} + \frac{\partial \hat{v}_1}{\partial \hat{y}} = 0$$

$$\left(\frac{W}{H}\right)^{\frac{1}{2}} \left(\hat{u}_0 \frac{\partial \hat{u}_0}{\partial \hat{x}} + \hat{v}_0 \frac{\partial \hat{u}_0}{\partial \hat{y}}\right) = - \frac{\partial \hat{p}_1}{\partial \hat{x}} + \hat{T}_1 + \frac{\partial^2 \hat{u}_1}{\partial \hat{x}^2} + \frac{\partial^2 \hat{u}_1}{\partial \hat{y}^2}$$

$$\left(\frac{W}{H}\right)^{\frac{1}{2}} \left(\hat{u}_0 \frac{\partial \hat{v}_0}{\partial \hat{x}} + \hat{v}_0 \frac{\partial \hat{v}_0}{\partial \hat{y}}\right) = - \frac{\partial \hat{p}_1}{\partial \hat{y}} + \frac{\partial^2 \hat{v}_1}{\partial \hat{x}^2} + \frac{\partial^2 \hat{v}_1}{\partial \hat{y}^2}$$

$$\left(N_{PR}\right)\left(\frac{W}{H}\right)^{\frac{1}{2}} \left(\hat{u}_0 \frac{\partial \hat{T}_0}{\partial \hat{x}} + \hat{v}_0 \frac{\partial \hat{T}_0}{\partial \hat{y}}\right) = \frac{\partial^2 \hat{T}_1}{\partial \hat{x}^2} + \frac{\partial^2 \hat{T}_1}{\partial \hat{y}^2}$$

with,

$$\hat{u}_1(\hat{x},0) = 0 \qquad \hat{u}_1(0,\hat{y}) = 0$$

$$\hat{v}_1(\hat{x},0) = 0 \qquad \hat{v}_1(0,\hat{y}) = 0$$

$$\hat{T}_1(\hat{x},0) = 0 \qquad \frac{\partial \hat{T}_1(0,\hat{y})}{\partial \hat{x}} = 0$$

(plus matching conditions with the vertical and horizontal wall boundary layers)

<u>Second-Order</u>

$$\frac{\partial \hat{u}_2}{\partial \hat{x}} + \frac{\partial \hat{v}_2}{\partial \hat{y}} = 0$$

$$\left(\frac{W}{H}\right)^{\frac{1}{2}} \left(\hat{u}_0 \frac{\partial \hat{u}_1}{\partial \hat{x}} + \hat{u}_1 \frac{\partial \hat{u}_0}{\partial \hat{x}} + \hat{v}_0 \frac{\partial \hat{u}_1}{\partial \hat{y}} + \hat{v}_1 \frac{\partial \hat{u}_0}{\partial \hat{y}}\right) = - \frac{\partial \hat{p}_2}{\partial \hat{x}} + \hat{T}_2 + \frac{\partial^2 \hat{u}_2}{\partial \hat{x}^2} + \frac{\partial^2 \hat{u}_2}{\partial \hat{y}^2}$$

$$\left(\frac{W}{H}\right)^{\frac{1}{2}} \left(\hat{u}_0 \frac{\partial \hat{v}_1}{\partial \hat{x}} + \hat{u}_1 \frac{\partial \hat{v}_0}{\partial \hat{x}} + \hat{v}_0 \frac{\partial \hat{v}_1}{\partial \hat{y}} + \hat{v}_1 \frac{\partial \hat{v}_0}{\partial \hat{y}}\right) = - \frac{\partial \hat{p}_2}{\partial \hat{y}} + \frac{\partial^2 \hat{v}_2}{\partial \hat{x}^2} + \frac{\partial^2 \hat{v}_2}{\partial \hat{y}^2}$$

$$\left(N_{PR}\right)\left(\frac{W}{H}\right)^{\frac{1}{2}} \left(\hat{u}_0 \frac{\partial \hat{T}_1}{\partial \hat{x}} + \hat{u}_1 \frac{\partial \hat{T}_0}{\partial \hat{x}} + \hat{v}_0 \frac{\partial \hat{T}_1}{\partial \hat{y}} + \hat{v}_1 \frac{\partial \hat{T}_0}{\partial \hat{y}}\right) = \frac{\partial^2 \hat{T}_2}{\partial \hat{x}^2} + \frac{\partial^2 \hat{T}_2}{\partial \hat{y}^2}$$

with,

$$\hat{u}_2(\hat{x},0) = 0 \qquad \hat{u}_2(0,\hat{y}) = 0$$

$$\hat{v}_2(\hat{x},0) = 0 \qquad \hat{v}_2(0,\hat{y}) = 0$$

$$\hat{T}_2(\hat{x},0) = 0 \qquad \frac{\partial \hat{T}_2(0,\hat{y})}{\partial \hat{x}} = 0$$

(plus matching conditions with the vertical and horizontal wall boundary layers)

APPENDIX B

INVESTIGATION OF ALTERNATIVE FORMS OF THE GOVERNING EQUATIONS FOR THE CORNER REGIONS

As shown in Chapter II:

$$(\hat{L}_{rx}\hat{v}_r) = (\bar{L}_{rx}\bar{v}_r) = \epsilon\ \nu_0\left(\frac{W}{H}\right)^{\frac{1}{2}} \tag{B.1}$$

$$\left(\frac{\hat{v}_r\hat{L}_{rx}}{\hat{u}_r\hat{L}_{ry}}\right) = 1 \tag{B.2}$$

or,

$$(\hat{u}_r\hat{L}_{ry}) = (\hat{v}_r\hat{L}_{rx}) = \epsilon\ \nu_0\left(\frac{W}{H}\right)^{\frac{1}{2}} \tag{B.3}$$

Thus;

$$\hat{u}_r = \left(\frac{\epsilon\ \nu_0}{\hat{L}_{ry}}\right)\left(\frac{W}{H}\right)^{\frac{1}{2}} \tag{B.4}$$

and,

$$\hat{v}_r = \left(\frac{\epsilon\ \nu_0}{\hat{L}_{rx}}\right)\left(\frac{W}{H}\right)^{\frac{1}{2}} \tag{B.5}$$

Substituting equations (B.2) and (B.5) in the energy equation (2.4d) and rearranging gives

$$\hat{u}\ \frac{\partial\hat{T}}{\partial\hat{x}} + \hat{v}\ \frac{\partial\hat{T}}{\partial\hat{y}} = \left(\frac{1}{N_{PR}}\right)\left(\frac{\hat{L}_{ry}}{\epsilon\ \hat{L}_{rx}}\right)\left(\frac{H}{W}\right)^{\frac{1}{2}}\frac{\partial^2\hat{T}}{\partial\hat{x}^2} + \left(\frac{1}{N_{PR}}\right)\left(\frac{\hat{L}_{rx}}{\epsilon\ \hat{L}_{ry}}\right)\left(\frac{H}{W}\right)^{\frac{1}{2}}\frac{\partial^2\hat{T}}{\partial\hat{y}^2} \tag{B.6}$$

This equation admits three possibilities for the coefficients of the terms in the right-hand member:

Case 1. $$\left(\frac{1}{N_{PR}}\right)\left(\frac{\hat{L}_{ry}}{\epsilon\ \hat{L}_{rx}}\right)\left(\frac{H}{W}\right)^{\frac{1}{2}} = 1 \tag{B.7}$$

Case 2. $$\left(\frac{1}{N_{PR}}\right)\left(\frac{\hat{L}_{rx}}{\epsilon\ \hat{L}_{ry}}\right)\left(\frac{H}{W}\right)^{\frac{1}{2}} = 1 \tag{B.8}$$

Case 3. $$\left(\frac{1}{N_{PR}}\right)\left(\frac{\hat{L}_{ry}}{\epsilon\ \hat{L}_{rx}}\right)\left(\frac{H}{W}\right)^{\frac{1}{2}} = \left(\frac{1}{N_{PR}}\right)\left(\frac{\hat{L}_{rx}}{\epsilon\ \hat{L}_{ry}}\right)\left(\frac{H}{W}\right)^{\frac{1}{2}}$$

or,

$$\hat{L}_{rx} = \hat{L}_{ry} \tag{B.9}$$

These three cases will now be investigated in a systematic fashion. This analysis will determine the correct values of the reference lengths, $\hat{L}_{rx}$ and $\hat{L}_{ry}$, and the reference velocities, $\hat{u}_r$ and $\hat{v}_r$, as well as the corresponding force balances in the momentum equations.

Case 1

As shown above, for Case 1

$$\left(\frac{1}{N_{PR}}\right)\left(\frac{\hat{L}_{ry}}{\epsilon\hat{L}_{rx}}\right)\left(\frac{H}{W}\right)^{\frac{1}{2}} = 1 \tag{B.7}$$

Thus,

$$\frac{\hat{L}_{ry}}{\hat{L}_{rx}} = \epsilon\ N_{PR}\left(\frac{W}{H}\right)^{\frac{1}{2}} \tag{B.10}$$

Substituting this result in the energy equation (B.6) gives

$$\hat{u}\ \frac{\partial\hat{T}}{\partial\hat{x}} + \hat{v}\ \frac{\partial\hat{T}}{\partial\hat{y}} = \frac{\partial^2\hat{T}}{\partial\hat{x}^2} + \left(\frac{1}{\epsilon^2}\right)\left(\frac{1}{N_{PR}^2}\right)\left(\frac{H}{W}\right)\ \frac{\partial^2\hat{T}}{\partial\hat{y}^2} \tag{B.11}$$

or, to the lowest order:

$$\frac{\partial^2\hat{T}_0}{\partial\hat{y}^2} = 0 \tag{B.12}$$

Integrating this result gives a linear function in $\hat{y}$ which is not acceptable since it cannot be matched with the solution of the bottom horizontal wall boundary layer. Therefore, Case 1 is rejected on this basis.

Case 2

For Case 2

$$\left(\frac{1}{N_{PR}}\right)\left(\frac{\hat{L}_{rx}}{\epsilon\ \hat{L}_{ry}}\right)\left(\frac{H}{W}\right)^{\frac{1}{2}} = 1 \qquad (B.8)$$

which gives

$$\frac{\hat{L}_{ry}}{\hat{L}_{rx}} = \left(\frac{1}{\epsilon\ N_{PR}}\right)\left(\frac{H}{W}\right)^{\frac{1}{2}} \qquad (B.13)$$

Substituting this result in the energy equation (B.6) gives

$$\epsilon^2 \left(\hat{u}\ \frac{\partial\hat{T}}{\partial\hat{x}} + \hat{v}\ \frac{\partial\hat{T}}{\partial\hat{y}}\right) = \left(\frac{1}{N_{PR}^2}\right)\left(\frac{H}{W}\right) \frac{\partial^2\hat{T}}{\partial\hat{x}^2} + \epsilon^2\ \frac{\partial^2\hat{T}}{\partial\hat{y}^2} \qquad (B.14)$$

or, to the lowest order:

$$\frac{\partial^2\hat{T}_0}{\partial\hat{x}^2} = 0 \qquad (B.15)$$

Integrating this result gives

$$\hat{T}_0 = \hat{x}\ g_1(\hat{y}) + g_2(\hat{y}) \qquad (B.16)$$

where: g_1, g_2 are unknown function of $\hat{y}$ only.

This expression (B.16) for $\hat{T}_0$ is a possible solution. The implications of this scaling on the force balances in the momentum equations must now be examined.

It is now assumed that the pressure force in the corner region is the same order as the pressure force in the vertical wall boundary layer, so that

$$\left.\frac{\partial\hat{p}}{\partial\hat{x}}\right|_r = \left.\frac{\partial\tilde{p}}{\partial\tilde{x}}\right|_r = \frac{\rho_0 \nu_0^2}{\epsilon^8 H^3} \qquad (B.17)$$

then,

$$\left.\frac{\partial \hat{p}}{\partial \hat{y}}\right|_r = \left(\frac{\hat{L}_{rx}}{\hat{L}_{ry}}\right)\left(\left.\frac{\partial \hat{p}}{\partial \hat{x}}\right|_r\right) \tag{B.18}$$

Substituting equations (B.13) and (B.17) in equation (B.18) gives:

$$\left.\frac{\partial \hat{p}}{\partial \hat{y}}\right|_r = \left(\frac{\rho_0 \nu_0^2 N_{PR}}{\epsilon^7 H^3}\right)\left(\frac{W}{H}\right)^{\frac{1}{2}} \tag{B.19}$$

Substituting equations (B.2), (B.4), (B.5), (B.13) and (B.19) in the $\hat{y}$-momentum equation (2.4c) and rearranging yields:

$$\left(\frac{\epsilon^3 N_{PR}}{\hat{L}_{rx}^3}\right)\left(\frac{W}{H}\right)\left(\hat{u}\frac{\partial \hat{v}}{\partial \hat{x}} + \hat{v}\frac{\partial \hat{v}}{\partial \hat{y}}\right) = -\left(\frac{N_{PR}}{\epsilon^7 H^3}\right)\frac{\partial \hat{p}}{\partial \hat{y}} + \left(\frac{\epsilon}{\hat{L}_{rx}^3}\right)\left[\frac{\partial^2 \hat{v}}{\partial \hat{x}^2} + (\epsilon^2 N_{PR}^2)\left(\frac{W}{H}\right)\frac{\partial^2 \hat{v}}{\partial \hat{y}^2}\right] \tag{B.20}$$

There are, in general, four possible force balances in this equation:

1. inertia - pressure - viscous force balance
2. inertia - pressure force balance
3. inertia - viscous force balance
4. pressure - viscous force balance

an examination of these force balances will determine the correct value of the reference length, $\hat{L}_{rx}$, for Case 2.

<u>Intertia - Pressure - Viscous Force Balance</u>

Equating the coefficients of these three terms in equation (B.20)

$$\left(\frac{\epsilon^3 N_{PR}}{\hat{L}_{rx}^3}\right)\left(\frac{W}{H}\right) = \left(\frac{N_{PR}}{\epsilon^7 H^3}\right) = \left(\frac{\epsilon}{\hat{L}_{rx}^3}\right) \tag{B.21}$$

From which:

$$\hat{L}_{rx} = \frac{\epsilon^{8/3} H}{N_{PR}^{1/3}} \tag{B.22}$$

Substituting this result back into the $\hat{y}$-momentum equation (B.20) yields

$$\epsilon^2 (N_{PR})\left(\frac{W}{H}\right)\left(\hat{u}\frac{\partial \hat{v}}{\partial \hat{x}} + \hat{v}\frac{\partial \hat{v}}{\partial \hat{y}}\right) = -\frac{\partial \hat{p}}{\partial \hat{y}} + \left[\frac{\partial^2 \hat{v}}{\partial \hat{x}^2} + \epsilon^2 (N_{PR}^2)\left(\frac{W}{H}\right)\frac{\partial^2 \hat{v}}{\partial \hat{y}^2}\right] \qquad (B.23)$$

Thus, an inertia - pressure - viscous force balance cannot be obtained for case 2 as the inertia terms are lost in the limit as ϵ approaches zero.

Inertia - Pressure Force Balance

Equation (B.20) gives

$$\left(\frac{\epsilon^3 N_{PR}}{\hat{L}_{rx}^3}\right)\left(\frac{W}{H}\right) = \left(\frac{N_{PR}}{\epsilon^7 H^3}\right) \qquad (B.24)$$

From which:

$$\hat{L}_{rx} = \epsilon^{10/3} H^{2/3} W^{1/3} \qquad (B.25)$$

Substituting this result back into the $\hat{y}$-momentum equation (B.20):

$$\epsilon^2\left(N_{PR}\right)\left(\frac{W}{H}\right)\left(\hat{u}\frac{\partial \hat{v}}{\partial \hat{x}} + \hat{v}\frac{\partial \hat{v}}{\partial \hat{y}}\right) = -\epsilon^2\left(N_{PR}\right)\left(\frac{W}{H}\right)\frac{\partial \hat{p}}{\partial \hat{y}} + \left[\frac{\partial^2 \hat{v}}{\partial \hat{x}^2} + \epsilon^2\left(N_{PR}^2\right)\left(\frac{W}{H}\right)\frac{\partial^2 \hat{v}}{\partial \hat{y}^2}\right]$$

(B.26)

Therefore, an inertia - pressure force balance is clearly impossible for Case 2 as both the inertia and pressure terms are lost in the limit as ϵ approaches zero.

Inertia Force - Viscous Force Balance

This gives:

$$\left(\frac{\epsilon^3 N_{PR}}{\hat{L}_{rx}^3}\right)\left(\frac{W}{H}\right) = \left(\frac{\epsilon}{\hat{L}_{rx}^3}\right) \qquad (B.27)$$

Since the Prandtl number, N_{PR}, and the aspect ratio, (W/H), are both O(1); the right- and left-hand members of equation (B.27) can never be of the same order, independent of the value of $\hat{L}_{rx}$. Thus, an inertia -

viscous force balance is also impossible for Case 2.

<u>Pressure - Viscous Force Balance</u>

This is the only remaining possible balance in Case 2. Equating the coefficients of the pressure force and viscous force terms in equation (B.20) gives

$$\frac{N_{PR}}{\epsilon^7 H^3} = \frac{\epsilon}{\hat{L}_{rx}^3} \tag{B.28}$$

Then;

$$\hat{L}_{rx} = \frac{\epsilon^{8/3} H}{N_{PR}^{1/3}} \tag{B.29}$$

Substituting equations (B.4), (B.5), (B.13), (B.17), (B.18), and (B.29) in the governing equations (2.4) gives

$$\frac{\partial \hat{u}}{\partial \hat{x}} + \frac{\partial \hat{v}}{\partial \hat{y}} = 0 \tag{B.30a}$$

$$\epsilon^4\left(N_{PR}^3\right)\left(\frac{W}{H}\right)^2\left(\hat{u}\,\frac{\partial \hat{u}}{\partial \hat{x}} + \hat{v}\,\frac{\partial \hat{u}}{\partial \hat{y}}\right) = -\frac{\partial \hat{p}}{\partial \hat{x}} + \hat{T} + \epsilon^2\left(N_{PR}^2\right)\left(\frac{W}{H}\right)\left[\frac{\partial^2 \hat{u}}{\partial \hat{x}^2} + \epsilon^2\left(N_{PR}^2\right)\left(\frac{W}{H}\right)\frac{\partial^2 \hat{u}}{\partial \hat{y}^2}\right] \tag{B.30b}$$

$$\epsilon^2\left(N_{PR}\right)\left(\frac{W}{H}\right)\left(\hat{u}\,\frac{\partial \hat{v}}{\partial \hat{x}} + \hat{v}\,\frac{\partial \hat{v}}{\partial \hat{y}}\right) = -\frac{\partial \hat{p}}{\partial \hat{y}} + \left[\frac{\partial^2 \hat{v}}{\partial \hat{x}^2} + \epsilon^2\left(N_{PR}^2\right)\left(\frac{W}{H}\right)\frac{\partial^2 \hat{v}}{\partial \hat{y}^2}\right] \tag{B.30c}$$

$$\epsilon^2\left(N_{PR}^2\right)\left(\hat{u}\,\frac{\partial \hat{T}}{\partial \hat{x}} + \hat{v}\,\frac{\partial \hat{T}}{\partial \hat{y}}\right) = \frac{\partial^2 \hat{T}}{\partial \hat{x}^2} + \epsilon^2\left(N_{PR}^2\right)\frac{\partial^2 \hat{T}}{\partial \hat{y}^2} \tag{B.30d}$$

where the pressure force - viscous force balance is obtained in the $\hat{y}$-momentum equation (B.30c).

To lowest order, these equations reduce to:

$$\frac{\partial \hat{u}_0}{\partial x} + \frac{\partial \hat{v}_0}{\partial \hat{y}} = 0 \qquad \text{(B.31a)}$$

$$\frac{\partial \hat{p}_0}{\partial \hat{x}} = \hat{T}_0 \qquad \text{(B.31b)}$$

$$\frac{\partial \hat{p}_0}{\partial \hat{y}} = \frac{\partial^2 \hat{v}_0}{\partial \hat{x}^2} \qquad \text{(B.31c)}$$

$$\frac{\partial^2 \hat{T}_0}{\partial \hat{x}^2} = 0 \qquad \text{(B.31d)}$$

Integrating the energy equation (B.31d) once gives:

$$\frac{\partial \hat{T}_0}{\partial \hat{x}} = h_1(\hat{y}) \qquad \text{(B.32)}$$

where: h_n's $\equiv$ functions of $\hat{y}$ only

Since the bottom horizontal wall is adiabatic:

$$\frac{\partial \hat{T}_0(0,\hat{y})}{\partial \hat{x}} = 0 \qquad \text{(B.33)}$$

This gives: $h_1(\hat{y}) = 0$ (B.34)

Therefore, a second integration gives

$$\hat{T}_0 = h_2(\hat{y}) \qquad \text{(B.35)}$$

Substituting this result in the $\hat{x}$-momentum equation (B.31b) and integrating yields:

$$\hat{p}_0 = \hat{x}\, h_2(\hat{y}) + h_3(\hat{y}) \qquad \text{(B.36)}$$

It has already been shown in Chapter II that the pressure distribution in the core is "impressed" on the vertical wall boundary layers. Thus; the pressure distribution in the vertical wall boundary layers is known to be:

$$\tilde{p}_0 = \tfrac{1}{2}\, c_1 \tilde{x}^2 + c_2 \tilde{x} \tag{B.37}$$

The pressure distributions in the right-hand vertical wall boundary layer and bottom right-hand corner regions will now be matched.

Pressure Matching

The corner region, or "inner", solution for the pressure distribution is given by equation (B.36) as:

$$\hat{p}_0 = \hat{x}\, h_2(\hat{y}) + h_3(\hat{y}) \tag{B.38}$$

Rewriting this solution in vertical wall boundary layer, or "outer", variables gives:

$$\tilde{p}_0 = \tilde{x}\, h_2\!\left[\epsilon^{1/3}\, N_{PR}^{4/3} \left(\frac{W}{H}\right)^{\frac{1}{2}} \tilde{y}\right] + \left(\frac{\epsilon^{8/3}}{N_{PR}^{1/3}}\right) h_3\!\left[\epsilon^{1/3} N_{PR}^{4/3} \left(\frac{W}{H}\right)^{\frac{1}{2}} \tilde{y}\right] \tag{B.39}$$

Taking the "outer limit" of this inner solution as $\epsilon \to 0$ yields:

$$\lim_{\epsilon \to 0} (\tilde{p}_0) = \tilde{x}\, h_2(0) \tag{B.40}$$

The vertical wall boundary layer, or outer, solution for the pressure distribution is given by equation (B.37) as:

$$\tilde{p}_0 = \tfrac{1}{2}\, c_1 \tilde{x}^2 + c_2 \tilde{x} \tag{B.41}$$

Rewriting this solution in corner, or inner, variables gives:

$$\hat{p}_0 = (\tfrac{1}{2})(c_1)\left(\frac{\epsilon^{8/3}}{N_{PR}^{1/3}}\right) \hat{x}^2 + c_2\, \hat{x} \tag{B.42}$$

Taking the "inner limit" of this outer solution as $\epsilon \to 0$ gives:

$$\lim_{\epsilon \to 0} (\hat{p}_0) = c_2\, \hat{x} \tag{B.43}$$

This limit may be rewritten in outer variables as:

$$\lim_{\varepsilon \to 0} (\hat{p}_0) = c_2 \tilde{x} \qquad (B.44)$$

The limit matching principle [34]

$$\begin{bmatrix}\text{inner limit} \\ \text{of the outer solution}\end{bmatrix} = \begin{bmatrix}\text{outer limit} \\ \text{of the inner solution}\end{bmatrix}$$

gives:

$$\tilde{x}\, h_2(0) = c_2 \tilde{x} \qquad (B.45)$$

or,

$$h_2(0) = c_2 \qquad (B.46)$$

Substituting the isothermal boundary condition on the right-hand vertical wall as given by

$$\hat{T}_0(\hat{x},0) = 1 \qquad (B.47)$$

in equation (B.46) yields

$$c_2 = 1 \qquad (B.48)$$

It is known from numerical solutions and experimental results such as Noble [11] and Elder [28], however, that:

$$c_2 = 0 \qquad (B.49)$$

Thus, Case 2 is rejected on this basis. (A physical argument for the impossibility of equation B.48 is given in Chapter III.)

Case 3

For Case 3

$$\hat{L}_{rx} = \hat{L}_{ry} \qquad (B.9)$$

Substituting equations (B.2), (B.4), (B.5), (B.9), and (B.18) in the $\hat{y}$-momentum equation (2.4c) gives

$$\left(\frac{\varepsilon^2}{\hat{L}_{rx}^3}\right)\left(\frac{W}{H}\right)\left(\hat{u}\frac{\partial\hat{v}}{\partial\hat{x}} + \hat{v}\frac{\partial\hat{v}}{\partial\hat{y}}\right) = -\left(\frac{1}{\varepsilon^8 H^3}\right)\frac{\partial\hat{p}}{\partial\hat{y}} + \left(\frac{\varepsilon}{\hat{L}_{rx}^3}\right)\left(\frac{W}{H}\right)^{\frac{1}{2}}\left(\frac{\partial^2\hat{v}}{\partial\hat{x}^2} + \frac{\partial^2\hat{v}}{\partial\hat{y}^2}\right) \tag{B.50}$$

There are, in general, four possible force balances in this equation:

1. inertia - viscous force balance
2. inertia - pressure - viscous force balance
3. inertia - pressure force balance
4. pressure - viscous force balance

an examination of these force balances will determine the correct value of the reference length, $\hat{L}_{rx}$, for Case 3.

<u>Inertia - Viscous Force Balance</u>

Inspection of equation (B.50) reveals that; since the aspect ratio, (W/H), is always O(1); the inertia force and viscous force terms can never be of the same order, independent of the value of $\hat{L}_{rx}$.

<u>Inertia - Pressure - Viscous Force Balance</u>

This balance cannot be obtained because the inertia force and viscous force terms can never be of the same order as shown above.

<u>Inertia - Pressure Force Balance</u>

Equating the coefficients of the inertia force and pressure force terms in equation (B.50) gives

$$\left(\frac{\varepsilon^2}{\hat{L}_{rx}^3}\right)\left(\frac{W}{H}\right) = \left(\frac{1}{\varepsilon^8 H^3}\right) \tag{B.51}$$

This yields:

$$\hat{L}_{rx} = \varepsilon^{10/3} W^{1/3} H^{2/3} \tag{B.52}$$

Substituting this result in the $\hat{y}$-momentum equation (B.50) and rearranging gives

$$\epsilon \left(\hat{u}\frac{\partial \hat{v}}{\partial \hat{x}} + \hat{v}\frac{\partial \hat{v}}{\partial \hat{y}}\right) = -\epsilon\frac{\partial \hat{p}}{\partial \hat{y}} + \left(\frac{H}{W}\right)^{\frac{1}{2}}\left(\frac{\partial^2 \hat{v}}{\partial \hat{x}^2} + \frac{\partial^2 \hat{v}}{\partial \hat{y}^2}\right) \qquad (B.53)$$

Thus, an inertia force-pressure force balance cannot be obtained as the inertia and pressure terms are lost in the limit as ϵ approaches zero.

<u>Pressure - Viscous Force Balance</u>

This is the only remaing possible force balance. Equating the coefficients of the pressure force and viscous force terms in equation (B.50) gives

$$\left(\frac{1}{\epsilon^8 H^3}\right) = \left(\frac{\epsilon}{\hat{L}_{rx}^3}\right)\left(\frac{W}{H}\right)^{\frac{1}{2}} \qquad (B.54)$$

so that:

$$\hat{L}_{rx} = \epsilon^3 H^{5/6} W^{1/6} \qquad (B.55)$$

Substituting this result in equation (B.9) gives

$$\hat{L}_{ry} = \hat{L}_{rx} = \epsilon^3 H^{5/6} W^{1/6} \qquad (B.56)$$

Substituting these results in equations (B.4), (B.5), and (B.18) yields

$$\hat{u}_r = \hat{v}_r = \left(\frac{\nu_0}{\epsilon^2 H}\right)\left(\frac{W}{H}\right)^{\frac{1}{2}} \qquad (B.57)$$

and,

$$\left.\frac{\partial \hat{p}}{\partial \hat{x}}\right|_r = \left.\frac{\partial \hat{p}}{\partial \hat{y}}\right|_r = \frac{\rho_0 \nu_0^2}{\epsilon^3 H^3} \qquad (B.58)$$

Substituting these reference quantities in equations (2.4) gives the following set of governing equations for the (bottom right-hand) corner region

$$\frac{\partial \hat{u}}{\partial \hat{x}} + \frac{\partial \hat{v}}{\partial \hat{y}} = 0 \qquad \text{(B.59a)}$$

$$\epsilon\left(\frac{W}{H}\right)^{\frac{1}{2}} \left(\hat{u}\,\frac{\partial \hat{u}}{\partial \hat{x}} + \hat{v}\,\frac{\partial \hat{u}}{\partial \hat{y}}\right) = -\,\frac{\partial \hat{p}}{\partial \hat{x}} + \hat{T} + \frac{\partial^2 \hat{u}}{\partial \hat{x}^2} + \frac{\partial^2 \hat{u}}{\partial \hat{y}^2} \qquad \text{(B.59b)}$$

$$\epsilon\left(\frac{W}{H}\right)^{\frac{1}{2}} \left(\hat{u}\,\frac{\partial \hat{v}}{\partial \hat{x}} + \hat{v}\,\frac{\partial \hat{v}}{\partial \hat{y}}\right) = -\,\frac{\partial \hat{p}}{\partial \hat{y}} + \frac{\partial^2 \hat{v}}{\partial \hat{x}^2} + \frac{\partial^2 \hat{v}}{\partial \hat{y}^2} \qquad \text{(B.59c)}$$

$$\epsilon\left(N_{PR}\right)\left(\frac{W}{H}\right)^{\frac{1}{2}}\left(\hat{u}\,\frac{\partial \hat{T}}{\partial \hat{x}} + \hat{v}\,\frac{\partial \hat{T}}{\partial \hat{y}}\right) = \frac{\partial^2 \hat{T}}{\partial \hat{x}^2} + \frac{\partial^2 \hat{T}}{\partial \hat{y}^2} \qquad \text{(B.59d)}$$

where the pressure force-viscous force balance is obtained in the $\hat{y}$-momentum equation (D.59c)

Thus, the only possible scaling for the corner regions is given by the following set of reference quantities:

$$\hat{L}_{rx} = \hat{L}_{ry} = \epsilon^3\, H^{5/6}\, W^{1/6} \qquad \text{(B.60a)}$$

$$\hat{u}_r = \hat{v}_r = \left(\frac{\nu_0}{\epsilon^2\, H}\right)\left(\frac{W}{H}\right)^{1/3} \qquad \text{(B.60b)}$$

$$\left.\frac{\partial \hat{p}}{\partial \hat{x}}\right|_r = \left.\frac{\partial \hat{p}}{\partial \hat{y}}\right|_r = \left(\frac{\rho_0 \nu_0^2}{\epsilon^8\, H^3}\right) \qquad \text{(B.60c)}$$